Dissertation

Structural dynamics of GABAergic axons in the face of changing neuronal activity

- A study in hippocampal slice cultures -

Dissertation of the Graduate School of Systemic Neurosciences
of the Ludwig-Maximilians-University Munich

Submitted by Anne Schümann

19.10.2012

Supervisor: Corette Wierenga, PhD
2nd reviewer: Prof. Dr. Stephan Kröger

Date of the oral defense: 20.12.2012

To my beloved family

Eidesstattliche Versicherung/Affidavit

Hiermit versichere ich an Eides statt, dass ich die vorliegende Dissertation „Structural dynamics of GABAergic axons in the face of changing neuronal activity - a study in hippocampal slice cultures“ selbstständig angefertigt habe, mich außer der angegebenen keiner weiteren Hilfsmittel bedient und alle Erkenntnisse, die aus dem Schrifttum ganz oder annähernd übernommen sind, als solche kenntlich gemacht und nach ihrer Herkunft unter Bezeichnung der Fundstelle einzeln nachgewiesen habe.

I hereby confirm that the dissertation „Structural dynamics of GABAergic axons in the face of changing neuronal activity - a study in hippocampal slice cultures“ is the result of my own work and that I have only used sources or materials listed and specified in the dissertation.

München, den 19.10.2012
Munich, 19.10.2012 Anne Schümann

Contributions

The following people contributed raw data or analysis tools to this work.

Corette Wierenga, PhD contributed the raw data for figures 9-12. Furthermore, she chiefly developed the software for analysis of GABAergic axons.
Dana Damohray and **Catherine Dippel**, two GSN students, performed two-photon imaging experiments with slices treated with 4-AP for 48 h during a lab rotation.
Agnieszka Klawiter, who contributed a part of the raw data for the electrophysiology experiments (Figure 20) during her summer stay as an Amgen scholar in the lab in 2011.
Dr. Birgit Manno (University of Göttingen) kindly provided the pABES plasmid (Takata et al., 1994).

Munich, 19.10.2012 Prof. Dr. Tobias Bonhoeffer

Table of Contents

List of Figures

Introduction

Materials and Methods

Results

Discussion

Summary

Synaptic plasticity is a key feature of neuronal networks, thought to underlie central processes like learning and memory. Structural plasticity is a very important aspect of synaptic plasticity, as it reflects the re-arrangement of synaptic connections and other "hard-wired" modifications of neuronal connectivity.

While many aspects of structural plasticity at excitatory synapses are relatively well known, similar mechanisms of inhibitory synapses have received considerably less attention. Since inhibitory plasticity appears to precede or even allow for excitatory plasticity in some systems and since the balance of excitation and inhibition is a crucial factor in many neurological diseases, this study was designed to add to the information about inhibitory plasticity. Work in this thesis was focused on structural plasticity of inhibitory synapses, where the gap of knowledge is especially prominent.

The first part of the thesis was focused on characterizing structural dynamics of inhibitory synapses under baseline conditions. For this purpose, GFP-positive axons in hippocampal slice cultures from GAD65-GFP mice were subjected to time-lapse two-photon imaging for several hours. In GAD65-GFP mice, a subset of mostly dendritically targeting, GABAergic interneurons express cytosolic GFP. The labeling of hippocampal interneurons of was sufficiently bright to allow for repeated two-photon imaging of individual GFP-positive axons over the course of several hours. About 80 % of the presynaptic GABAergic boutons on the imaged axons were present successively throughout the imaging period, large, showed little volume variations, and to a large part

co-localized with both pre- and postsynaptic markers. These "persistent boutons" were assumed to mostly represent rather mature, *bona fide* synapses. The remainder of the boutons (~20 %) was present intermittently, small, showed comparatively large volume variations and co-localized to a lesser extend with pre- and postsynaptic markers as persistent boutons did. This population was termed "non-persistent boutons" and dependent on their average lifetime suggested to represent synapses in the process of formation or degradation, to occupy stop sites for synaptic material along the axon, or to represent general axonal transport events. Persistent and non-persistent boutons were suggested to avoid clustering with boutons from the same category along the axon.

The second part of the thesis focused on changes in the structural dynamics of GABAergic axons during the manipulation of neuronal activity. Acute (4 h) manipulation of neuronal activity was found to affect the structural dynamics of GABAergic axons. While reducing activity with TTX decreased synapse formation and degradation as well as synapse-related transport events, enhancing activity with 4-AP destabilized persistent boutons and increased transport processes along the axon. The high-activity induced changes in the structural dynamics of GABAergic axons were found to critically depend on the activation of $GABA_A$ receptors. This suggests that $GABA_A$ receptors are part of a feedback mechanism which assesses the level of GABA release in a network and adjusts structural plasticity accordingly. Interestingly, the acute changes in axonal dynamics did not result in changes in synapse density after several days (48 h to 7 d). This suggests (a) that other than structural plasticity mechanisms govern the long-term adaptation of GABAergic synapses to changes in network activity or (b) that the initial changes in bouton turnover and volume dynamics represent the rearrangement of synaptic connections which is complete after several days of activity manipulations.

The last part of this thesis was concerned with determining the spatial scale of the plasticity mechanisms that were found in the previous parts. Reducing neuronal activity in only a small region of the slice culture led to the conclusion that the plasticity observed here does not require activity changes in the entire network to be evoked. Furthermore, initial experiments preparing the manipulation of individual cells were performed, to set the stage for later experiments on this spatial scale.

In summary, the data of this thesis contribute to the understanding of the structural plasticity of inhibitory synapses and other axonal structures both under baseline conditions and following the manipulation of neuronal activity in the network. These experiments set the stage for further experiments investigating the spatial scale or molecular mechanisms of structural GABAergic plasticity.

Abbreviations

3D	Three dimensions
4-AP	4-aminopyridine
ABES	Human beta actin promoter (modified)
ACSF	Artificial cerebrospinal fluid
AMPA	α-amino-3-hydroxy-5-methyl-4-isoxazolepropionic acid
Ara-C	Arabinofuranosyl Cytidine
Arc	Activity-regulated cytoskeleton-associated protein
ATP	Adenosine triphosphate
BDNF	Brain derived neurotrophic growth factor
BME	Basal medium eagle
CA1/2/3	Cornu ammonis, region 1, 2, or 3
CAG	Combination of the CMV early enhancer and the chicken beta actin promoter
CaMKII/V	Calcium-calmodulin-dependent kinase II/V
CDK5	Cyclin-dependent kinase 5
CGE	Caudal ganglionic eminence
CMV	Human cytomegalus virus immediate early promoter
CV	Coefficient of variation
DIV	Days *in vitro* after preparation (day of preparation = DIV 1)
DSG	Dystrophin-glycoprotein complex
EF1a	Human elongation factor 1 alpha promoter
ER	Endoplasmatic reticulum
FGF	Fibroblast growth factor
GABA	Gamma aminobutyric acid
$GABA_A$ receptor	GABA receptor, type A
GABARAP	$GABA_A$ receptor associated proteins
GAD65/67	Glutamate decarboxylase, 65 kDa/67 kDa
GBSS	Grey's balanced salt solution
GFP	Green fluorescent protein

GTP	Guanosine triphosphate
HBSS	Hank's balanced salt solution
HEPES	2-(4-(2-Hydroxyethyl)- 1-piperazinyl)-ethansulfonsäure
KCC2	Potassium/chloride co-transporter, member 5
LTD	Long-term depression
LTP	Long-term potentiation
MGE	Medial ganglionic eminence
MHC	Major histocompatibility complex
mEPSC	Miniature excitatory postsynaptic currents
mIPSC	Miniature inhibitory postsynaptic currents
NA	Numerical aperture
NCAM	Neural cell adhesion molecule
NeuN	Neuronal nuclei
NL-1	Neuroligin-1
NL-2	Neuroligin-2
NMDA	N-Methyl-D-aspartic acid
Nrg1	Neuregulin 1
PBS	Phosphate buffered saline
PCR	Polymerase chain reaction
PFA	Paraformaldehyde
Plk2	Polo-like kinase 2
PSA	Polysialic acid
PSD	Postsynaptic density
PSD-95	Postsynaptic density protein 95
PTV	Piccolo transport vesicles
PVP	Polyvinylpyrollidone
s.d.	Standard deviation
STV	Synaptic transport vesicles
TNFα	Tumor necrosis factor α
TTX	Tetrodotoxin

UB	Human ubiquitin C promoter
v/v	Volume per volume
VGAT	Vesicular GABA transporter
VGLUT	Vesicular glutamate transporter
VIP	Vasoactive intestinal peptide
w/v	Weight per volume

Introduction

The brain achieves incredibly complex tasks every minute of the day. It is responsible for steering the organism through its environment and adapting its behavior to changes in that environment. Neuronal processes such as learning and memory mediate these functions. The complex and specific connections between the neurons of the brain - their synapses - are considered to be essential for these processes: Synaptic specificity and strength determine which neurons can activate each other, and how strong this activation will be. This precise connectivity is believed to form the physiological correlate of memory. Consequently, the formation of new memories – learning – must involve modifications of synaptic connections. Biological processes that result in such changes in network connectivity or that change synaptic strength are termed synaptic plasticity.

While the bulk (~ 80 %) of central neurons is excitatory (Hendry et al., 1987), key network functions rely on proper synaptic inhibition. Inhibition is for instance required to balance overall network excitation, to control neuronal integration, and is thought to underlie neuronal oscillations, which serve complex tasks including perception and memory (Buzsaki et al., 1992; Pouille and Scanziani, 2001; Chattopadhyaya and Cristo, 2012). Consequently, malfunctions of the inhibitory system have been linked to severe neurological disorders such as schizophrenia, autism spectrum disorders, and epilepsy (Baulac et al., 2001; Ma et al., 2005; Craddock et al., 2010; Rossignol, 2011; Yizhar et al., 2011; Chattopadhyaya and Cristo, 2012).

Understanding synapse formation and plasticity of both the excitatory and the inhibitory system are therefore necessary to understand brain function in health and disease. The present study is focused on the plasticity of inhibitory synapses, a subject which has gained more and more attention in recent years.

1. Synapse formation

1.1 The structure of synapses

Neurons communicate by means of synapses. The majority of these synapses are so-called chemical synapses. Chemical synapses typically comprise a presynaptic varicosity, a postsynaptic specialization, and a synaptic cleft between pre- and postsynapse. In response to an electrical signal, a chemical neurotransmitter is released from the presynapse. Following neurotransmitter-binding to receptors in the postsynaptic membrane, a postsynaptic potential is generated and further processed at the soma of the postsynaptic cell.

Depending on their mode of action, chemical synapses can be classified as excitatory, inhibitory, or modulatory. In the mature mammalian central nervous system, glutamatergic synapses make up the bulk of excitatory synapses, while GABAergic synapses account for the majority of inhibitory neurotransmission (Curtis et al., 1970; Iversen et al., 1971). In addition, glycine is a major inhibitory neurotransmitter in the brain stem and the spinal cord (Curtis et al., 1968a; Curtis et al., 1968b). Well-known modulatory neurotransmitters include dopamine and acetylcholine.

The presynaptic site is characterized by an axonal varicosity, very often along the length of the axon, an *en passant* bouton. Ultrastructurally, that part of the presynaptic bouton which is directly opposed to the postsynaptic specialization contains an electron dense network of proteins, the cytomatrix of the active zone, and neurotransmitter-filled synaptic vesicles (Gray, 1963). Except for the type of neurotransmitter used, presynaptic sites of excitatory and inhibitory synapses are believed to have a similar molecular composition (Garner et al., 2006). Synaptic vesicles are filled with neurotransmitters by vesicular transporters. In excitatory, glutamatergic neurons, this task is achieved by the vesicular glutamate transporter (VGLUT) (Bellocchio et al., 2000; Takamori et al., 2000). In inhibitory, GABAergic neurons the vesicular GABA transporter (VGAT) fills the synaptic vesicles (McIntire et al., 1997). As a proteinogenic amino acid, glutamate is abundant in all cells, including neurons. GABA however is unique to GABAergic neurons. It needs to be synthesized from glutamate by the two forms of the glutamic acid decarboxylase (GAD) (Roberts and Frankel, 1950, 1951). The bulk of GABA is synthesized by GAD67, which is associated with cytosolic GABA stores. GAD65, on the other hand, is associated with presynaptic terminals (Soghomonian and Martin, 1998).

The active zone is a dense mesh of proteins that provides a structural grid for presynaptic components, or assists in synaptic vesicle fusion with the synaptic membrane, or is necessary for synaptic vesicle endocytosis. Structural proteins found in the active

zone include the large proteins piccolo and bassoon (Richter et al., 1999; Garner et al., 2000). Proteins like synaptotagmin, Vamp, and Snap-25 are involved in synaptic vesicle exocytosis (Sudhof and Rizo, 2011), and proteins like clathrin and dynamin mediate synaptic vesicle endocytosis (Royle and Lagnado, 2010).

The space between pre- and postsynapse is termed the synaptic cleft. It is bridged by a variety of transsynaptic adhesion proteins, some of which are specific for excitatory or inhibitory synapses. On the one hand, homomeric Syncam pairs, as well as EphrinB - EphB, and Neuroligin-1 (NL-1) - neurexin β pairs localize preferentially to excitatory synapses (Song et al., 1999; Dalva et al., 2007). Neuroligin-2 (NL-2) - neurexin α/β pairs, on the other hand, are found rather at inhibitory synapses and the same holds true for the dystrophin-glycoprotein complex (Patrizi et al., 2008; Sassoe-Pognetto et al., 2011).

The postsynaptic specialization of excitatory synapses typically is a dendritic spine with a postsynaptic density containing the neurotransmitter receptors at the bulbous head of the spine. Molecularly, the postsynaptic density is characterized by a protein scaffold, through which neurotransmitter receptors are anchored in the membrane, and through which a connection to the cytoskeleton is maintained. The most well-known constituent of this scaffolding matrix in glutamatergic synapses is PSD-95, a member of the membrane-associated guanylate kinase (MAGUK) family of proteins (Cho et al., 1992). Neurotransmitter receptors found in this type of synapse are AMPA and NMDA receptors - glutamatergic, ionotropic receptors. PSD-95 can directly bind glutamatergic receptors. Therefore, the amount of PSD-95 at a synapse is correlated with the strength of the postsynaptic response (Xu, 2011).

By contrast, inhibitory synapses are formed directly onto the dendritic shaft (Harris and Kater, 1994; Megias et al., 2001; Wierenga et al., 2008). GABAergic postsynaptic specializations are characterized by a scaffold of gephyrin molecules (Pfeiffer et al., 1982; Sassoe-Pognetto et al., 1995). Based on a dimerization and a trimerization domain, gephyrin molecules are thought to form a hexagonal lattice in the postsynaptic density (Saiyed et al., 2007; Fritschy et al., 2008). Other components of the postsynaptic density of GABAergic synapses include collybistin, a molecule binding both to gephyrin and to $GABA_A$ receptors, the intracellular part of the dystrophin-glycoprotein complex (DSG), and S-SCAM/MAGI-2 (Sassoe-Pognetto et al., 2011). $GABA_A$ receptors are the major ionotropic GABA receptor and are found at most GABAergic synapses. $GABA_A$ receptors are heteropentameric receptors typically comprising two α-, two β-, and one γ- or δ-subunits (McKernan and Whiting, 1996). Multiple different isoforms have been described for α-, β-, and γ- subunits, equipping the receptor with different functional

attributes (such as kinetics, sensitivity, channel open and close time, etc.) (Owens and Kriegstein, 2002; Luscher et al., 2011). In total, about 26 different functional receptor isoforms are known to be assembled from the subunits, eleven of which are expressed broadly in the nervous system (Luscher et al., 2011). Each receptor subunit has four transmembrane domains, an extracellular N-terminus, and a large intracellular loop between the third and fourth transmembrane domain. This loop is subject to various post-translational and activity-dependent modifications such as phosphorylation, palmitoylation, and ubiquitination, and seems to be the major site for regulating receptor function and receptor residence time in the membrane (Rudolph and Mohler, 2004; Tretter and Moss, 2008). $GABA_A$ receptors are inserted into the postsynaptic membrane at extrasynaptic sites and rapidly enter the postsynaptic specialization via lateral diffusion (Thomas et al., 2005). In the postsynaptic specialization, diffusion kinetics are much slower, suggesting that the receptors are interacting with parts of the postsynaptic density matrix (Jacob et al., 2005), such as gephyrin and collybistin. $GABA_A$ receptors are internalized from the postsynaptic membrane via clathrin mediated endocytosis, and can be recycled back into the membrane or be subjected to lysosomal degradation (Kittler et al., 2004; Tretter and Moss, 2008) (Figure 1).

In the case of an action potential in the inhibitory axon, the Ca^{2+} concentration in the presynaptic bouton is increased through opening of voltage-gated Ca^{2+}-channels and Ca^{2+} release from intracellular stores. Ca^{2+} then facilitates fusion of GABA-filled vesicles with the presynaptic membrane and the release of GABA into the synaptic cleft. The released GABA binds to postsynaptic $GABA_A$ receptors and causes these chloride channels to open. In mature neurons, the equilibrium potential of chloride is typically more negative than the resting membrane potential. The opening of $GABA_A$ receptors therefore leads to an influx of chloride and a hyperpolarization of the postsynaptic neurons (inhibitory postsynaptic potential, IPSP).

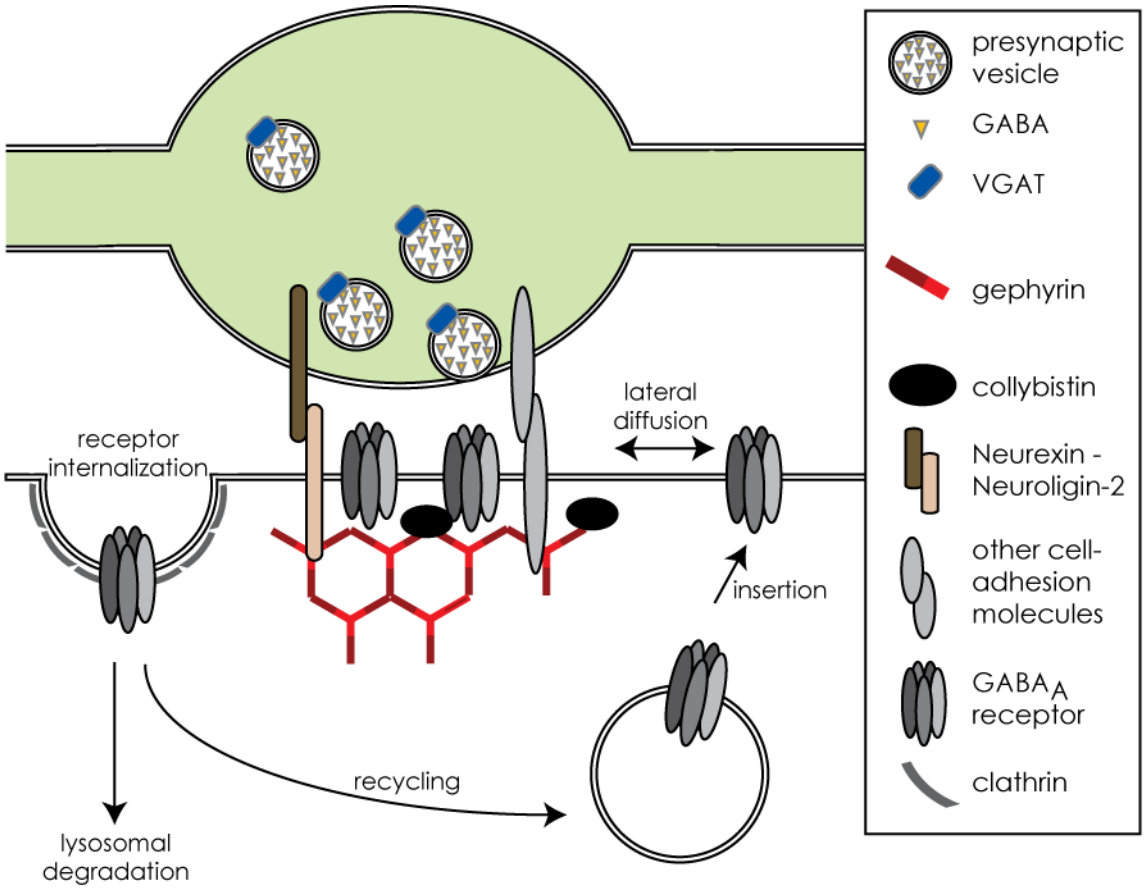

Figure 1 - Schematic drawing of a GABAergic synapse. The presynaptic bouton (green) contains GABA filled vesicles. The vesicular GABA transporter VGAT (blue) fills the vesicles with GABA. The synaptic cleft is bridged by cell adhesion molecules, for instance pairs of neurexin and neuroligin-2. The main receptor type in the postsynaptic specialization is the $GABA_A$ receptor. The postsynaptic specialization is furthermore characterized by the structural protein gephyrin (red) and collybistin, which binds both $GABA_A$ receptors and gephyrin. $GABA_A$ receptors are inserted into the extrasynaptic membrane, from where they are also endocytosed via clathrin-mediated endocytosis.

1.2 The development of GABAergic interneurons

In order to process information adequately and not fall prey to runaway excitation or quiescence, neuronal activity in a network needs to be controlled precisely. This task is typically realized by the concerted action of many different types of GABAergic interneurons, which accurately control neuronal activity. In addition to highly divergent functional properties, different types of GABAergic interneurons also target very specific postsynaptic cells, or even selected cellular compartments (Somogyi and Klausberger, 2005; Klausberger and Somogyi, 2008). The development of such specific innervation patterns must require a tightly organized process.

Most GABAergic interneurons are generated in the ventral telencephalon, or, more specifically, in either the medial or the caudal ganglionic eminence (MGE or CGE, respectively) (Wonders and Anderson, 2006). Already the place of birth defines different GABAergic subtypes, owing to the differential expression of transcription factors and gradients of signaling molecules. The MGE for instance gives rise to parvalbumin and somatostatin/calretinin positive interneurons, while CGE derived interneurons express calretinin, the vasoactive intestinal peptide (VIP), or cholecystokinin (Butt et al., 2005; Fogarty et al., 2007; Liodis et al., 2007). GABAergic interneurons that are labeled in the current study mostly belong to the latter family (Wierenga et al., 2010) (Figure 2). Interneurons then migrate tangentially to the cortex, into which they subsequently migrate in a radial fashion (Ang et al., 2003). The process of migration into the cortex appears to be enhanced by GABA signaling via $GABA_A$Rs (Cuzon et al., 2006; Bortone and Polleux, 2009).

Once in their target region, axons need to establish contact to their postsynaptic target cells and finally form *bona fide* synapses with often very high specificity. While dendritic filopodia are believed to mediate contact between excitatory axons and most of their target dendrites (Ziv and Smith, 1996; Yuste and Bonhoeffer, 2004), neither dendritic nor axonal protrusions are involved in the formation of inhibitory synapses (Wierenga et al., 2008). Neither GABAergic axons nor postsynaptic target dendrites can use filopodia or spines to bridge the space to further-away targets. Therefore, only those axonal spots that are in close apposition to postsynaptic dendrites can be used as presynaptic sites by GABAergic neurons. Remarkably, axonal spots specialized for synapse formation even exist in glutamatergic synapses: synapses preferentially form at locations on glutamatergic axons, where synaptic transport vesicles frequently stop, and where vesicles might cycle with the axonal membrane (Sabo et al., 2006; Antonova et al., 2009). The existence of such specialized axonal domains is an intriguing concept for synapse formation.

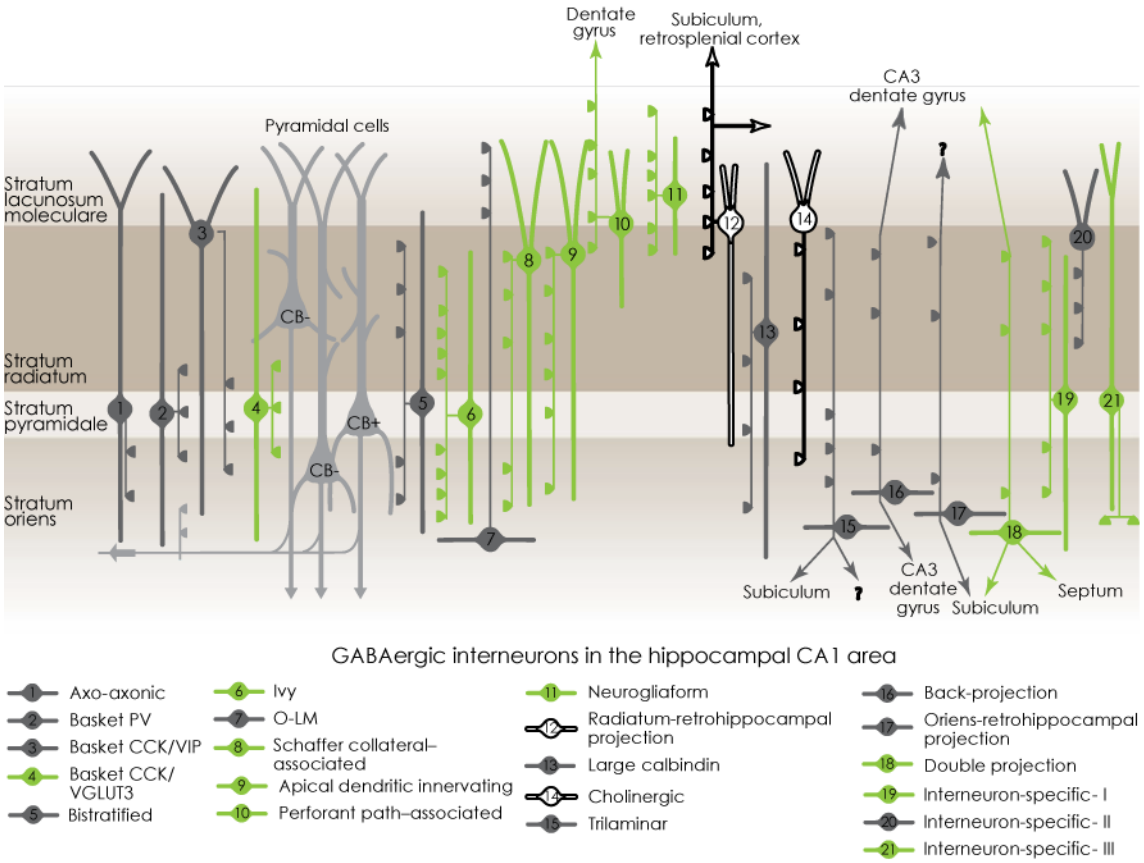

Figure 2 - GABAergic interneurons in hippocampal CA1. At least 21 different types of interneurons have been identified in the CA1 area of the hippocampus. In GAD65-GFP mice, mostly dendritically targeting interneurons are labeled with GFP (green). Cell populations that are largely un-labeled in GAD65-GFP mice are filled with a dark grey color, those populations that could not be assigned to GAD65-GFP mice positive or negative phenotypes based on current literature are filled white. Pyramidal cells were given a light grey coloring. *Adapted from Klausberger et Somogyi (Science, 2008).*

Interestingly, the cellular architecture of GABAergic axons differs significantly from axons of glutamatergic pyramidal cells. While glutamatergic axons cross the tissue in a rather straight fashion, seemingly "unaware" of potential synaptic targets, GABAergic axons are much more tortuous (Stepanyants et al., 2004), maybe reflecting target-guided growth. Furthermore, overlaying the anatomy of GABAergic axons with their target cells shows significantly more overlay than the same method applied to pyramidal cells (Stepanyants et al., 2004). Because inhibitory synapses are usually formed on the dendritic shaft, dendritic spines or axonal filopodia cannot "bridge" between the axon and the target dendrite. A geometrical wiring as described for GABAergic axons above might compensate for the lack of spines by creating as many contacts with potential target cells as possible. The interneuron might then activate these potential synaptic sites by the formation of a new synapse, whenever the situation in the neuronal network requires it.

1.3 The development of GABAergic synapses

The astounding target specificity of inhibitory synapses is thought to be achieved by a combination of molecular clues. Cell adhesion molecules, secreted, and extracellular factors have been implied in synaptogenesis and synapse maturation. Recently, the list of molecules promoting predominantly inhibitory synapse formation and maturation has grown considerably.

The probably most well-known transsynaptic pair of adhesion molecules is neuroligin (NL) and neurexin. While NL-1 and its interaction with beta neurexins are predominantly found at excitatory synapses, NL-2 is found mainly in inhibitory postsynaptic sites. NL-2 can establish heterophilic interactions with both alpha- and beta-neurexins in the presynaptic membrane (Song et al., 1999; Graf et al., 2004; Varoqueaux et al., 2004; Chubykin et al., 2007). Nonetheless, both NL-1 and NL-2 can promote the formation of inhibitory synapses. The effect of NL-2, however, is much stronger than that of NL-1 (Dong et al., 2007). The family of neurexins is a potential candidate for mediating very specific interactions (such as defining target cell-types or regions), because they can undergo extensive alternative splicing. More than 1000 neurexin isoforms can arise through such alternative splicing, and the expression of different neurexin isoforms has been shown to be variable across brain regions (Ullrich et al., 1995). Other pairs of trans-synaptic adhesion and signaling molecules specific for GABAergic synapses include Slitrk3 (postsynapse) and PTPδ (presynapse) (Takahashi et al., 2012), as well as Nrg1 (diffusible) and ErbB4 (presynapse) (Fazzari et al., 2010). In addition, NCAM seems to promote GABAergic synapse formation. This effect can be regulated by PSA (Di Cristo et al., 2007). Secreted factors such as the brain-derived neurotrophic factor (BDNF) and the fibroblast growth factor 7 (FGF7) also seem to play an important role in the formation and/or functional maturation of GABAergic synapses (Umemori et al., 2004; Hong et al., 2008; Terauchi et al., 2010). Moreover, Sema4D, a membrane-bound member of the semaphorin family was shown to specifically enhance the formation of GABAergic synapses, primarily by acting on the postsynaptic specialization (Paradis et al., 2007).

Finally, neurotransmitters themselves appear to influence synapse formation. The excitatory neurotransmitter glutamate, for instance, can elicit the formation of new and functional spines following focal uncaging in the immediate vicinity of a postsynaptic dendrite (Kwon and Sabatini, 2011), and has furthermore been shown to regulate synapse formation in the mouse retina (Kerschensteiner et al., 2009). As glutamate release can lead to calcium influx via NMDA-type glutamate receptors, these effects are often explained by the role of calcium as a second messenger, activating calcium-sensitive enzymes, like protein kinase A or CaMKII (Kwon and Sabatini, 2011). GABA mainly acts through

$GABA_A$ receptors, which pass chloride ions, and those have not been associated with any second messenger functions so far. Nonetheless, many studies argue for a role of GABA release in GABAergic synaptogenesis. These studies should be separated into those investigating the role of GABA in early nervous system development, when GABA still acts as an excitatory neurotransmitter, and those exploring later phases of synaptogenesis, when GABA has resumed its classical role as an inhibitory neurotransmitter.

Until early postnatal development, GABA acts as an excitatory neurotransmitter, due to a more positive chloride reversal potential in immature neurons (Chen et al., 1996; Owens et al., 1996; Rivera et al., 1999). In this mode of operation, GABA can excite postsynaptic neurons, and cause calcium influx. Calcium-mediated signaling pathways and BDNF release have been shown to halt neuronal proliferation and induce differentiation (Berninger et al., 1995; LoTurco et al., 1995; Maric et al., 2001).

But the effect of GABA on interneuron development and synaptogenesis exceeds these early developmental periods. For instance, it has been shown that GABA signaling is required for successful development of perisomatic GABAergic innervation (Chattopadhyaya et al., 2007). Reducing GABA levels by a conditional knockout of the rate-limiting enzyme for GABA synthesis, GAD67, in individual cells, strongly reduced formation of synapses and axon branching of the affected cells. Recent work has added to these findings. A study in which a complete knockout of GABA synthesis was used, led to the interpretation that GABAergic signaling does not promote synapse formation per se, but rather induces elimination of nascent contacts (Wu et al., 2012). Consequently, GABAergic signaling in development is now believed to work as a "proofreading" mechanism, stabilizing some synapses and eliminating others. In addition, $GABA_A$ receptors seem to be involved in the stabilization of a subset of inhibitory synapses, as has been demonstrated by restraining cerebellar Purkinje cells from expressing $GABA_A$ receptors (Fritschy et al., 2006) and by preventing $GABA_A$ receptor clustering in hippocampal neurons (Li et al., 2005). These findings could indicate a role for trans-synaptic GABA signaling in the stabilization of inhibitory contacts.

After successful contact formation, contacts mature into fully functional synapses through a process involving the recruitment of synaptic proteins to the nascent contact sites. It has been suggested, that during these processes, the formation of the presynapse precedes that of the postsynapse (Friedman et al., 2000; Dobie and Craig, 2011).

Different mechanisms govern the accumulation of pre- and postsynaptic material. It has been suggested, that presynaptic material accumulates in a quantal fashion, by the recruitment of transport packets containing synaptic vesicles and proteins

(Shapira et al., 2003). Two different transport entities have been described in glutamatergic axons: (a) piccolo transport vesicles (PTVs), containing components of the active zone, such as piccolo and bassoon (Zhai et al., 2001; Shapira et al., 2003), and (b) synaptic transport vesicles (STVs), containing for instance calcium channels and synaptic vesicles (Ahmari et al., 2000). Given the high similarity of glutamatergic and GABAergic presynaptic terminals (Garner et al., 2006) as well as a demonstrated co-localization of GABA receptors and bassoon (Zhai et al., 2000), one can speculate that similar arrangements are present in GABAergic axons, too. In contrast to presynaptic specializations, the postsynaptic site appears to assemble by gradual recruitment of its components (Bresler et al., 2004).

The recruitment of synaptic proteins to pre- and postsynaptic sites likely depends on molecular tags that attract transport packets or individual molecules traveling along the axon to these sites. So far the nature of these tags has not been investigated in GABAergic axons. However, similar processes have been described in glutamatergic axons: Sites along excitatory axons at which synapses are preferentially formed, might contain intrinsic local signals such as adhesion molecules, second messengers (e.g. Ca^{2+}, cAMP), or activated enzymes that define these sites (Sabo et al., 2006; Bury and Sabo, 2011) and attract transport vesicles with synaptic proteins. A wealth of proteins have been certified a role in presynaptic terminal assembly (e.g. CASK, syntenin, RIM, piccolo and bassoon), however, none of them was found to be essential for synapse formation (Bury and Sabo, 2010). This leads to the hypothesis that for presynaptic terminal formation, presynaptic material might make use of their capacity to self-assemble (Klassen et al., 2010), without necessitating the involvement of a "master-organizer" (Bury and Sabo, 2010). It might be possible to expand this concept from glutamatergic to GABAergic presynaptic terminals.

Studies investigating the assembly of GABAergic postsynaptic specializations have mostly focused on dynamics and clustering of the $GABA_A$ receptor (Luscher et al., 2011). In GABAergic axons, $GABA_A$ receptors can be found as synaptic clusters and as an extrasynaptic, diffuse population (Jacob et al., 2005). There is constant exchange between these two receptor pools (Jacob et al., 2005; Thomas et al., 2005). $GABA_A$ receptors are believed to accumulate at postsynaptic sites because of their interactions with gephyrin and other scaffolding proteins in the inhibitory postsynaptic density (Essrich et al., 1998; Kneussel et al., 1999; Jacob et al., 2005). Collybistin has also been shown to be required for $GABA_A$ receptor clustering in the postsynaptic membrane, an effect that might rely on the mutual interaction of $GABA_A$ receptors and collybistin with gephyrin (Papadopoulos et al., 2007). Furthermore, neurexins have been reported to induce clustering of $GABA_A$

receptors, as have other cell adhesion molecules (see previous sections). What mechanisms these adhesion molecules employ to induce synapse formation, however, is far from clear.

It seems conceivable that mature neurons might generate new synapses by employing mechanisms which resemble those described for developing neurons. However, in addition to the de novo recruitment of pre- and postsynaptic proteins described above, another mechanism of synapse formation has been reported, too. It was shown that release-competent fragments of presynaptic specializations could be liberated from an existing terminal to form new functional synapses (Krueger et al., 2003). Formation of new synapses in mature neuronal networks is an aspect of synaptic plasticity which will be discussed in further detail below.

2. Plasticity of GABAergic synapses

Generally, synaptic plasticity is understood as "[…] the ability of individual synaptic junctions to respond to use and disuse by appropriate changes in transmissive efficacy […]" (Eccles and McIntyre, 1951). The term includes any activity-induced changes in synaptic transmission, lasting from seconds to years, involving structural or only functional changes, and affecting the pre- or the postsynapse. Synaptic plasticity is a prerequisite for learning and memory, two fundamental features of complex nervous systems. Therefore, synaptic plasticity is an important field of neuroscience research. Over the past years, various types of plasticity have been identified primarily for excitatory (glutamatergic) synapses. Jointly with the recently increased awareness of the vital role of inhibition in neuronal network function, attention has been given to plasticity mechanisms in inhibitory (GABAergic) synapses, too.

2.1 GABAergic plasticity during development

Although synapse formation per se seems independent of neuronal activity (Verhage et al., 2000; Varoqueaux et al., 2002; Harms and Craig, 2005), many processes during synapse development can be influenced by neuronal activity. As far as GABAergic synapses are concerned, these phenomena should be separated into (a) an early, mostly embryonic and early postnatal period, where GABA still acts as an excitatory neurotransmitter, and (b) later developmental stages – such as critical periods of certain sensory systems – where the nervous system continues to develop or mature, but GABA has resumed its classical role as an inhibitory transmitter.

2.1.1 GABAergic plasticity in early development

Several examples illustrate that proper development and function of GABAergic synapses is influenced by neuronal activity or neurotransmitter release in early development. Activity-dependent transcription of the neurotrophin BDNF has been shown to play an important role in the development of GABAergic synapses (Hong et al., 2008; Jiao et al., 2011). Introducing a mutation into the BDNF gene that blocks its activity-dependent transcription decreased the number of inhibitory synapses in these mice. This result highlights the important role that neuronal activity plays in the development of inhibitory synapses (Hong et al., 2008). Furthermore, the developmental switch of GABA function itself appears to be induced by neuronal activity and/or GABA release and signaling. The developmental switch is characterized by an upregulation of KCC2

expression – a potassium-chloride co-transporter which maintains a low intracellular chloride concentration and allows for the inhibitory action of GABA. The initiation of this change in KCC2 expression levels can be prevented by the addition of $GABA_A$ receptor antagonists or induced prematurely by increasing activity (Ganguly et al., 2001; Leitch et al., 2005). BDNF might be involved in these processes, too (Carmona et al., 2006). However, not all groups find this relationship between neuronal activity and the switch in GABA function, indicating differences in experimental systems and/or preparations (Ludwig et al., 2003).

2.1.2 GABAergic plasticity during network maturation

Later in development, when connections are mostly being refined, the role of neurotransmission and neuronal activity becomes increasingly important for the precise regulation of synaptic connectivity and for establishing proper network function.

It has been shown that the maturation of a certain population of GABAergic synapses is an essential factor for critical period plasticity, for instance in the mouse or cat visual system. Reducing perisomatic GABAergic inhibition (brought about by fast-spiking basket cells) prevents the onset of ocular dominance plasticity, which is a hallmark of the critical period for experience-dependent plasticity in the visual system (Hensch et al., 1998). Visual experience has been shown to be indispensable for the maturation of this form of GABAergic inhibition, and therefore critical period plasticity (Morales et al., 2002). Blocking activity in slice cultures furthermore suggests that the role of visual experience might be to increase neuronal activity and GABA release in the system (Chattopadhyaya et al., 2004).

In the tadpole, research has demonstrated the influence of neuronal activity on the refinement of circuits, too. Matching receptive fields of excitatory and inhibitory neurons, for instance, depends on the correct level of GABAergic inhibition (Tao and Poo, 2005). In addition, visual input can act to stabilize presynaptic puncta in the axons of tadpole retinal ganglion cells (Ruthazer et al., 2006), suggesting an important role for neuronal activity in mediating synaptic plasticity.

2.2 GABAergic plasticity in a developed neuronal network

In a mature neuronal network, plasticity acts to adapt the circuit to changing conditions in the environment. These processes can include learning paradigms or short-term adaptations.

Two forms of long-term plasticity work hand in hand to ensure proper function of the nervous system, so-called Hebbian plasticity and homeostatic plasticity. Hebbian plasticity mechanisms strengthen synapses between simultaneously active neurons and weaken those between asynchronously active neurons (Hebb, 1949; Bliss and Lomo, 1973). However, exclusive application of this learning mechanism would ultimately drive a network "towards runaway excitation or quiescence" (Turrigiano and Nelson, 2004), which would hamper the flow of information within the network (Miller, 1996; Turrigiano, 1999). Such cases illustrate the importance of homeostatic plasticity, which restrains neuronal activity in a network to certain limits. Homeostatic plasticity is typically understood as a form of plasticity "that acts to stabilize the activity of a neuron or neuronal circuit in the face of perturbations […] that alter excitability"(Turrigiano, 2008).

2.2.1 Hebbian plasticity

Long-term potentiation (LTP) and long-term depression (LTD) are the two phenomena that are typically understood as Hebbian plasticity. LTP strengthens synapses between those cells that are active together, while LTD weakens those whose activity is not coordinated. Neither LTP nor LTD are mechanistically uniform, and to date different sub-categories of each process employing different molecular pathways have been identified (Citri and Malenka, 2008). Although most research on Hebbian plasticity has focused on excitatory synapses, some publications demonstrate that such mechanisms also exist at inhibitory synapses. In some cases, Hebbian plasticity at excitatory and inhibitory synapses appears to occur concurrently and modify the synapses in opposite directions (i.e. in the same system LTP at excitatory synapses is paralleled by LTD at inhibitory synapses). In the hippocampus, such a relationship has been demonstrated at several sites: high-frequency stimulation of mossy fibers, for instance, induced LTP of mossy fiber boutons (contacting excitatory cells) and LTD of neighboring mossy fiber filopodia (contacting inhibitory cells) (Pelkey and McBain, 2008). Furthermore, high-frequency stimulation in CA3 induced LTP at synapses onto pyramidal cells and LTD at synapses onto interneurons (Gibson et al., 2008; McBain and Kauer, 2009). Moreover, this experiment provides evidence for the intriguing concept that synapses made by the same axon can be regulated very differently depending on their postsynaptic target.

While the most well-known form of Hebbian plasticity at excitatory synapses – NMDA receptor dependent LTP and LTD – is accomplished by a regulation of the amount of AMPA-type glutamate receptors in the postsynaptic membrane, Hebbian plasticity at inhibitory synapses has been reported to be mediated by local changes in

KCC2 expression. KCC2 regulates the intracellular chloride concentration: A high KCC2 expression would yield a low intracellular chloride concentration, thereby increasing the driving force for chloride and upregulating the level of inhibition. A low KCC2 expression would have the opposite effect. Local changes of KCC2 expression can therefor regulate the strength of inhibition at a subcellular level. This effect seems to rely on calcium influx through either voltage-gated calcium channels (Woodin et al., 2003) or NMDA receptors (Lee et al., 2011). As BDNF can regulate KCC2 expression both in development and during plasticity paradigms in mature networks, it might induce Hebbian plasticity at GABAergic synapses in a similar way as described above (Rivera et al., 2002; Rivera et al., 2004; Fiumelli and Woodin, 2007).

Other forms of long-term, "Hebbian", plasticity at GABAergic synapses include endocannabinoid-dependent LTD and NMDA receptor-dependent LTP of GABAergic synapses. Endocannabinoid-dependent LTD of GABAergic synapses has been demonstrated in the hippocampus, where it is induced by high-frequency stimulation. This effect is initiated by the release of endocannabinoids from the postsynapse that activate the cannabinoid receptors 1 at the GABAergic presynapse. Activation of these receptors inactivates protein kinase A and activates the phosphatase calcineurin, thereby reducing GABA release (Chevaleyre et al., 2007; Heifets et al., 2008). Induction of endocannabinoid-dependent LTD furthermore requires the activation of metabotropic glutamate receptors, and therefore does not solely rely on GABAergic synapses (Castillo et al., 2011).

NMDA receptor dependent LTP of GABAergic synapses has been demonstrated following a stimulus which is known to result in LTD of excitatory synapses - mild activation of NMDA receptors. The surface expression of $GABA_A$ receptors was increased under these conditions, which led to a strengthening of inhibition. This effect required the activation of CaMKII and the $GABA_A$ receptor trafficking protein GABARAP (Marsden et al., 2007).

2.2.2 *Homeostatic plasticity*

Homeostatic plasticity is an important mechanism when it comes to restraining network activity to a working range. It was first described for excitatory synapses (Turrigiano et al., 1998), but has soon been expanded to inhibitory synapses, as well (Kilman et al., 2002). Interestingly, also homeostatic plasticity has been suggested to occur simultaneously at both excitatory and inhibitory synapses within the same system. Just as described for Hebbian plasticity, homeostatic plasticity of excitatory and inhibitory

synapses occurred simultaneously and regulated excitatory and inhibitory synapses in opposite directions (Kilman et al., 2002; De Gois et al., 2005; Swanwick et al., 2006).

Typically, homeostatic plasticity is understood as a scaling mechanism that uniformly scales the strength of all synapses up or down, thereby preserving individual synaptic weights and the information stored through these. Such scaling has been shown to occur network-wide (Rutherford et al., 1998; Stellwagen and Malenka, 2006), as well as restricted to a small area within the network, or even cell-autonomously (Turrigiano and Nelson, 2004; Sutton et al., 2006; Hou et al., 2008).

Several molecules and other determinants have been suggested to play a role in the induction of homeostatic plasticity. As far as neuronal activity is concerned, postsynaptic spiking appears to be sufficient for the induction of homeostatic plasticity (Ibata et al., 2008). A wide range of molecules were suggested to be involved in homeostatic plasticity. These include the secreted factors BDNF (Rutherford et al., 1998), and TNFα (a cytokine) (Stellwagen and Malenka, 2006; Kaneko et al., 2008), the transmembrane proteins β3-integrin (Cingolani and Goda, 2008) and MHC1 (an antigen presenting protein, mostly known for its functions in the immune system) (Goddard et al., 2007), as well as the cytoplasmic proteins CaMKIV (Thiagarajan et al., 2002; Ibata et al., 2008), Arc (a member of the family of immediate early genes) (Rial Verde et al., 2006; Shepherd et al., 2006), Plk2 and CDK5 (Seeburg et al., 2008). The expression locus of homeostatic plasticity can be both presynaptic and postsynaptic, involving changes in release probability (Burrone et al., 2002; Wierenga et al., 2006; Tokuoka and Goda, 2008) and postsynaptic receptor density (Turrigiano, 2007; Rannals and Kapur, 2011).

Several components of inhibitory synapses have been shown to be regulated by homeostatic plasticity mechanisms, most prominently $GABA_A$ receptors. Prior to their insertion into the plasma membrane, $GABA_A$ receptors are assembled from individual subunits in the endoplasmatic reticulum (ER). Here, $GABA_A$ receptors can get targeted for ER-associated degradation, a process which is mediated by the ubiquitin-proteasome system. Targeting for this pathway (or ubiquitination of the receptors) was upregulated following a 24 h reduction in network activity, and resulted in decreased surface expression of $GABA_A$ receptors, and consequently reduced the strength of inhibitory transmission (Saliba et al., 2007). This mechanism was shown to rely on the activation of voltage-gated calcium channels (Saliba et al., 2009). Furthermore, 48 h of increased network activity (induced by a high-potassium medium) was shown to increase the size of $GABA_A$ receptor clusters in the postsynaptic membrane, as well as mIPSC amplitude and frequency. This effect seemed to be caused by a reduced internalization of the receptors (Rannals and Kapur, 2011).

But also other components of GABAergic synapses are subject to homeostatic regulation. Blocking network activity for two days with TTX for instance, reduced GABA levels, as shown by a reduction in GAD67, GAD65, and GABA immunoreactivity. Conversely, enhancing network activity for two days with picrotoxin increased neuronal GABA-levels (Lau and Murthy, 2012). Similarly, another study found a decrease in VGAT levels, following two days of TTX treatment. Again, enhancing activity for two days (in this case with bicuculline) increased VGAT levels (De Gois et al., 2005). Interestingly, this study also found an opposite regulation of inhibitory synapses (identified by VGAT staining) and excitatory synapses (identified by VGLUT staining), following the same paradigm. In line with these findings, a third study could observe a reduction in the size of axonal varicosities and a decrease in the motility of postsynaptic gephyrin clusters following 48 h treatment with TTX. This study, too, observed a reduction in mIPSC amplitude and frequency (Kuriu et al., 2011).

Together, these studies demonstrate a regulation of GABAergic synapses in response to homeostatic plasticity paradigms. Again, different (molecular) mechanisms might exist that produce similar phenomena of homeostatic plasticity, depending on the specific experimental conditions used.

2.3 Structural plasticity

While short-term plasticity mechanisms include changes in the probability of presynaptic neurotransmitter release or postsynaptic receptor responsiveness, many long-lasting plasticity mechanisms necessitate hard-wired modifications of neuronal connectivity. These can range from the strengthening or weakening of existing synapses, a phenomenon tightly linked to synaptic size (Matsuzaki et al., 2001; Weyhersmuller et al., 2011), over the formation or elimination of synapses to – more rarely – the remodeling of entire neurites. All these phenomena are combined in the term “structural plasticity”.

2.3.1 Structural plasticity of excitatory synapses

In recent years, structural plasticity of excitatory synapses has been studied extensively, probably also because dendritic spines go through impressive structural changes when confronted with plasticity-inducing paradigms such as LTP or LTD (Matsuzaki et al., 2004; Bosch and Hayashi, 2011). It has been shown that the formation of new dendritic spines is associated with the induction of LTP (Engert and Bonhoeffer, 1999), and that Hebbian-type plasticity phenomena seem to be expressed at the level of individual spines (Matsuzaki et al., 2004). In addition, structural correlates have been

described for homeostatic plasticity paradigms. They for instance include increases in synaptic size and transmitter release (Murthy et al., 2001). Furthermore, blocking activity with TTX has been shown to increase the PSD-95 content at excitatory synapses, while increasing activity decreased it (Minerbi et al., 2009).

Experiments *in vivo* furthermore suggest that the formation and elimination of dendritic spines is associated with plasticity paradigms such as sensory deprivation or motor learning tasks. Focal retinal lesions, for instance, induced an enormous turnover of dendritic spines in the lesion projection zone in primary visual cortex (Keck et al., 2008). This phenomenon was suggested to correspond to the re-wiring in this part of cortex: the nervous tissue undertakes new tasks (and therefore needs to be connected differently), because its original tasks have become obsolete due to the lesion in its corresponding part of the retina. Another experiment demonstrated that monocular deprivation (a paradigm where one eye is closed for a couple of days) increased spine formation and density in the binocular visual cortex. Many of these spines were maintained beyond the period of monocular deprivation (Hofer et al., 2009).

Some of the experiments described above, already indicate that absolute spine density and variations of this characteristic factor, might not be the most informative measure for answering some questions about synaptic plasticity. In fact, it seems as if the structural dynamics, reflecting re-wiring of neurons, enclose valuable information about synaptic plasticity. Recent data support this view. Stabilization of dendritic spines was reported to be associated with learning behavior (Xu et al., 2009; Yang et al., 2009), suggesting that maybe not the gain, but rather the remodeling of spines could be considered to be the correlate of learning and memory (Bednarek and Caroni, 2011; Caroni et al., 2012). Interestingly, spines that occur only transiently within an imaging period are typically smaller than those which are stable throughout the period (Holtmaat et al., 2005), suggesting a correlation between the morphology of a spine and its (recent) function.

Besides dendritic spines, axonal boutons exhibit structural plasticity, as well (Holtmaat and Svoboda, 2009). An increase in activity was shown to increase the dynamics (i.e. gain and loss within one day) of axonal boutons in hippocampal slices (De Paola et al., 2003). On an even smaller scale, it has been found that a fraction of transmitter-filled vesicles is not restricted to a particular axonal bouton, but is rather shared between neighboring boutons. Vesicles in this "superpool" are release competent and interestingly, their dynamics can be influenced by BDNF (BDNF application increases dynamics), which has been implicated in a variety of plasticity paradigms (Staras and Branco, 2010; Staras et al., 2010).

2.3.2 *Structural plasticity of inhibitory synapses*

Maybe partially due to the lack of prominent postsynaptic structures like dendritic spines (Figure 3 A), data on structural plasticity of inhibitory synapses is rather scarce. However, it is not less important. In fact, plasticity of inhibitory synapses might even precede and allow for plasticity of excitatory synapses. It has been reported that a loss of sensory input seems to reduce the inhibitory tone, which might allow for the subsequent re-organization of excitatory synapses (Chen et al., 2011; Keck et al., 2011; van Versendaal et al., 2012). In line with these data, structural plasticity of inhibitory synapses following 4 days of monocular deprivation was shown to cluster spatially with plasticity of excitatory synapses, highlighting the significant link between excitatory and inhibitory plasticity (Chen et al., 2012).

As mentioned above, postsynaptic specializations of inhibitory synapses typically do not occupy a prominent structure, such as a spine. Therefore, many studies investigating inhibitory postsynaptic sites make use of markers for the inhibitory postsynaptic site (such as $GABA_A$ receptors or gephyrin) to identify it. Often, also presynaptic markers are used to investigate the effect on GABAergic presynaptic structures in parallel (results summarized in Figure 3).

Already the short-term dynamics of GABAergic synapses (range of several seconds) seem to be affected by neuronal activity. Increasing activity with 4-AP increased the diffusion of individual $GABA_A$ receptors and decreased the fluorescence intensity of individual clusters, suggesting a dispersion of $GABA_A$ receptor clusters. This phenomenon was dependent on calcium influx (Bannai et al., 2009). Another study analyzed the rapid dynamics of gephyrin clusters in response to 4-AP or TTX treatment. Treatment with 4-AP (to enhance neuronal activity) reduced gephyrin dynamics (timescale of seconds), compared to treatment with TTX (to reduce neuronal activity). Interestingly, this effect of 4-AP could be reduced by blocking neurotransmitter receptors (GABAergic or glutamatergic), suggesting that synaptic transmission plays a role in modulating the short-term dynamics of gephyrin clusters at inhibitory postsynaptic sites (Hanus et al., 2006). The results of the latter study seem to be at odds with the aforementioned one. The first study reports enhanced dynamics of components of the GABAergic postsynapse in response to increased network activity, while the second one reports reduced dynamics. Both dynamics are measured over the scale of several seconds. However, the two studies investigate dynamics of very different components of

GABAergic synapses ($GABA_A$ receptors and gephyrin), which might be a possible explanation for this discrepancy.

Several experiments have also demonstrated structural plasticity of inhibitory synapses related to Hebbian plasticity phenomena. First, as a method to mimic LTP, two recent studies have exposed hippocampal slices to oxygen-glucose deprivation. Electron microscopy of the tissue subjected to this treatment, has revealed a growth of both pre- and postsynaptic structures of excitatory synapses (Lushnikova et al., 2009), as well as in an increase of complex inhibitory PSDs within only one hour of the treatment (Lushnikova et al., 2011). The size of the inhibitory PSD was correlated with that of the presynaptic bouton, again highlighting the predictive value of synaptic size of estimations of synaptic strength (Lushnikova et al., 2011). Another study employing electron microscopy could demonstrate an increase of the size of inhibitory synapses paralleled by a decrease in synapse density two hours after the induction of LTP (Bourne and Harris, 2011) in hippocampal slices. LTP inducing paradigms therefore seem to increase the size of GABAergic synapses, while decreasing their density.

In addition, more general manipulations of activity were shown to influence GABAergic synapses. Already after just four hours of elevated network activity, the intensity as well as puncta number in immunocytochemistry staining for VGAT, GAD65, and $GABA_A$ receptors was increased. This effect seemed to depend on BDNF release (Peng et al., 2010) and suggests that neuronal activity mediates both the formation and growth of GABAergic synapses. Furthermore, paradigms used to induce homeostatic plasticity, affected GABAergic synapses. For instance, 48 h of elevated activity have been reported to induce (a) an increase in the size of $GABA_A$ receptor clusters, based on a reduced internalization of $GABA_A$ receptors (Rannals and Kapur, 2011), and (b) an increase in the density of $GABA_A$ receptor or gephyrin clusters (Marty et al., 2004). Conversely, 48 h of decreased neuronal activity decreased the dynamics of postsynaptic gephyrin clusters and simultaneously decreased the size of (presynaptic) axonal varicosities (Kuriu et al., 2011), and the density of $GABA_A$ receptor or gephyrin clusters (Marty et al., 2004).

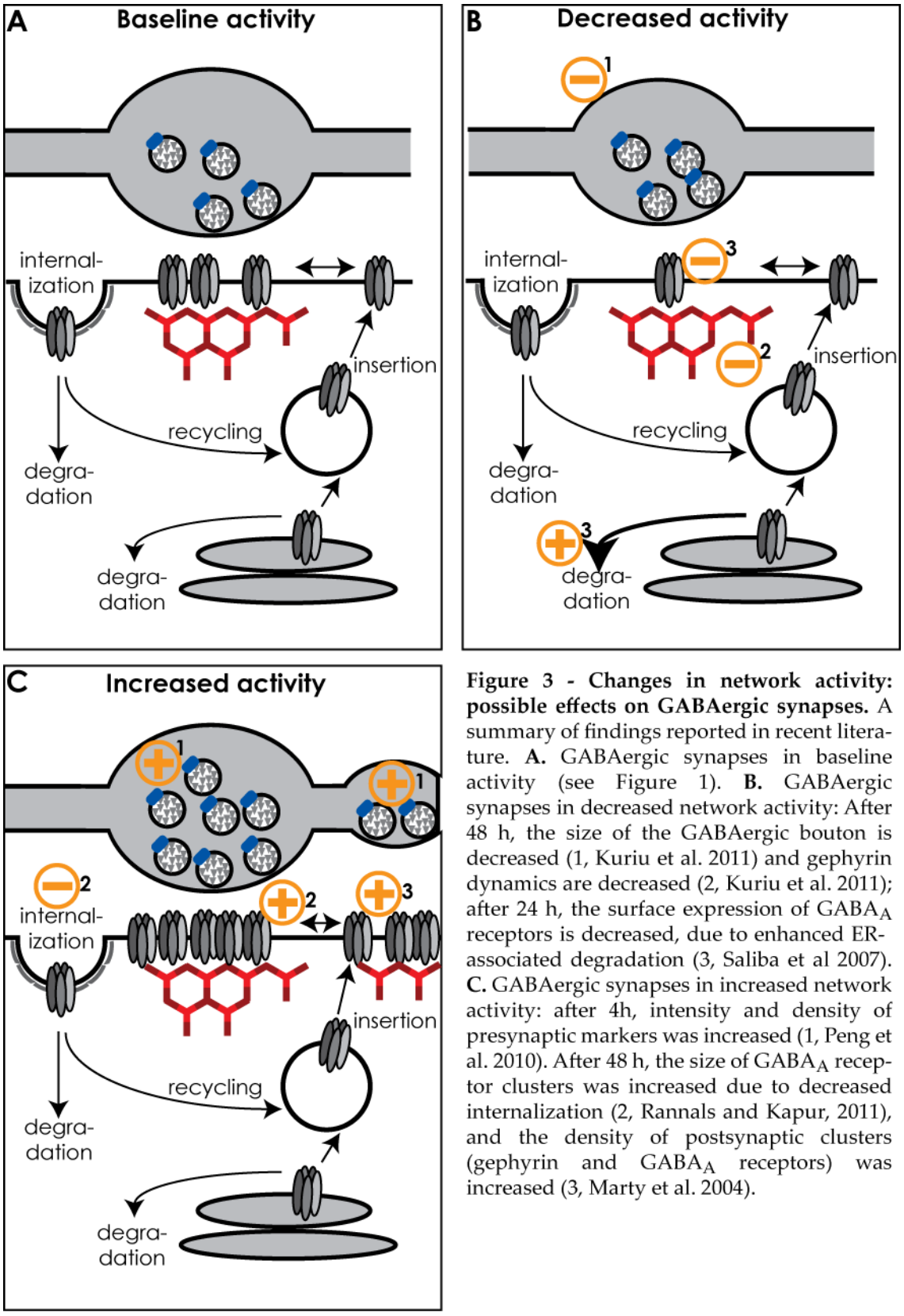

Figure 3 - Changes in network activity: possible effects on GABAergic synapses. A summary of findings reported in recent literature. **A.** GABAergic synapses in baseline activity (see Figure 1). **B.** GABAergic synapses in decreased network activity: After 48 h, the size of the GABAergic bouton is decreased (1, Kuriu et al. 2011) and gephyrin dynamics are decreased (2, Kuriu et al. 2011); after 24 h, the surface expression of $GABA_A$ receptors is decreased, due to enhanced ER-associated degradation (3, Saliba et al 2007). **C.** GABAergic synapses in increased network activity: after 4h, intensity and density of presynaptic markers was increased (1, Peng et al. 2010). After 48 h, the size of $GABA_A$ receptor clusters was increased due to decreased internalization (2, Rannals and Kapur, 2011), and the density of postsynaptic clusters (gephyrin and $GABA_A$ receptors) was increased (3, Marty et al. 2004).

So far, only one study has investigated the activity-dependent dynamics of GABAergic presynaptic structures. Kuriu and colleagues found that the size of axonal varicosities was decreased following 48 h of TTX treatment. They did not observe any change in structural dynamics or density of these boutons (Kuriu et al., 2011).

In addition to different temporal manipulations, spatially variable manipulations of neuronal activity have been applied to GABAergic synapses, as well. However, the results of these studies are inconsistent regarding the spatial extent of GABAergic plasticity mechanisms. While Hartman and colleagues reported that the induction of a form of homeostatic plasticity of inhibitory synapses required network-wide manipulations of activity (Hartman et al., 2006), other studies suggest that local or even cell-autonomous mechanisms suffice for the induction of different forms of structural inhibitory plasticity (Liu, 2004; Chattopadhyaya et al., 2007; Peng et al., 2010).

3. Aim of this study

Plasticity of inhibitory, GABAergic synapses is an important building block of functional neuronal networks. *In vivo*, plasticity of GABAergic synapses has been shown to precede plastic changes of excitatory synapses in response to decreased sensory input and *in vitro*, GABAergic synapses were shown to change their strength in response to manipulations of network activity (Rutherford et al., 1997; Kilman et al., 2002; Swanwick et al., 2006; Rannals and Kapur, 2011). To date, few studies have explored the structural plasticity of GABAergic synapses, but these studies typically omit the early phase of plasticity induction (Chen et al., 2011; Keck et al., 2011; Kuriu et al., 2011). In addition, these studies often investigate a snapshot in time, analyzing GABAergic synapse strength and density only once after the induction of plasticity. However, early structural dynamics of GABAergic synapses could indicate a remodeling of existing connections which later gives rise to changes in synaptic strength or GABAergic connectivity.

Therefore, this study was designed to investigate the structural dynamics of GABAergic synapses in the first hours after the induction of plasticity in greater detail. First, the study investigated the baseline structural dynamics of GABAergic axons. Second, changes of these baseline dynamics following manipulations of network activity were analyzed. These data should aid the understanding of the development of GABAergic plasticity.

For the analysis of baseline structural dynamics, hippocampal slice cultures from GAD65-GFP mice were imaged with two-photon microscopy for four hours at 30 minute intervals. Imaging GABAergic axons in a 100 µm * 100 µm * 50 µm volume (1024 * 1024 pixels in xy and a z-increment of 0.5 µm) allowed for the analysis of stretches of GABAergic axons and their structural dynamics over the imaging period. For the analysis of structural dynamics during changes in network activity, the slice cultures were subjected to pharmacological manipulations of network activity for the duration of the imaging experiment described above. To investigate long-term changes in GABAergic synapses over longer periods of time, axons were treated with the pharmacological agent for 48 h or 7 d before the imaging experiment.

The study has described many structural characteristics and dynamics of GABAergic axons, such as different types of GABAergic boutons and baseline structural dynamics of these boutons which might correspond to material transport along the axon. Analyzing the effect of network activity on these dynamics suggested furthermore that acute manipulation of activity modifies structural GABAergic bouton dynamics. In addition, this study has started to investigate the spatial scale of GABAergic plasticity and set the stage for further experiments that could clarify questions in this regard.

Materials and Methods

4. Material

4.1 Equipment

Equipment	Supplier
40x, 1.2 NA water immersion objective	Zeiss (Oberkochen, Germany)
Bandpass filter ET510/80m-2p	Chroma Technology (Bellows Falls (VT), USA)
Bandpass filter ET605/70m-2p	Chroma Technology
Cell Counter plugin for ImageJ	K. De Vos, (University of Sheffield, Academic Neurology, UK)
Confocal microscope SP2UV	Leica Microsystems (Wetzlar, Germany)
Dichroic mirror CH-700DCXR2638	LOT Oriel (Darmstadt, Germany)
Dichroic mirror T560lpxr	Chroma Technology
Electro-optical modulator	Polytech (Waldbronn, Germany)
Helios Gene Gun Kit	Bio-Rad Laboratories (Hercules (CA), USA)
ImageJ 1.37v	W. Rasband (NIH, Bethedsa (MD), USA)
Inverted microscope, IX70	Olympus (Hamburg, Germany)
ITCN plugin for ImageJ	Kuo and Byun (UCSB (CA), USA)
LabView	National Instruments (Austin (TX), USA)
Lambda half-wave plate	Thorlabs (Dachau, Germany)
Mai Tai Ti:Sapphire laser	Spectra Physics (Newport) (Irvine (CA), USA)
Matlab R2010b	MathWorks (Natick (MA), USA)
McIlwain Tissue Chopper	The Mickle Laboratory Engineering Co. (Surrey, UK)
Microsoft Excel 2010	Microsoft (Redmond (WA), USA)
P-97 Flaming/Brown Micropipette puller	Sutter Instruments (Novato (CA), USA)
Photomultiplier tubes R6357	Hamamatsu (Hamamatsu, Japan)
Polarizing beam splitter	Thorlabs
Scanhead Yanus II	TILL Photonic (Graefelfing, Germany)
Statistica, Version 7	StatSoft (Tulsa (OK), USA)
Tubing Prep Station	Bio-Rad Laboratories

4.2 Chemicals

Chemical	Supplier
4-aminopyridine (4-AP)	Sigma-Aldrich (St. Louis (MO), USA)
5-Fluoro-2′-deoxyuridine	Sigma-Aldrich
Adenosine 5′-triphosphate magnesium salt (Mg^{2+}-ATP)	Sigma-Aldrich
Alexa Fluor 568 hydrazide, sodium salt	Invitrogen (Carlsbad (CA), USA)
Ara-C Hydrochloride	Sigma-Aldrich
Baclofen hydrochloride	Sigma-Aldrich
Basal medium eagle (BME)	Invitrogen
Bicuculline methiodide	Sigma-Aldrich
Calcium chloride ($CaCl_2 * 2H_2O$)	Merck Chemicals (Darmstadt, Germany)
Cesium methanesulfonate (CH_3CsO_3S)	Sigma-Aldrich
Chicken plasma	Sigma-Aldrich
Compressed helium gas	Westfalen (Münster, Germany)
D(+)-Glucose monohydrate ($C_6H_{12}O_6 * H_2O$)	Merck Chemicals
Disodium phosphate (Na_2HPO_4)	Merck Chemicals
Ethanol, 100 %	Sigma-Aldrich
Gabazine (SR-95531)	Tocris Bioscience (Ellisville, USA)
Goat serum	Bethyl Laboratories Inc. (Montgomery (TX), USA)
Guanosine 5′-triphosphate sodium salt (Na^+-GTP)	Sigma-Aldrich
Hank's balanced salt solution (HBSS)	Invitrogen
HEPES (2-(4-(2-Hydroxyethyl)- 1-piperazinyl)-ethansulfonsäure)	Roth Sochiel (Lauterbourg, France)
Horse Serum	Invitrogen
Hydrochloric acid (HCl; 1 M)	Merck Chemicals
Kynurenic acid	Sigma-Aldrich
L-glutamine (200 mM)	Invitrogen
Magnesium chloride hexahydrate ($MgCl_2 * 6H_2O$)	Merck Chemicals
Magnesium sulfate heptahydrate ($MgSO_4 * 7H_2O$)	Merck Chemicals

Chemical	Supplier
Monopotassium phosphate (KH_2PO_4)	Merck Chemicals
Monosodium phosphate ($NaH_2PO_4 * H_2O$)	Merck Chemicals
Muscimol	Tocris Bioscience
Paraformaldehyde (PFA; $OH(CH_2O)_nH$)	Merck Chemicals
Phosphocreatine disodium salt hydrate	Sigma-Aldrich
Polyvinylpyrollidone (PVP)	Sigma-Aldrich
Potassium chloride (KCl)	Merck Chemicals
QX-314 (bromide salt)	Alomone labs (Jerusalem, Israel)
Sodium chloride (NaCl)	Merck Chemicals
Sodium hydrogen carbonate ($NaHCO_3$)	Merck Chemicals
Sodium hydroxide (NaOH; 1N)	Merck Chemicals
Sodium Pyruvate ($C_3H_4O_3Na$)	Sigma-Aldrich
Spermidine	Sigma-Aldrich
Tetrodotoxin (TTX)	Sigma-Aldrich
Thrombin	Merck Chemicals
Triton X-100	Sigma-Aldrich
Trolox (6-hydroxy-2,5,7,8-tetramethylchroman-2-carboxylic acid)	Sigma-Aldrich
Uridine	Sigma-Aldrich

4.3 DNA

Plasmid DNA	Supplier
pABESpuroII	Gift from Dr. Birgit Manno, University of Göttingen (cellular and molecular immunology), original vector (pABESpuro) published (Takata et al., 1994)
pCAGEN (plasmid 11160)	Addgene
pEF-GFP (plasmid 11154)	Addgene
pEGFP-N	Clontech (Mountain View (CA), USA)
pUB-GFP (plasmid 11155)	Addgene (Cambridge (MA), USA)
pZeoSV2	Invitrogen (Carlsbad (CA), USA)

PCR primers	Metabion (Martinsried, Germany)
EGFP_forward (+ EcoRI restriction site)	5'-gcagtgcgaattccgccaccatggtgag-3'
EGFP_reverse (+ EcoRV restriction site)	5'-cacgctgatatcggccgctttacttgtac-3'

4.4 Enzymes

Enzyme	Supplier
EcoRI	New England Biolabs (Ipswich (MA), USA)
EcoRV	New England Biolabs
T4 Ligase	New England Biolabs
Taq Polymerase	Fermentas/Thermo Scientific (Waltham (MA), USA)

4.5 Consumables

Only consumables that differ from regular labware are listed.

Gähwiler slice cultures	
Glass coverslips (12 x 24 mm), # 00	Menzel Glaeser, Braunschweig, Germany
Roller incubator tubes	Nunc (ThermoFisher) (Waltham (MA), USA)

Biolistic transfection	
Gold particles, 1.6 µm diameter	Bio-Rad Laboratories (Hercules (CA), USA)
Nylon mesh, 90 µm	Small Parts (Miami Lakes (FL), USA)
Tubing	Bio-Rad Laboratories (Hercules (CA), USA)
Local superfusion	
Glass micropipettes, 200 µl	Brand GmbH (Wertheim, Germany)
Other	
Qiagen Mini and Maxi Prep Kits	Qiagen (Hilden, Germany)
Borosilicate glass capillaries (GC 150 F-10)	Harvard Instruments (Holliston (MA), USA)

4.6 Media

ACSF		
Chemical	**concentration**	
NaH_2PO_4	1.25 mM	Phosphate buffer
$NaHCO_3$	26 mM	
NaCl	126 mM	Ringer
KCl	2.5 mM	
$CaCl_2$	2.5 mM	
$MgCl_2$	1.3 mM	
Glucose ($C_6H_{12}O_6$)	20 mM	
Pyruvate ($C_3H_4O_3$)	1 mM	
Trolox	1 mM	

ACSF was carbogenated with 95% O_2 and 5% CO_2 to saturate the solution with oxygen. Tenfold stock solutions of Phosphate buffer and Ringer solution were prepared and kept at 4 °C. 1 M stock solution of glucose and 1 M stock solutions of pyruvate were prepared and stored at -20 °C.

Intracellular solution for patch pipettes (Internal solution)

Intracellular solution for whole-cell recordings from CA1 pyramidal cells to measure spontaneous synaptic currents contained 20 mM KCl, 100 mM CH_3CsO_3S, 10 mM

HEPES, 4 mM Mg-ATP, 0.3 mM Na-GTP, 10 mM phosphocreatine disodium salt and 3 mM QX-314 bromide. The osmolarity of the solution was adjusted to ~305 mosmol, then the solution was sterile filtered and stored in aliquots at -20 °C before use.

Preparation medium for organotypic slice cultures

GBSS (1.5 mM $CaCl_2$, 4.96 mM KCl, 0.22 mM KH_2PO_4, 1.03 mM $MgCl_2$, 0.07 mM $MgSO_4$, 136.89 mM NaCl, 2.7 mM $NaHCO_3$, 0.85 mM Na_2HPO_4, 5.55 mM D-glucose), 1 mM kynurenic acid, 0.05 mM D-glucose; pH set to 7.2 with 1 M HCl, sterile filtrated.

Gähwiler medium

50 % (v/v) BME, 25 % (v/v) horse serum, 25 % (v/v) HBSS, 1 mM L-glutamine, 5 mg/ml D-glucose. Sterile filtrated and stored at 4 °C.

Phosphate-buffered saline (PBS)

2.7 mM KCl, 1.47 mM KH_2PO_4, 138 mM NaCl, 7.24 mM Na_2HPO_4. pH was adjusted to 7.4 with 10 N NaOH.

Chicken plasma solution

50 % (v/v) solution in H_2O. Sterile filtrated and stored at -20 °C.

Mitotic inhibitor solution

0.33 mM uridine, 0.33 mM Ara-C, 0.33 mM 5-Fluoro-2'-deoxyuridine in H_2O. Sterile filtrated and stored in aliquots at -20 °C.

Thrombin solution

0.5 g thrombin were dissolved in 50 ml H_2O and 50 ml GBSS (0.5 % (w/v) solution). Stored at -20 °C.

Fixative

To fix organotypic slice cultures for post-hoc immunohistochemistry, a solution of 4 % PFA (w/v) in PBS was used. A 16 % (w/v) PFA stock solution was stored at -20 °C. 4 ml stock solution and 12 ml PBS were mixed to obtain the fixative.

4.7 Antibodies

Primary Antibodies

Antibody	Dilution	Supplier
α-c-fos (rabbit, polyclonal)	1:5000	Merck (Darmstadt, Germany)
α-gephyrin	1:400	Synaptic Systems (Göttingen, Germany)
α-GFP (chicken, polyclonal)	1:1000	Millipore (Billerica (MA) USA)
α-NeuN (mouse, monoclonal)	1:100	Millipore (Billerica (MA) USA)
α-VGAT	1:200	Synaptic Systems (Göttingen, Germany)

Secondary antibodies

Antibody	Dilution	Supplier
α-chicken-Alexa488	1:200	Invitrogen (Carlsbad (CA), USA)
α-mouse-Alexa633	1:200	Invitrogen (Carlsbad (CA), USA)
α-mouse-cy3	1:200	Dianova (Hamburg, Germany)
α-rabbit-Alexa633	1:200	Invitrogen (Carlsbad (CA), USA)
α-rabbit-cy3	1:200	Dianova (Hamburg, Germany)

5. Methods

5.1 Organotypic slice cultures

Hippocampal slices were prepared from postnatal day 2-6 GAD65-GFP mice (Lopez-Bendito et al., 2004), and maintained in a roller incubator, according to the Gähwiler method (Gähwiler, 1981). The entire preparation procedure was carried out under a laminar flow. Briefly, mice pups were decapitated, the brain was removed from the skull and stored in fresh, ice-cold preparation medium. Hippocampi were removed and cut in 350 μm transversal slices using a tissue chopper. Slices were then stored in preparation medium and separated using fine forceps. To allow for removal of debris and regeneration, slices were stored in preparation medium at 4 °C for 30-60 min. Afterwards, slices were transferred to a drop of 10 μl chicken plasma solution on a glass coverslip. 10 μl thrombin solution was added to the slice to induce coagulation of a plasma clot, and slices were oriented to their final position on the coverslip. The plasma clot with the hippocampal slice was allowed to dry for approximately 30 min, before the coverslip was placed in a roller incubator tube containing 750 μl of prewarmed Gähwiler medium and transferred to the roller incubator. Slices were maintained at 35 °C. After three or four days in culture, 10 μl mitotic inhibitor solution were added to each slice. 16-24 h afterwards, the medium was changed (500 μl of the old Gähwiler medium were exchanged with fresh, pre-warmed Gähwiler medium). Subsequently, medium was changed once per week in the same way. Slices were kept in culture for at least ten days before the experiments (range: 10-17 days *in vitro* (DIV)). Hippocampal slice cultures are an experimental system, in which the time course and pattern of GABAergic synapse formation have been shown to resemble the same processes *in vivo* (De Simoni et al., 2003).

In GAD65-GFP mice, ~20 % of all hippocampal CA1 interneurons express GFP (Wierenga et al., 2010), and the expression level is stable from the early embryonic age to adulthood (Lopez-Bendito et al., 2004). Furthermore, the GFP signal in GAD65-GFP hippocampal slice cultures is sufficiently bright to identify individual boutons along axons and sufficiently sparse to identify individual axons in the tissue.

5.2 Time-lapse two-photon imaging of GABAergic boutons in hippocampal slice cultures

For the imaging experiments, organotypic hippocampal slice cultures were transferred to a heated recording chamber (35 °C), where they were continuously perfused with carbogenated (95% O_2, 5% CO_2) ACSF.

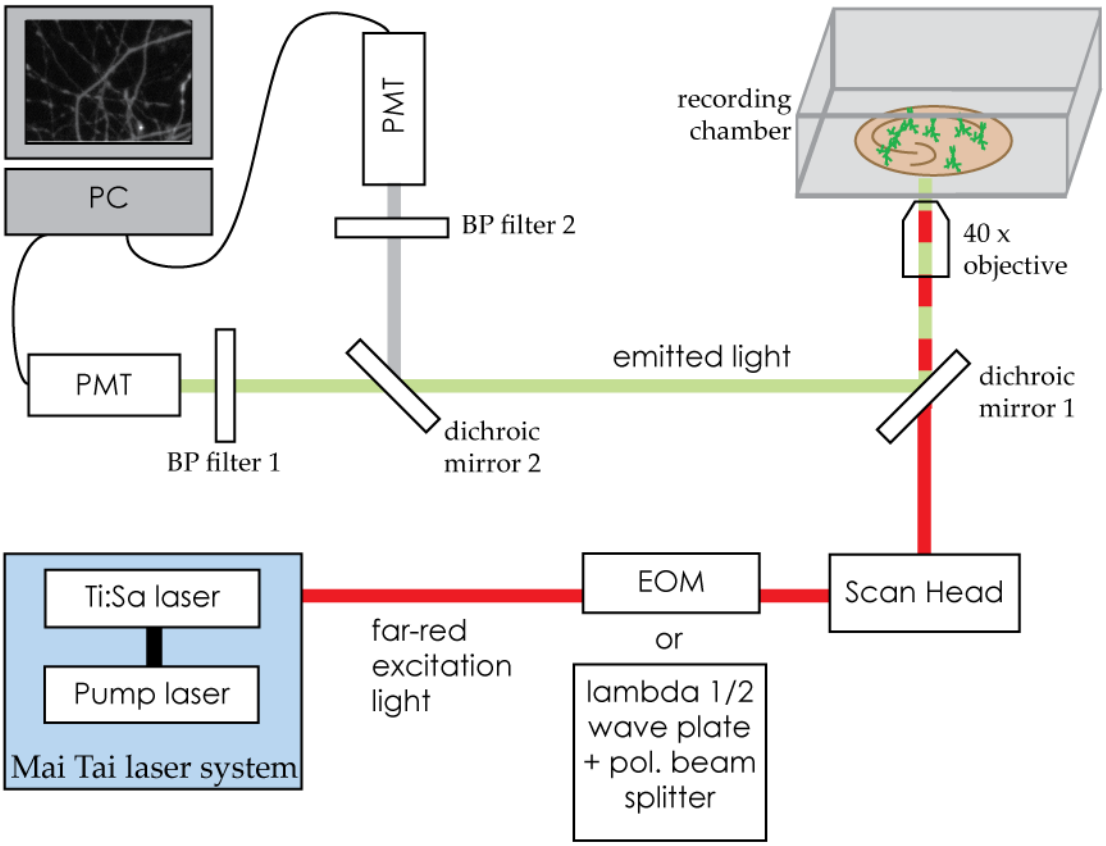

Figure 4 - Schematic drawing of the two-photon imaging setup. The laser beam from a Mai Tai Titanium:Sapphire (**Ti:Sa**) laser system is routed through an electro-optical modulator (**EOM**) or a lambda 1/2 wave plate followed by a polarizing beam splitter to adjust laserpower. It then enters the Scanbox (**Scan Head**), which scans the laser beam across the sample in xy. Emitted light is reflected by a dichroic mirror (1) and split into the red and green channel by a second dichroic mirror (2) and filtered by adequate bandpass filters (**BP filters**). Emission light is then detected by a photomultiplier tube (**PMT**) which is installed behind each bandpass filter. Data from the PMTs is used by a computer (**PC**) to compute the final image.

For monitoring structural changes of GFP-positive axons, a custom-built two-photon microscope, based on an Olympus IX70 inverted microscope was used. To excite GFP and (if applicable) Alexa 568, the laser beam from a Mai Tai HP laser system was tuned to either 910 nm (excitation of GFP only) or to 950 nm (simultaneous excitation of GFP and Alexa 568). The power of the laser beam was adjusted to a power of ~ 2.8 mW after the objective using either a λ half-wave plate followed by a polarizing beam splitter

or an electro-optical modulator (earlier version of the microscope). Owing to different absorption properties of parts of the microscope, the laserpower had to be adjusted slightly for a wavelength of 950 nm. The laser beam was routed through a laser scanhead and a dichroic mirror (passing excitation light and reflecting emitted light from the probe) before reaching the probe through a 40x water immersion objective. The emitted green and red fluorescence was reflected by the dichroic mirror, split into green and red light by an appropriate dichroic mirror, filtered by suitable bandpass filters, and detected with two external photomultiplier tubes (Figure 4).

3D image stacks (spanning 100 × 100 μm in xy, and 40-50 μm in z; using 1024 x 1024 pixels in xy, and 0.5 μm steps in z) were acquired every 30 min for a total experiment duration of 4 h in the CA1 region of the slice culture. Before the acquisition of each image, minute adjustments were made to the position of the slice culture if necessary, such that exactly the same region of the slice was imaged in every time point.

5.3 Pharmacological treatments of hippocampal slice cultures

For acute pharmacological treatments, the ACSF was supplemented with one or more of the following substances: 0.1 μM TTX, 50 μM 4-AP, 20 μM bicuculline methiodide, 10 μM gabazine (SR-95531), 10 μM muscimol, and 20 μM baclofen hydrochloride. For long-term pharmacological treatments, the substances were added to the slice medium and renewed every day by exchanging 500 μl of the culture medium (in controls and treated cultures). For each pharmacological treatment, data were obtained from treated slice cultures and untreated sister cultures (control). Obtaining data from sister cultures had the advantage of reducing data variations caused by changes to the microscope or variations in slice quality over time.

5.4 Immunohistochemistry

Post-hoc immunohistochemistry for the pre- and postsynaptic markers of GABAergic synapses was carried out as described previously (Wierenga et al., 2008). Briefly, after two-photon imaging slices were fixed with 4 % w/v PFA, washed extensively in PBS and removed from their glass coverslips to be processed as free floating slices. They were incubated with 0.4 % v/v Triton X-100 and 10 % v/v horse serum in PBS for permeabilization of the tissue and blocking of unspecific epitopes. Subsequently, primary antibodies were applied over-night in 0.4 % v/v Triton X-100 and 5 % v/v horse serum in PBS, and secondary antibodies were applied after extensive washing and incubated over-night. High-resolution confocal image stacks (Δz = 0.35-0.4 μm) were taken to analyze the

immunohistochemical staining. Marker content of individual boutons was determined in single z sections after filtering and thresholding each channel independently.

Post-hoc immunohistochemistry for the immediate early gene c-fos was performed following a similar protocol. Briefly, slices were fixed with 4 % w/v pre-warmed PFA in PBS (30 min at 35 °C, then 4 h at 4 °C). After fixation, slices were washed extensively in PBS and removed from their glass coverslip to be processed as free-floating slices. They were incubated in 1 % v/v Triton X-100 and 10 % goat serum in PBS for 24 h to achieve permeabilization and blocking of unspecific epitopes. Primary antibodies (against c-fos, NeuN, and GFP) were applied over-night at 4 °C in 1 % v/v Triton X-100 and 5 % v/v goat serum in PBS. After thorough washing in PBS, slices were incubated with appropriate secondary antibodies diluted in 5 % v/v goat serum in PBS. Slices were imaged with a commercial confocal microscope (Leica SPUV, 20x objective) to analyze c-fos-positive nuclei. Images were taken in the CA1 region, spanning both the stratum radiatum and the stratum pyramidale. Images spanned 508 x 508 μm in xy (resolution of 512 x 512 pixel) and 40-50 μm in z (Δz = 1 μm). For analysis of c-fos positive nuclei, a region spanning 150 x 150 pixels in xy and 30 μm in z was selected both in the stratum radiatum and the stratum pyramidale for each slice. A z-projection of the c-fos channel of this area was analyzed with the ITCN plugin for ImageJ, which can count cell bodies or nuclei. This cell count was normalized to the intensity of the NeuN staining in this region to account for differences in neuron density.

5.5 Local superfusion

To manipulate a small area of the slice culture (local superfusion), the technique described by Veselovsky and colleagues was used in a slightly modified way (Veselovsky et al., 1996). Briefly, two glass pipettes, between which a superfusion solution was flowing through gravity flow, were lowered to the top of the slice culture. The area affected by the superfusion was approximately 300 μm × 300 μm in size. The superfusion solution consisted of carbogenated ACSF with 10 μM Alexa 568 and, when indicated, 0.1 μM TTX. High-resolution two-photon image stacks (dimensions: 100 x 100 μm in xy (1024 x 1024 pixel), 40-50 μm in z (Δz = 0.5 μm)) were acquired both inside and outside the superfusion spot for 4 h at 30 min intervals. The superfusion spot was controlled between images to ascertain that its dimensions remained stable.

5.6 Electrophysiological recordings

Somatic whole-cell recordings were obtained from visually identified pyramidal cells in the CA1 area of the hippocampal slice cultures. Glass pipette electrodes (resistance: 2-4 MΩ) were pulled from borosilicate capillaries and filled with sterile filtered pipette internal solution.

To measure spontaneous synaptic currents, the reversal potentials for chloride and for glutamatergic currents were determined by clamping the cell to different potentials in 5 mV increments. The average reversal potential for chloride was -44.1 ± 1.3 mV, and the average reversal potential for glutamatergic currents was 4.2 ± 1.7 mV. For recording spontaneous excitatory currents, cells were clamped to the reversal potential of inhibitory currents, and vice versa. In the presence of bicuculline, the reversal potential of chloride could not be measured ($GABA_A$ receptors as major chloride channels were blocked by bicuculline). Therefore, excitatory currents were measured at -40 mV. Synaptic currents were recorded for 5 min, in 1.5 second sweeps. Data were acquired using custom-written LabView software.

Only neurons for which a membrane potential (V_m) below -50 mV, an input resistance (R_{in}) above 150 MΩ, and a series resistance below 25 MΩ were measured, were included in the analysis. Data analysis was performed with custom-written Matlab software. Total excitatory and inhibitory charge was calculated as the integral of negative and positive currents in the respective recordings and represented as the total charge per second recording time.

5.7 Data analysis – two-photon imaging

Image analysis was performed on raw images. For illustration purposes, some images in this work have been filtered. Image stacks were visually inspected in ImageJ and xyz coordinates of exemplary points along individual axons were selected at every time point using the CellCounter plugin for ImageJ.

Subsequent analysis of the selected axons was carried out in a semi-automated manner using software written in Matlab. xyz coordinates of each axon, as determined with ImageJ beforehand, were used by the software to generate a 3D intensity profile at every time point. For this purpose, at each point of the axon, the total intensity of a small area in the orthogonal plane was determined (16 pixels on orthogonal line × 4 z-layers). The bouton threshold was determined for each time point in a two-step process. First, a local axon threshold was calculated for each image to distinguish the axon from the background (2 standard deviations (s.d.) above mean intensity). Second, a local threshold

(0.5 s.d. above mean axon intensity) was calculated for all peaks of the 3D intensity profile and the 33-percentile of the distribution of all local thresholds was taken as the bouton threshold for the entire axon. This axon threshold was then used to identify boutons along the axon. This procedure was found to be optimal for detecting weak boutons, independent of bright neighboring boutons. Each image stack was visually examined to remove false positives and negatives. Only structures with ten or more pixels above bouton threshold were considered as boutons.

The axon was then aligned across time points, such that the presence of any bouton could be determined in every time point of the imaging period. The output of this analysis was a "presence matrix", indicating each bouton and its presence (1 = bouton present, 0 = bouton absent) in all time points recorded. In addition, axon length and the average position of every bouton along the axon were calculated.

Bouton volumes were calculated as the summed intensity of all pixels above bouton threshold, divided by the bouton threshold. An alternative volume measurement (number of pixels above bouton threshold) led to comparable results (Figure 5). The output of the volume analysis was a "volume matrix", which was analogous to the presence matrix, but contained volume values whenever a bouton was present.

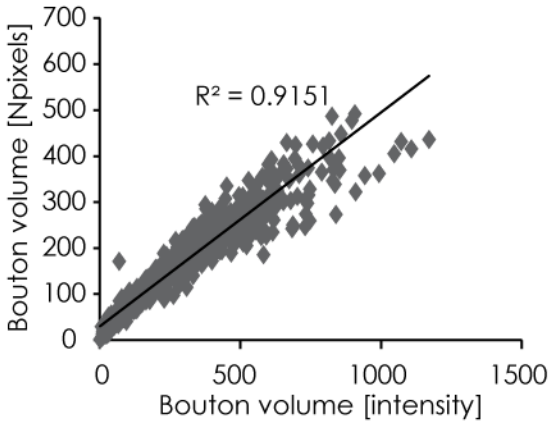

Figure 5 - Correlation of the two different volume measurements. Bouton volume of control boutons measured as the number of pixels above bouton threshold (Npixels, y-axis), and as The summed intensity above threshold, normalized by the threshold (Intensity, x-axis). The two volume measurements show a strong correlation. n = 1128 boutons.

Subsequent analysis was carried out with Microsoft Excel, to calculate different measures of bouton plasticity (turnover, survival fraction, volume CV), bouton density, bouton volume, and lifetime. Bouton volume CV was calculated as the ratio of the standard deviation of bouton volume and the mean bouton volume over all imaging time points. Bouton turnover is defined as the fraction of boutons appearing and disappearing at every time point, it is then averaged over all time points. Persistent bouton density was defined as the number of persistent boutons divided by axon length. For the calculation of the density of transient and short-lived boutons, the number of transient or short-lived boutons at each timepoint was divided by axon length, then, the average of these densities

was calculated. A growth coefficient of bouton volume was calculated to analyze the extent of bouton growth and shrinkage: growth coefficient = $(V_2 – V_1) / (V_2 + V_1)$, in which V_1 and V_2 are the average volumes of the first two (V_1) and last two (V_2) imaging time points. A positive value of the growth coefficient indicates bouton growth while a negative value indicates bouton shrinkage.

5.8 Simulation of bouton distribution along axons

Absolute positions and numbers of persistent and transient boutons along analyzed control axons were used to simulate these axons *in silico* with Matlab-based functions. For the simulation, the positions of boutons on an analyzed axon were randomly assigned to the same number of persistent and transient boutons that were found in the experimental data. For each axon, this simulation was repeated 1000 times. Analysis was carried out on the entire population of control axons, as axons were too short to be analyzed individually.

Data obtained from experiments and simulations were analyzed for clustering with three different methods.

(1) Analysis of relative bouton distance

For this purpose, the number of different category boutons between neighboring boutons of the same category was counted.

(2) Analysis of a boutons' neighborhood / "cluster coefficient"

Here, the identity of the next and the second-to-next bouton to the sides of each bouton were analyzed. For every bouton that belonged to the same category as the center bouton, the "cluster coefficient" was increased by one, leading to cluster coefficients between 0 (no clustering with same-category boutons) and 4 (all neighboring boutons belong to the same category = high clustering).

(3) Analysis of absolute bouton distance

Here, the absolute distance between neighboring boutons of the same category were calculated by comparing their absolute positions along the axon (in μm).

Comparisons of experimental and simulated data were tested for statistical significance using the Chi Square test. Distributions were considered to be significantly different if the p-value was below 0.05. Significance levels: *: $p < 0.05$, **: $p < 0.01$, ***: $p < 0.005$.

5.9 Biolistic transfection of individual cells

To express the gene of interest in individual cells within the slice culture, biolistic, gene-gun mediated gene transfer was used. Here, gold particles were coated

with the plasmid DNA of interest (for a complete list, see section 4.3) with a method adapted from McAllister and colleagues (McAllister, 2000).

Briefly, 12.5 mg of 1.6 μm diameter gold particles were mixed with 100 μl of 50 mM spermidine solution, vortexed and sonicated for 5 s to separate the gold particles. Plasmid DNA was added to the gold solution to reach a final concentration of 3-5 μg DNA/mg gold. While vortexing, 100 μl of a 1 M $CaCl_2$ solution were added to the gold-DNA mixture dropwise. This procedure allowed for a precipitation of the plasmid DNA onto the gold particles. After 10 min the gold was pelleted with a minicentrifuge, and washed three times with 100 % ethanol. The gold pellet was then resuspended in 3 ml of a 0.09 mg/ml PVP solution in ethanol. Then, the solution was filled into tubing, which had been purged with N_2 for 30 min beforehand, and the filled tubing was inserted into the BioRad tubing prep station. The gold was allowed to settle for 30 min before the fluid was slowly removed from the tubing, and the tubing was rotated for 30 s. Finally, the tubing was dried by steady N_2 flow through it while rotating. The dried tubing was then cut into 0.5 inch pieces that would fit into the gene-gun cartridge. These "bullets" were stored at 4 °C in a plastic container with a desiccant pellet to avoid humidification of the bullets.

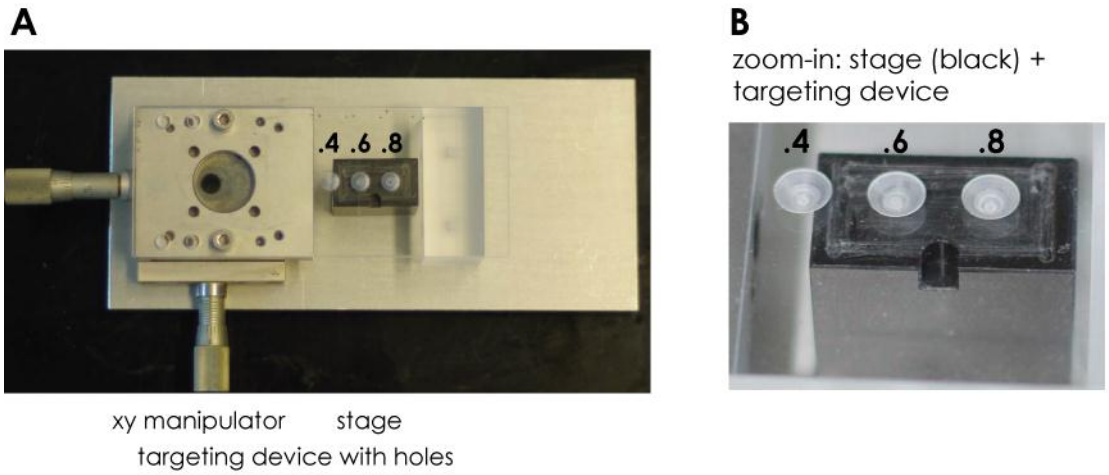

Figure 6 - Device for (targeted) biolistic transfection of Gähwieler hippocampal slice cultures. **A.** The device consisted of a targeting device (a 3 mm plastic board with 3 holes (0.4, 0.6, and 0.8 mm in diameter). A xy manipulator could be used to move this targeting device across a slice culture which was put onto the stage (black cuboid). The stage had been carved to exactly fit the glass coverslips on which the slice cultures were mounted. Furthermore, it had a cavity which allowed for easy positioning and removal of the coverslip. **B.** Detailed view of stage and the holes in the targeting device.

Before the transfection of cells, gene-gun cartridge, barrel liner and a piece of nylon mesh were sterilized with ethanol. Subsequently, under a sterile hood, the gene-gun cartridge was loaded with the "bullets". The barrel liner of the gene-gun was covered with a nylon mesh which would disperse the DNA-loaded gold particles being shot

towards the slice. Under the sterile hood, organotypic slice cultures were removed from their tube and placed in a well of a sterile 6-well plate or onto a custom-made device (Fig. 6), that allowed for targeted transfection and better handling of the glass coverslips. They were shot once with the hand-held gene-gun from a distance of 15-20 cm by passing compressed helium at a pressure of ~ 180 psi through the gene-gun. Slice cultures were quickly placed back into their tube and returned to the incubator. 1-2 days after GFP transfection, transfected cells showed bright green fluorescence.

5.10 Generation of plasmid DNA

Plasmid DNA for gene-gun mediated gene transfection of individual cells was designed, generated, and amplified using standard molecular biology techniques.

In brief, to generate the pCAGEN-GFP, pABESII-GFP, and pZeoSV2-GFP plasmids, GFP was amplified from the pEGFP-N vector using PCR (with the Taq polymerase enzyme). The restriction site EcoRI was incorporated into the forward primer, while a restriction site for EcoRV was incorporated into the reverse primer of this reaction. As a result, the product from the PCR reaction comprised GFP, flanked by an EcoRI restriction site in front, and an EcoRV restriction site at the end. The PCR product was then digested with the two restriction enzymes and gel-purified using agarose gel-electrophoresis. In parallel, the plasmid vectors (pCAGEN, pABESII, and pZeoSV2) were digested with the same restriction enzymes and gel-purified as well. Now the opened vectors and the PCR product had matching ends (EcoRI and EcoRV restriction sites). They were then ligated (each vector with the PCR product) using the T4 ligase enzyme. Competent DH5α bacteria were transformed with the product of the ligase reaction using a heat shock. Bacteria carrying the plasmid were selected based on their resistance to certain antibiotics (usually ampicillin, in the case of pZeoSV2 zeocin), a feature of the plasmid DNA, and amplified. Finally plasmid DNA was purified from the bacteria using the Qiagen Mini and Maxi Prep Kits, and the identity of the plasmid was confirmed using test restriction and DNA sequencing.

pUB-GFP and pEF-GFP were ordered in their final form from the addgene library and amplified using the Qiagen Mini and Maxi Prep Kits.

5.11 Statistics

Data are reported as mean ± standard error unless otherwise stated. Statistical significance of differences between mean values for treated slices and matched untreated controls was tested using the two-tailed t-test. Multiple comparisons were made by an ANOVA followed by a post-hoc Fisher test, unless stated otherwise. Differences were considered significant if the p-value was below 0.05. Significance levels: * $p < 0.05$, ** $p < 0.01$, *** $p < 0.005$.

Results

6. Characterizing baseline structural dynamics of GABAergic axons

6.1 Time-lapse two-photon imaging of GABAergic axons reveals persistent and non-persistent presynaptic boutons.

To characterize the structural dynamics of GABAergic axons, time-lapse two-photon imaging was performed on hippocampal slice cultures from GAD65-GFP mice. These mice express GFP in ~20 % of all hippocampal interneurons. Most of these interneurons target the dendrites of nearby pyramidal cells and express reelin or VIP (Wierenga et al., 2010). Sparse, yet bright and uniform GFP labeling makes these mice an ideal model system for analyzing the structural dynamics of GABAergic axons (Figure 7A). Individual axons can be identified and imaged several times at high resolution without noticeable bleaching of the fluorophore GFP. For the experiments, high-resolution image stacks (100*100 μm, 1024*1024 pixels, z-increment of 0.5 μm over a depth of 50 μm) of the same CA1 region were acquired every 30 min for a total imaging period of 4 h. Subsequently, the same axon was selected in each of the eight image stacks and boutons along the axon were detected in a semi-automatic manner from the 3D intensity profile of the axon (for a more detailed description, see section 5.7). Potential boutons (peaks of the 3D intensity profile selected by the automatic detection procedure) were visually verified in the original image stack. Boutons were only included in the analysis if the intensity of ten or more connected pixels exceeded the bouton threshold.

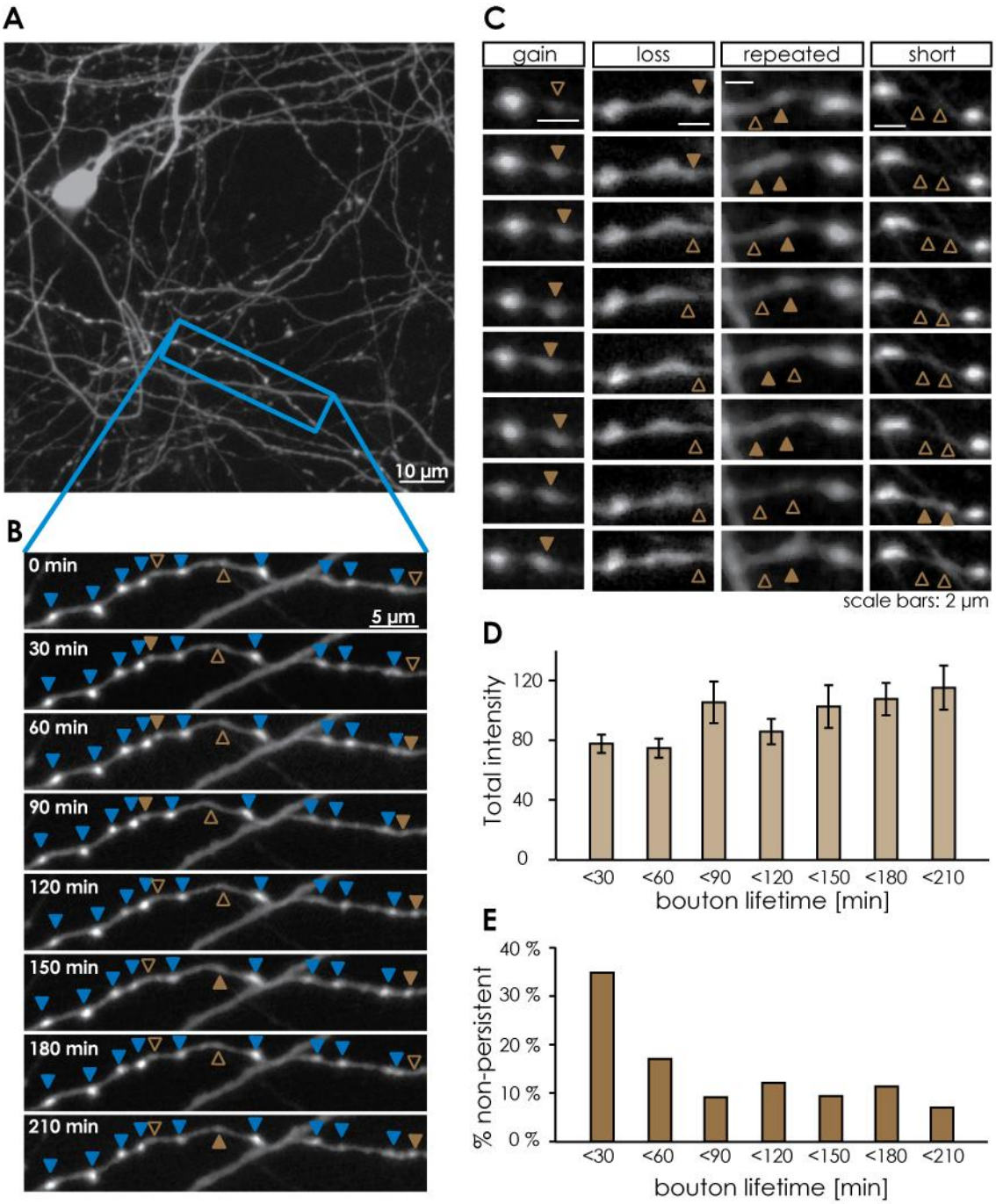

Figure 7 – Time-lapse imaging of GABAergic axons reveals persistent and non-persistent presynaptic boutons. A. Average intensity projection image from the CA1 region of a GAD65-GFP hippocampal slice culture, showing GABAergic interneurons, dendrites, and axons. **B.** Average intensity projection image of a GABAergic axon indicated by a blue box in A in eight consecutive time points/image stacks. Boutons appear as bright axonal varicosities (filled arrowheads). Boutons that occurred in every timepoint were termed persistent boutons (blue arrowheads), whereas boutons that did not occur in every timepoint were termed non-persistent boutons (open (= absent) and filled (= present) brown arrowheads). **C.** Different non-persistent bouton dynamics: gain, loss, repeated occurrence or short occurrence. **D.** Non-persistent bouton volumes separated by bouton lifetime. **E.** Non-persistent boutons separated by lifetime. Note that many transient boutons were short-lived (<60 min lifetime). 405 non-persistent boutons from 39 control-treated axons were included in this analysis.

Two different bouton populations were found on the imaged GABAergic axons. The majority of boutons (~80 % at each time point) were present successively throughout the imaging period. They were termed persistent boutons. The remaining boutons were present intermittently within the imaging period. They were termed non-persistent boutons (Figure 7 B; blue arrowheads: persistent boutons, filled and open brown arrowheads: absent and present non-persistent boutons, respectively). On average, non-persistent boutons appeared at three imaging time points (corresponding to 60-90 minutes total bouton lifetime), with a broad spectrum of temporal appearance patterns (for examples see Figure 7 C). Most non-persistent boutons could not be separated into non-overlapping categories such as new or lost. Nonetheless, bouton lifetime (total number of time points that a bouton was present) appeared to be correlated with bouton volume: longer-lived boutons tended to be slightly larger than shorter-lived boutons (Figure 7 D). Because of this slight volume difference and - more importantly – because of differences in the co-localization with synaptic markers (section 6.2, see for instance Figure 10), non-persistent boutons were separated into two categories: transient and short-lived boutons. Transient boutons had a lifetime of three or more time points (or more than 60 min). Short-lived boutons had a lifetime of one or two imaging time points (or less than 60 min). A large part (~50 %) of the non-persistent boutons fell into the category of short-lived boutons (Figure 7 E). At each time point short-lived boutons made up ~4 % of all boutons on the axon. Due to their longer lifetime, transient boutons corresponded to ~17 % of all boutons at each time point. As new synapses take a few hours until they show properties of functional synapses, it can be assumed that most short-lived boutons do not represent *bona fide* synapses. Transient boutons living for more than two imaging time points are therefore more likely to represent synapses.

Persistent boutons were on average three times as large as transient or short-lived boutons (Figure 8 A; persistent boutons: 311 ± 7, transient boutons: 102 ± 5, short-lived boutons: 77 ± 5 [total normalized intensity], $p < 0.005$). In addition, their volume was more stable: the coefficient of variation (CV) of persistent boutons volume was smaller than that of transient or short-lived boutons (Figure 8 B; persistent boutons: 31 ± 0.6 %, transient boutons: 54 ± 2 %, short-lived boutons: 50 ± 4 %, $p < 0.005$). The CV is a measure for the variation of bouton volume in relation to the average bouton volume (see section 5.7). The bouton volume CV was not correlated between neighboring boutons and therefore not due to variations in the experimental measurement but to true biological variation. Bouton volume CV reflects growth and shrinkage of GABAergic boutons, which might be evoked by material transport into and out of the boutons.

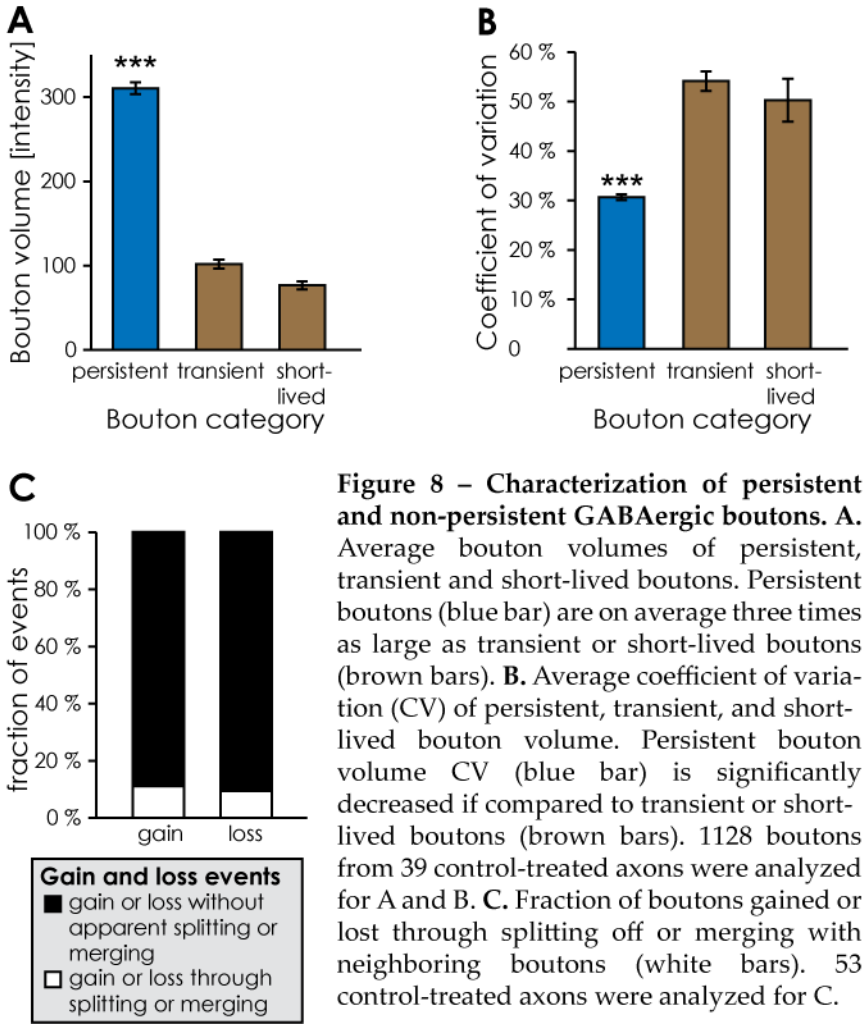

Figure 8 – Characterization of persistent and non-persistent GABAergic boutons. A. Average bouton volumes of persistent, transient and short-lived boutons. Persistent boutons (blue bar) are on average three times as large as transient or short-lived boutons (brown bars). **B.** Average coefficient of variation (CV) of persistent, transient, and short-lived bouton volume. Persistent bouton volume CV (blue bar) is significantly decreased if compared to transient or short-lived boutons (brown bars). 1128 boutons from 39 control-treated axons were analyzed for A and B. **C.** Fraction of boutons gained or lost through splitting off or merging with neighboring boutons (white bars). 53 control-treated axons were analyzed for C.

Bouton gain and loss were frequently observed throughout the imaging period. Under control conditions, 8.0 ± 0.2 % of boutons were gained and 8.7 ± 0.4 % of boutons were lost at each time point (represented as the fraction of all boutons at this time point). In general, new boutons were observed to appear via de novo accumulation on the axonal shaft (see for instance Figure 7 C). Only rarely (~11 % of all observed bouton gain events), a bouton was generated by a clear splitting off a neighboring bouton. Similarly, boutons were rather lost through gradual extinction than by merging with another bouton (~9 % of all observed bouton loss events; Figure 8 C). Both splitting and merging of GABAergic boutons occurred at a similar frequency of 1.8 ± 0.2 splitting and 1.5 ± 0.2 merging events per 100 μm of axon over the entire experiment duration (4 h). It should be noted that the imaging frequency used (2/h) might be too slow for detecting all split- and merge-events. Therefore, the fraction of boutons generated by splitting off or lost by merging with existing boutons might be considerably underestimated in this study.

6.2 Analyzing the co-localization with synaptic marker proteins reveals differences between persistent and non-persistent GABAergic boutons.

Co-localization with pre- and postsynaptic markers has often been used to assess the likelihood of axonal or dendritic structures to represent functional synapses (Wierenga et al., 2008; Dobie and Craig, 2011; Kuriu et al., 2011). The differences of the structural characteristics (volume and volume CV) and temporal appearance patterns of persistent, transient, and short-lived boutons prompted the question whether they would also co-localized with synaptic markers differently. Such data could help to elucidate the role of the different bouton populations on the axon. If all boutons co-localized with synaptic markers to a similar extent, they could be assumed to have a similar function on the axon. If they differed with respect to their co-localization with synaptic markers, some bouton populations would be more likely to represent functional synapse then others. In addition, the co-localization with synaptic markers of growing versus shrinking boutons could be vastly different, or variations in bouton (volume) dynamics might indicate different subcategories of GABAergic boutons.

To shed light on such questions, hippocampal slice cultures were fixed after time-lapse two-photon imaging sessions to be subjected to post-hoc immunohistochemistry (Figure 9 A). Slices were stained for GFP to identify previously imaged axons and boutons, for the presynaptic GABAergic marker VGAT (vesicular GABA transporter), and for the postsynaptic marker gephyrin (a major scaffolding molecule at inhibitory synapses). Confocal imaging of these preparations allowed for the identification of previously imaged boutons and their co-localization with synaptic markers. This information could then be correlated with their structural dynamics prior to fixation (Figure 9 B, C).

Bouton lifetime was positively correlated with synaptic marker content. Most persistent, but only few transient and even less short-lived boutons co-localized with synaptic markers (Figure 10 A; persistent boutons: 63.0 % VGAT + gephyrin, 18.1 % VGAT only, 4.7 % gephyrin only, 13.0 % no synaptic marker, 1.3 % of boutons were not found back in the immunohistochemistry image; transient boutons: 24.4 % VGAT + gephyrin, 16.3 % VGAT only, 7.3 % gephyrin only, 33.3 % no synaptic marker, 18.7 % of boutons were not found back in the immunohistochemistry image; short-lived boutons: 5.6 % VGAT + gephyrin, 5.6 % VGAT only, 1.4 % gephyrin only, 34.7 % no synaptic marker, 52.8 % of boutons were not found back in the immunohistochemistry image).

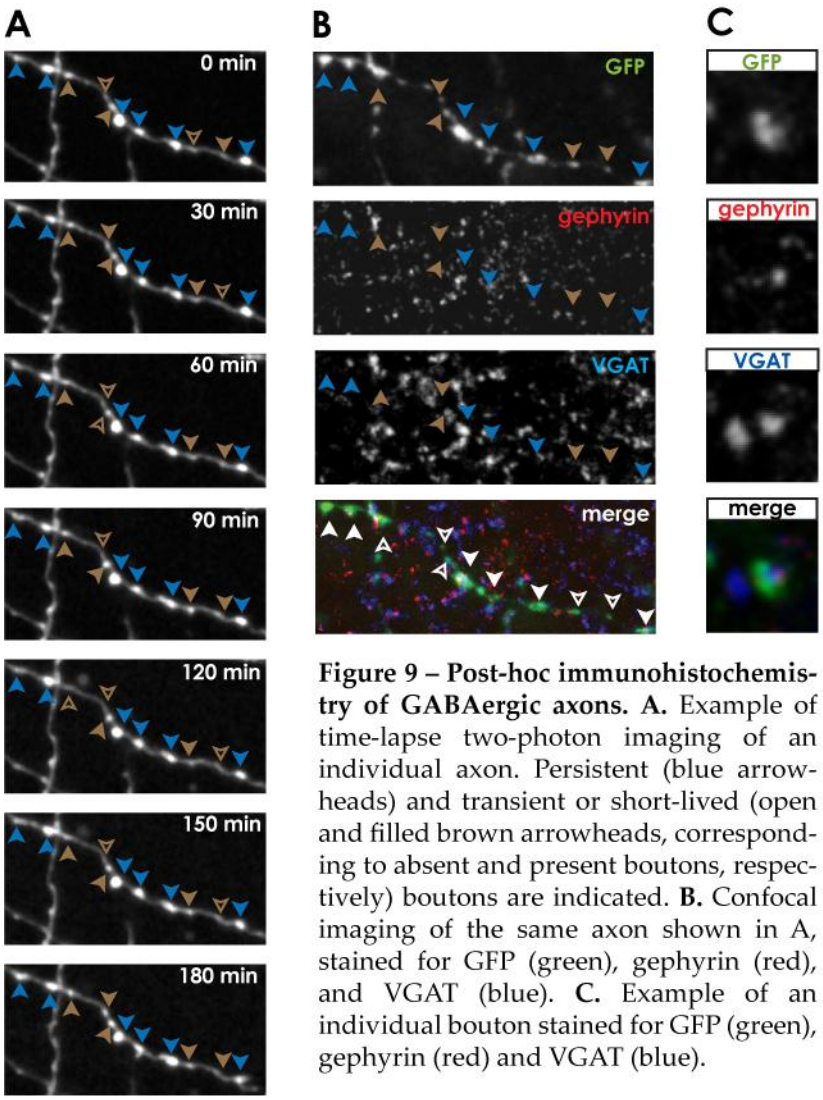

Figure 9 – Post-hoc immunohistochemistry of GABAergic axons. A. Example of time-lapse two-photon imaging of an individual axon. Persistent (blue arrowheads) and transient or short-lived (open and filled brown arrowheads, corresponding to absent and present boutons, respectively) boutons are indicated. **B.** Confocal imaging of the same axon shown in A, stained for GFP (green), gephyrin (red), and VGAT (blue). **C.** Example of an individual bouton stained for GFP (green), gephyrin (red) and VGAT (blue).

Interestingly, a very short bouton lifetime (one or two imaging time points or < 60 min), predicted a much lower co-localization with synaptic markers, even if the bouton was present right before fixation (Figure 10 B, C). The apparent lack of synaptic markers co-localizing with short-lived boutons and the notion of the slightly smaller volume of short-lived boutons (Figure 8), were the decisive factors for the separation of non-persistent boutons into "transient" and "short-lived" boutons.

Not more than 48 % of transient boutons contained any synaptic marker (Figure 10 A). It was shown previously, that new GABAergic boutons assemble over the course of a few hours and that the appearance of transient boutons at axon-dendrite crossings often precedes synapse formation at these sites (Wierenga et al., 2008). It is therefore feasible to assume that transient boutons, which are present for three or more time points at the same site during a 4 h imaging period, represent GABAergic synapses in the process of formation or degradation. In addition, they might represent axonal stop sites for synaptic

material which are frequently occupied by transport entities (Sabo et al., 2006). As little as 13 % of short-lived boutons co-localized with any synaptic marker, suggesting that they do not represent synapses but maybe rather transport events of (synaptic) material along the axon. Conversely, most persistent boutons co-localized with either VGAT or gephyrin (86 %), or even both synaptic markers (63%), cementing previous reports of their synaptic nature (Wierenga et al., 2008).

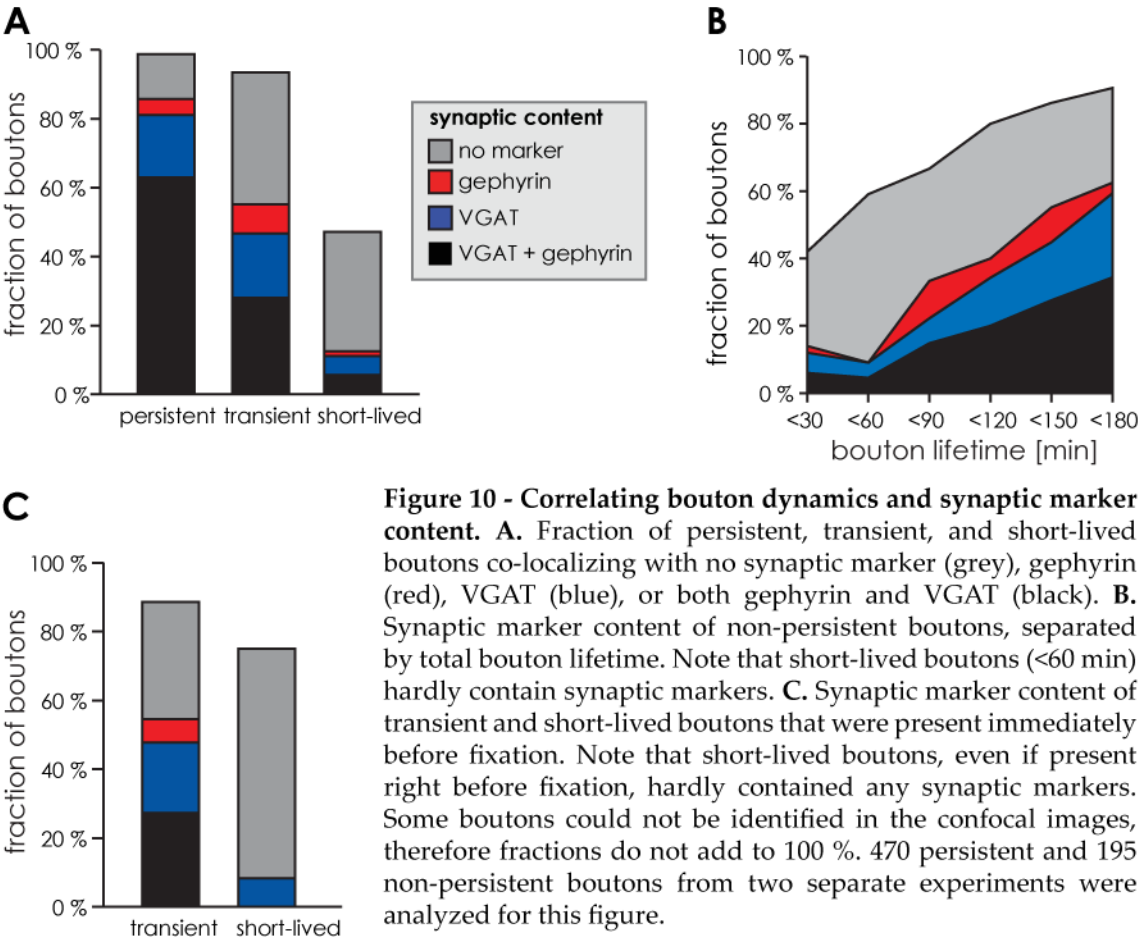

Figure 10 - Correlating bouton dynamics and synaptic marker content. A. Fraction of persistent, transient, and short-lived boutons co-localizing with no synaptic marker (grey), gephyrin (red), VGAT (blue), or both gephyrin and VGAT (black). **B.** Synaptic marker content of non-persistent boutons, separated by total bouton lifetime. Note that short-lived boutons (<60 min) hardly contain synaptic markers. **C.** Synaptic marker content of transient and short-lived boutons that were present immediately before fixation. Note that short-lived boutons, even if present right before fixation, hardly contained any synaptic markers. Some boutons could not be identified in the confocal images, therefore fractions do not add to 100 %. 470 persistent and 195 non-persistent boutons from two separate experiments were analyzed for this figure.

6.3 Co-localization with synaptic marker proteins predicts different structural characteristics.

Interestingly, the structural characteristics of persistent boutons differed, depending on their co-localization with synaptic markers. Persistent GABAergic boutons, which contained both pre- and postsynaptic markers, were found to be significantly larger than those co-localizing with only one or no synaptic marker (Figure 11 A; both VGAT and gephyrin: 311.4 ± 9.3, VGAT: 245.5 ± 13.5, gephyrin: 201.6 ± 18.3, no marker: 183.8 ± 11.5 [total normalized intensity], $p < 0.005$). In addition, persistent, VGAT-containing GABAergic boutons were larger than those co-localizing with no synaptic

marker (Figure 11 A, p = 0.01). A similar trend was observed for transient boutons (Figure 11 B). These data suggest that rather mature boutons (co-localizing with both pre- and postsynaptic markers) are larger than more immature boutons. Although the average volume correlated with synaptic marker content, bouton size was not a limiting factor for detecting synaptic markers in this experiment. It was confirmed that boutons co-localizing with both pre- and postsynaptic markers could be as small as those co-localizing with less synaptic markers. In line with other data, these analyses confirm the correlation between synaptic size and function (Schikorski and Stevens, 1997; Matsuzaki et al., 2001; Weyhersmuller et al., 2011). In addition, transient bouton lifetime seemed to be slightly longer for those boutons that contained either both synaptic markers or VGAT alone (Figure 11C), indicating that boutons acquire more synaptic markers as they mature.

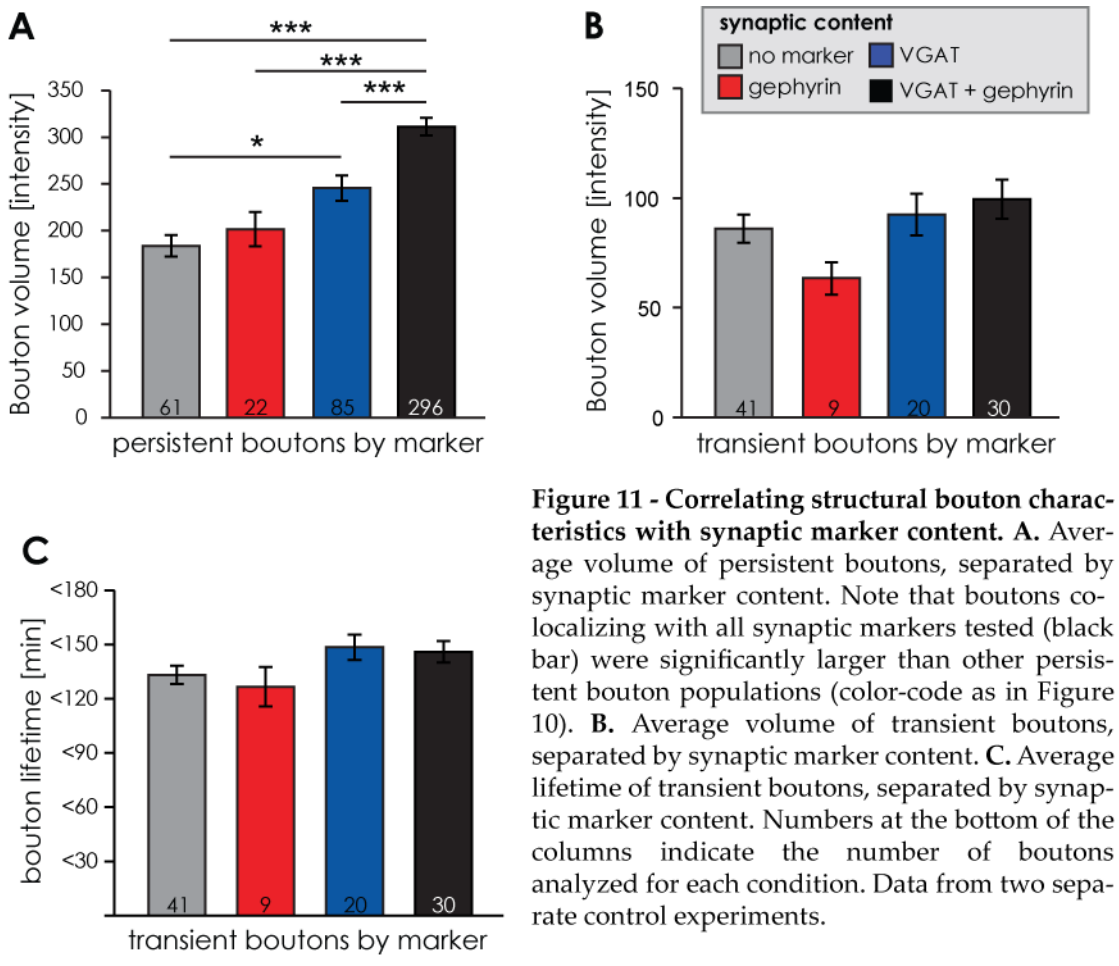

Figure 11 - Correlating structural bouton characteristics with synaptic marker content. A. Average volume of persistent boutons, separated by synaptic marker content. Note that boutons co-localizing with all synaptic markers tested (black bar) were significantly larger than other persistent bouton populations (color-code as in Figure 10). **B.** Average volume of transient boutons, separated by synaptic marker content. **C.** Average lifetime of transient boutons, separated by synaptic marker content. Numbers at the bottom of the columns indicate the number of boutons analyzed for each condition. Data from two separate control experiments.

In the process of synapse formation and degradation, synaptic markers are acquired in a sequential fashion (Friedman et al., 2000; Okabe et al., 2001; Wierenga et al., 2008; Dobie and Craig, 2011). Therefore, it is feasible to hypothesize that synapses containing only one synaptic marker might be passing through such a process. The

transport of synaptic material into or out of a synapse is inevitable for synapse formation and degradation, respectively. Consequently, synapses in the process of formation can be assumed to grow, while those in the process of degradation supposedly shrink. To quantify bouton growth of shrinkage before fixation, a growth coefficient (between -1 and 1) was computed. The growth coefficient was defined such that it would be negative for shrinking boutons and positive for growing boutons, while its magnitude would be a measure for the extent of bouton growth or shrinkage (see section 5.7). A cumulative distribution of the growth coefficient furthermore indicates the fraction of shrinking boutons at its crossing with the vertical axis.

Although the population of persistent boutons did not grow or shrink significantly (average growth coefficient = -0.002 ± 0.009), individual boutons showed significant growth or shrinkage (Figure 12 A). Interestingly, the fraction of shrinking boutons was found to be largest for boutons co-localizing with gephyrin alone (68 %), while it was smallest for boutons co-localizing with VGAT alone (46 %; Figure 12 B). Accordingly, the average growth coefficient showed a tendency for being larger in VGAT-positive boutons and smaller in gephyrin-positive boutons (VGAT: 0.035 ± 0.021; gephyrin: -0.046 ± 0.056). Boutons containing both VGAT and gephyrin seemed to favor neither growth nor shrinkage (fraction of shrinking boutons: 52 %; average growth coefficient: -0.007 ± 0.010). These data demonstrate that VGAT containing boutons tend to grow, while gephyrin containing boutons tend to shrink. Analysis of the 25 % most growing and shrinking boutons for each marker category supports this notion. Boutons co-localizing only with VGAT were growing most strongly, while boutons co-localizing only with gephyrin were shrinking most strongly. Boutons containing both pre- and postsynaptic markers were growing and shrinking least, despite having the largest volume. This is in agreement with the interpretation that they represent rather mature and stable synapses, which exchange only small quantities of material with neighboring synapses (Figure 12 C). Data presented elsewhere (Friedman et al., 2000; Okabe et al., 2001; Wierenga et al., 2008; Dobie and Craig, 2011) suggest that during synapse formation, assembly of the presynapse precedes assembly of the postsynapse. The data presented here support this hypothesis. Boutons co-localizing with VGAT alone are rather prone to grow, suggesting that they are in the process of synapse formation. These boutons do not co-localize with gephyrin yet. Therefore, it is feasible to assume that newly forming GABAergic synapses acquire VGAT before gephyrin. Boutons co-localizing with gephyrin alone are prone to shrink, suggesting that they are in the process of degradation. The lack of VGAT in these shrinking boutons indicates that in the process of degradation, GABAergic synapses loose VGAT before gephyrin.

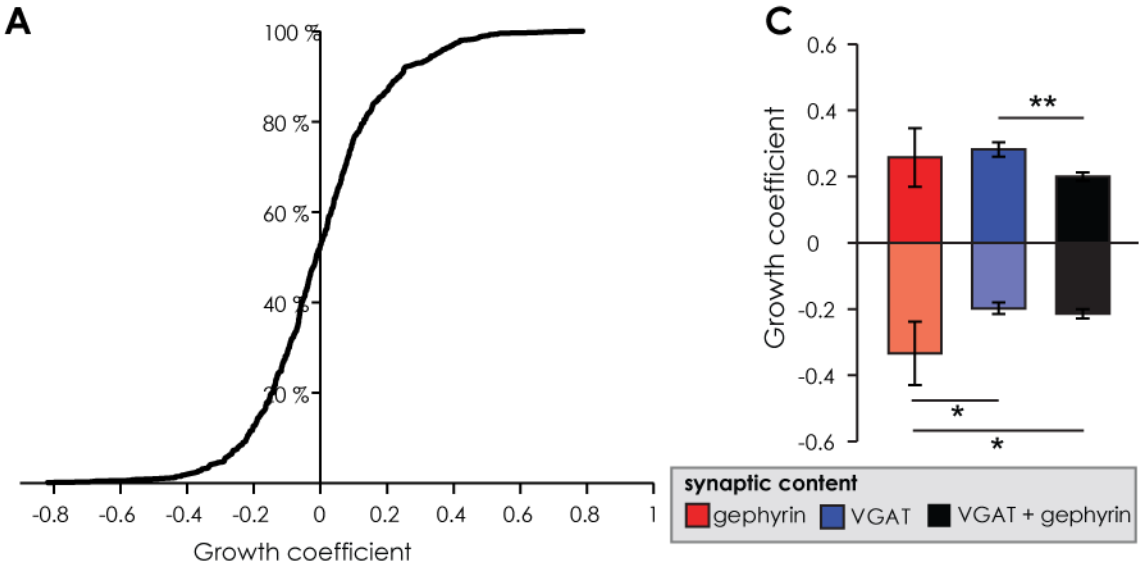

Figure 12 – Relationship between synaptic marker content and persistent bouton volume dynamics (growth coefficient). A. Cumulative distribution of persistent bouton growth coefficient (all persistent boutons). **B.** Cumulative distribution of GABAergic bouton growth coefficient separated by marker content. Red: gephyrin, blue: VGAT, black: both gephyrin and VGAT. **C.** Growth coefficient of the 25 % most growing or shrinking boutons in each staining category. 470 persistent boutons from two separate experiments were included in this analysis.

7. Characterizing structural dynamics of GABAergic axons following manipulations of network activity

7.1 GABAergic bouton turnover and density are changed during acute manipulations of network activity.

Characterization of GABAergic boutons suggested that different bouton categories diverge with respect to their co-localization with synaptic markers (section 6). Persistent boutons seem to represent *bona fide* synapses, while transient boutons might be in the process of formation or degradation, and short-lived boutons seem to embody the transport of (synaptic) material along the GABAergic axon. These different bouton populations might be regulated differently in the face of changing network activity. Furthermore, axonal dynamics – which might represent transport or exchange processes – were suggested to play an important role in synaptic plasticity (Krueger et al., 2003; McAllister, 2007; Staras and Branco, 2010). Therefore, the regulation of bouton populations and axonal dynamics in response to changes in network activity were tested in GABAergic neurons.

Network activity in hippocampal slice cultures was manipulated with two different drugs. To reduce activity, slices were treated with 0.1 µM TTX throughout the 4 h imaging period. The pufferfish toxin TTX is a sodium channel blocker (Narahashi et al., 1960), and consequently prevents the generation of action potentials. To enhance activity, slices were treated with 50 µM 4-AP, a potassium channel blocker (Pelhate and Pichon, 1974). Blocking potassium channels prolongs the repolarization phase of the action potential and thereby reduces the action potential threshold for a longer time (consequently promoting increased action potential firing). While the slice cultures were subjected to enhanced or reduced network activity, GABAergic axons were monitored with time-lapse two photon imaging (4 h, 30 min intervals).

Bouton formation and degradation could be observed frequently along the imaged axons. In control-treated slice cultures, this bouton turnover amounted to 8.0 ± 0.2 % bouton gain and 8.7 ± 0.4 % bouton loss between consecutive time points. Reducing network activity with TTX significantly decreased bouton turnover (bouton gain: 80.9 ± 8.5 %, bouton loss: 73.4 ± 8.1 % of control values; $p = 0.073$ and $p = 0.009$, respectively), while enhancing network activity with 4-AP increased bouton turnover (bouton gain: 124.5 ± 7.7 %, bouton loss: 135.4 ± 11 % of control values; $p = 0.089$ and $p = 0.041$, respectively) (Figure 13 A).

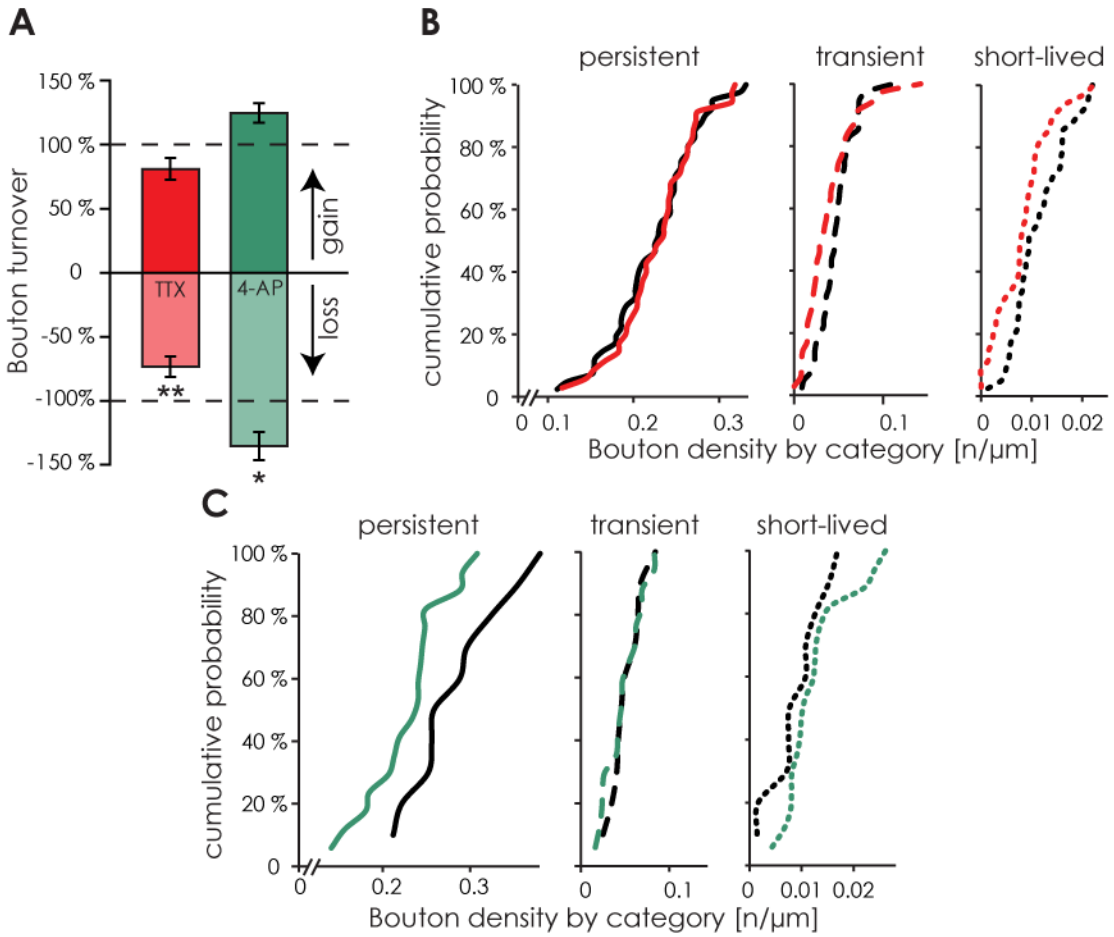

Figure 13 – Acute changes in network activity manipulate GABAergic bouton dynamics. A. GABAergic bouton gain and loss following 4 h reduction of network activity with TTX (red bars) or 4 h increase of network activity with 4-AP (green bars), normalized to control. **B.** Cumulative distribution of the density of persistent (solid lines), transient (dashed lines), and short-lived boutons (dotted lines) during 4 h treatment with TTX (red) or control ACSF (black). **C.** Cumulative distribution of the density of persistent, transient, and short-lived boutons during acute treatment with 4-AP (green) or control ACSF (black). TTX series: Control: 41 axons, TTX: 34 axons; 4-AP series: control: 10 axons, 4-AP: 17 axons.

The observed alterations in bouton turnover could be attributable to modifications of any of the identified bouton populations. Therefore, density and fraction of persistent, transient, and short-lived boutons were analyzed in treated slice cultures and untreated sister cultures (controls). Blocking activity with TTX did not affect the density of persistent boutons (Figure 13 B; average values: control: 22.4 ± 0.8, TTX: 22.8 ± 0.8 boutons per 100 µm axon, $p = 0.74$). However, axons tended to have lower densities of transient and short-lived boutons (Figure 13 B; average values: transient boutons: control: 4.7 ± 0.3, TTX: 3.9 ± 0.5 boutons per 100 µm axon, $p = 0.16$; short-lived boutons: control: 1.1 ± 0.1, TTX: 0.8 ± 0.1 boutons per 100 µm axon, $p = 0.01$). Consequently, this resulted in an increase of the fraction of persistent boutons, while the fraction of transient and short-lived boutons was decreased, indicating a stabilizing effect of decreased network activity

on GABAergic axons (persistent boutons: control: 61.4 ± 1.6 %, TTX: 69.3 ± 2.6 %, p = 0.009; transient boutons: control: 20.2 ± 1.3 %, TTX: 17.5 ± 1.7 %, p = 0.21; short-lived boutons: control: 18.5 ± 1.2 %, TTX: 13.2 ± 1.5 %, p = 0.006).

Quite the opposite situation was observed following treatment with 4-AP. This treatment induced a strong reduction in the density of persistent boutons and a clear trend for an increase in the density of short-lived boutons (Figure 13 C; average values: persistent boutons: control: 28.4 ± 1.8, 4-AP: 22.9 ± 1.1 boutons per 100 μm axon, p = 0.01; transient boutons: control: 5.3 ± 0.6, 4-AP: 4.9 ± 0.5 boutons per 100 μm axon, p = 0.66; short-lived boutons: control: 0.9 ± 0.1, 4-AP: 1.3 ± 0.2 boutons per 100 μm axon, p = 0.16). As a result, the fraction of persistent boutons was decreased in 4-AP treated axons, at the expense of short-lived boutons (persistent boutons: control: 67.9 ± 2.9 %, 4-AP: 60.2 ± 1.9 %, p = 0.03; transient boutons: control: 19.4 ± 1.9 %, 4-AP: 20.5 ± 2.1 %, p = 0.73; short-lived boutons: control: 12.7 ± 2.2 %, 4-AP: 19.3 ± 1.7 %, p = 0.03).

The data presented here demonstrate an opposite regulation of GABAergic bouton turnover in response to decreased and increased network activity, respectively. Note that these effects might be mechanistically different: while activity deprivation mainly reduces transient and short-lived boutons, enhancing activity appears to destabilize persistent boutons.

7.2 GABAergic bouton volumes are only partially affected by acute manipulations of network activity.

Data presented here (Figure 11) show that boutons co-localizing with both pre- and postsynaptic markers are on average larger than their counterparts that co-localize with less synaptic markers. This suggests that larger boutons are more likely to represent functional synapses. Other studies have reached similar conclusions by correlation presynaptic bouton volume with synaptic strength (Schikorski and Stevens, 1997; Weyhersmuller et al., 2011). The analysis of boutons volumes can therefore yield important information about synaptic strength or even function. Consequently, bouton volumes were analyzed following 4 h manipulations of network activity to reveal plasticity mechanisms acting on the level of synaptic strength rather than synapse formation.

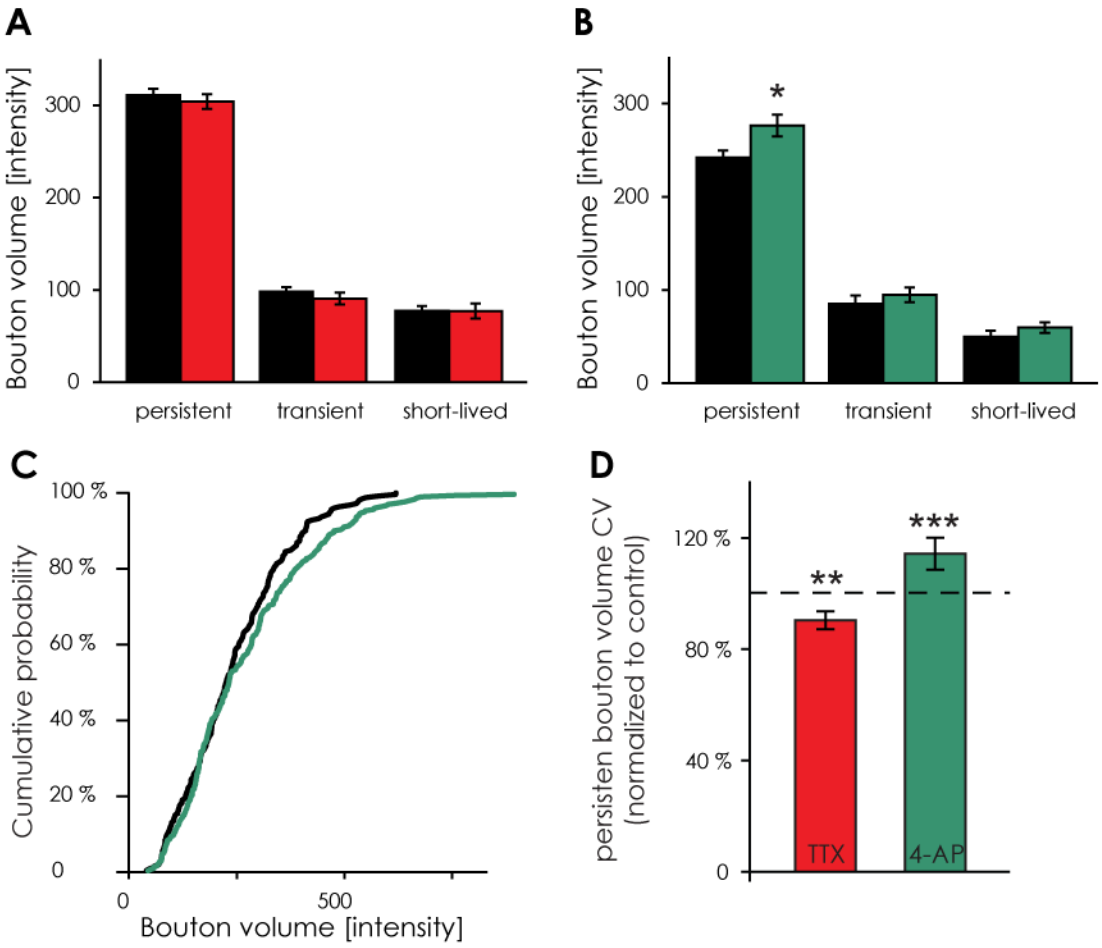

Figure 14 - Acute changes in network activity partially affect GABAergic bouton volumes. A. Volume of persistent, transient, and short-lived boutons during 4 h treatment with TTX (red bars) or control ACSF (black bars). **B.** Volume of persistent, transient, and short-lived boutons during 4 h treatment with 4-AP (green bars) or control ACSF. **C.** Cumulative distribution of average persistent bouton volumes during 4 h 4-AP treatment. **D.** CV of persistent bouton volume during 4 h treatment with TTX (red bar) or 4-AP (green bar), normalized to the respective control values (dashed line). Same datasets as in Figure 13.

As in control bouton populations, persistent boutons were on average 3-fold larger than transient or short-lived boutons during treatment with TTX or 4-AP. Bouton volumes were largely unaffected by changes in network activity (Figure 14 A, B; TTX experiment series: persistent boutons: control: 311 ± 7, TTX: 304 ± 8, $p = 0.51$; transient boutons: control: 98 ± 5, TTX: 91 ± 6, $p = 0.36$; short-lived boutons: control: 77 ±5, TTX: 77 ± 8, $p = 0.97$; 4-AP experiment series: persistent boutons: control: 242 ± 8, 4-AP: 276 ± 12, $p = 0.02$; transient boutons: control: 85 ± 9, 4-AP: 95 ± 8, $p = 0.42$; short-lived boutons: control: 50 ± 7, 4-AP: 60 ± 6, $p = 0.46$). However, a small but specific volume increase in the fraction of large persistent boutons was observed in response to 4-AP treatment (Figure 14 C). This might reflect either an acute strengthening of existing synapses, or a specific loss of small persistent boutons. To get a better idea which of the above scenarios is happening during

acute 4-AP treatment, control volume data were modulated in different ways to mimic these scenarios. Removing the smallest persistent boutons from the control dataset until the average density matched that of the 4-AP dataset resulted in a different cumulative volume distribution as observed in the 4-AP dataset (Figure 14 C, Figure 15 A). However, reducing bouton density globally and increasing the volume of the largest 50% of the boutons by additive growth (i.e. adding the same amount of volume to each bouton) resulted in a similar cumulative distribution (Figure 15 B).

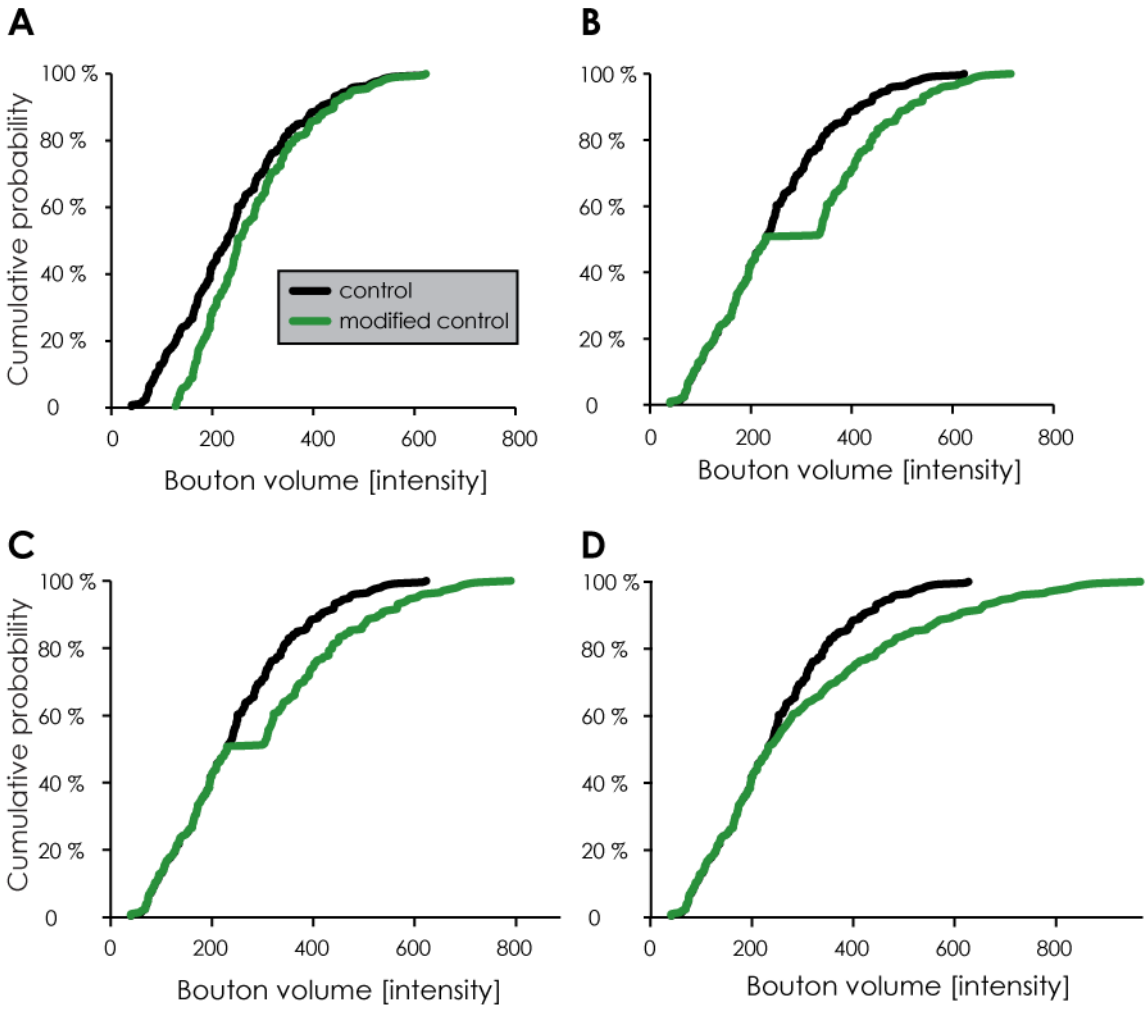

Figure 15 - Scenarios of persistent bouton volume changes induced by acute 4-AP treatment. **A.** The control boutons from the 4-AP dataset (black line; Figure 13) were modified (green line) such that the smallest persistent boutons were lost to achieve a density as measured during 4-AP treatment. **B.** The modification of control boutons consisted of a general loss of boutons (to achieve the density measured during 4-AP treatment), accompanied by an additive growth of large persistent boutons (adding the same amount of volume units to each large persistent bouton). Control volumes: black line, modified control volumes: green line. **C.** The modification of control boutons consisted of a general loss of control boutons (to achieve the density measured during 4-AP treatment), accompanied by a multiplicative growth of large persistent boutons (multiplication of the volume with the same factor). **D.** The modification of control boutons consisted of a general loss of control boutons, accompanied by a multiplicative growth of large persistent boutons that was proportionate to the initial volume (larger bouton volumes were multiplied with a larger factor than the smaller boutons).

Furthermore, reducing bouton density globally and increasing bouton volume by multiplication with the same factor resulted in a more similar distribution (multiplicative growth; Figure 15 C). Finally, increasing the volume of the largest 50% of the boutons such that larger boutons grew stronger than smaller boutons, came even closer to the real data (Figure 15 D). This growth was achieved by multiplying the initial volume of the boutons with a factor that was linearly increasing from the smallest to the largest bouton. The average over all factors was equal to the factor used for multiplicative growth shown in Figure 15 C. Therefore, it is reasonable to assume that acute 4-AP treatment increases the volume of larger boutons proportionally to their initial volume. Together with increased bouton turnover and a reduction in the density of persistent boutons, these data support the idea that enhanced activity results in an increased exploration of novel synaptic partners (more dynamic boutons). Particularly strong (i.e. large) synapses, however, are stabilized and grow even further.

Unlike bouton volumes, the variations of bouton volume were affected by changes in network activity. During treatment with TTX, the CV of persistent boutons was decreased, suggesting a reduced material transport into and out of GABAergic synapses. Conversely, the CV of persistent bouton volume was increased during treatment with 4-AP, suggesting increased material transport along the GABAergic axon (Figure 14 D; TTX: 90.4 ± 3.2 % of control values, $p = 0.007$; 4-AP: 114.3 ± 5.7 % of control values, $p = 0.003$). Note that changes in persistent bouton volume CV go hand in hand with the effects of network activity on bouton turnover. Bouton stabilization, as observed during TTX treatment, would require less material transport along the axon. This hypothesis is supported by the reduction in persistent bouton volume CV, which might reflect such transport events. In turn, the destabilization of GABAergic synapses as it was observed during 4-AP treatment would predict enhanced material transport along the axon. Again, this hypothesis is supported by an increase in persistent bouton volume CV. The data presented here therefore suggest that not only bouton stability but also material transport along the axon are affected by changes in network activity.

7.3 GABAergic bouton turnover and density are not affected by prolonging manipulations of network activity to 48 h.

Changes in GABAergic bouton dynamics (Bouton turnover, CV of bouton volume) might affect the rate of bouton formation or degradation. Consequently, changes in bouton dynamics might translate into changes of bouton density after a few days, to change the overall level of inhibition in the slice culture.

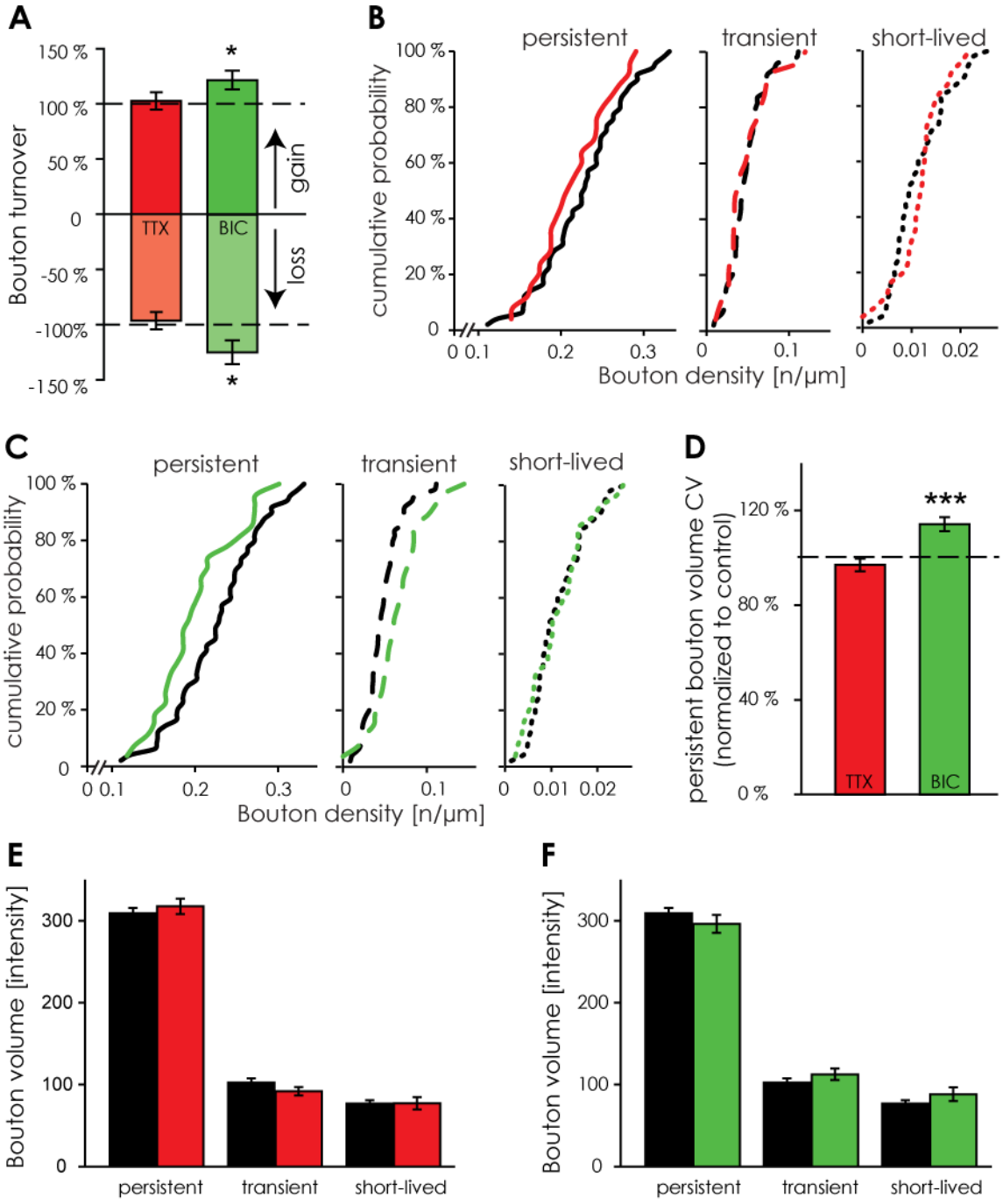

Figure 16 - Effects of 48 h manipulations of network activity on GABAergic boutons. A. GAB-Aergic bouton gain and loss following 48 h treatment with TTX (red bar) or bicuculline (green bar). **B.** Density of persistent (solid lines), transient (dashed lines) and short-lived (dotted lines) GABAergic boutons following 48 h treatment with TTX (red) or control ACSF (black). **C.** Density of persistent, transient and short-lived boutons following 48 h treatment with bicuculline (green) or control ACSF (black). **D.** CV of persistent bouton volume following 48 h treatment with TTX (red bar) or bicuculline (green bar), represented as a fraction of control values. **E and F.** Bouton volume of persistent, transient, and short-lived boutons following 48 h treatment with TTX (**E**, red bars) or bicuculline (**F**, green bars) compared to control treated sister slice cultures (black bars). Control: 49 axons, TTX: 25 axons, Bicuculline: 27 axons.

Several *in vivo* studies have reported a reduction in inhibitory bouton density after the reduction of sensory input, suggesting that similar changes will occur upon a

reduction of neuronal activity in culture, as well (Rosier et al., 1995; Marik et al., 2010; Chen et al., 2011; Keck et al., 2011). However, in dissociated cell cultures, such an effect on synapse density seems to be rather of a developmental nature, as experiments with older cultures did not reveal an effect of network activity on bouton density (Marty et al., 2004; Kuriu et al., 2011; Rannals and Kapur, 2011). It is not clear, whether changes in the density of GABAergic synapses are specific for intact animals, e.g. if sensory input is required for such drastic changes, or if it represents a general mechanism of intact neural tissue to cope with changed activity levels. Therefore, organotypic hippocampal cultures were subjected to 48 h manipulations of network activity before performing time-lapse two-photon imaging experiments as described before.

Following two days of decreased activity (0.1 μM TTX), bouton turnover was not distinguishable from control (Figure 16 A; bouton gain: 102.7 ± 7.9 %, boutons loss: 96.5 ± 7.9 % of control values, $p = 0.77$ and $p = 0.73$, respectively). In addition, neither persistent, nor transient or short-lived boutons showed a difference in density (Figure 16 B; average values: persistent boutons: control 22.7 ± 0.7, TTX: 21.4 ± 0.9 boutons per 100 μm axon, $p = 0.31$; transient boutons: control 4.8 ± 0.3, TTX: 4.7 ± 0.5 boutons per 100 μm axon, $p = 0.98$; short-lived boutons: control 1.1 ± 0.1, TTX: 1.2 ± 0.1 boutons per 100 μm axon, $p = 0.84$). Finally, analyzing boutons volumes did not reveal differences between control and untreated sister cultures with respect to either bouton volume or the CV of persistent bouton volume (Figure 16 D, E; CV: 96.7 ± 2.8 % of control values, $p = 0.32$).

Treating the slice cultures with 50 μM 4-AP for 48 h, strongly impaired slice health. Therefore, network activity was increased with 20 μM bicuculline, a $GABA_A$ receptor antagonist (Curtis et al., 1970). This did not impair slice health within the first 48 h of treatment. In contrast to treatment with 4-AP, acute (4 h) treatment with bicuculline did affect neither GABAergic bouton turnover (Figure 17 A; bouton gain: 94.9 ± 9.2 %, bouton loss: 90.7 ± 8.6 % of control values, $p = 0.65$ and $p = 0.39$, respectively) nor density (Figure 17 B; average values: persistent boutons: control 22.4 ± 0.8, bicuculline: 20.7 ± 0.9 boutons per 100 μm axon, $p = 0.17$; transient boutons: control 4.7 ± 0.3, bicuculline: 4.4 ± 0.5 boutons per 100 μm axon, $p = 0.55$; short-lived boutons: control 1.1 ± 0.1, bicuculline: 1.0 ± 0.1 boutons per 100 μm axon, $p = 0.39$). In contrast to these negligible effects of acute bicuculline treatment, 48 h bicuculline treatment led to a strong increase in bouton turnover (Figure 16 A; bouton gain: 121.3 ± 8.5 %, bouton loss: 123.6 ± 10.8 % of control values, $p = 0.04$ and $p = 0.04$, respectively). Analogous to the effects of acute 4-AP treatment, 48 h bicuculline treatment also decreased the density of persistent boutons, while the density of transient boutons was increased (Figure 16 C; average values: persistent boutons: control 22.7 ± 0.7, bicuculline: 20.1 ± 0.9 boutons per 100 μm axon, p =

0.03; transient boutons: control 4.8 ± 0.3, bicuculline: 6.5 ± 0.6 boutons per 100 µm axon, p = 0.01; short-lived boutons: control 1.1 ± 0.1, bicuculline: 1.1 ± 0.1 boutons per 100 µm axon, p = 1.0). In addition, persistent bouton volume CV was increased (Figure 16 D; 115.0 ± 4.0 % of control values, p < 0.005). These data resemble those obtained during acute 4-AP treatment (see Figure 13, 14). As bicuculline has no acute effect on GABAergic bouton dynamics, these data might suggest a role for the activation of $GABA_A$ receptors in mediating a fast response of GABAergic axon structure to enhanced activity.

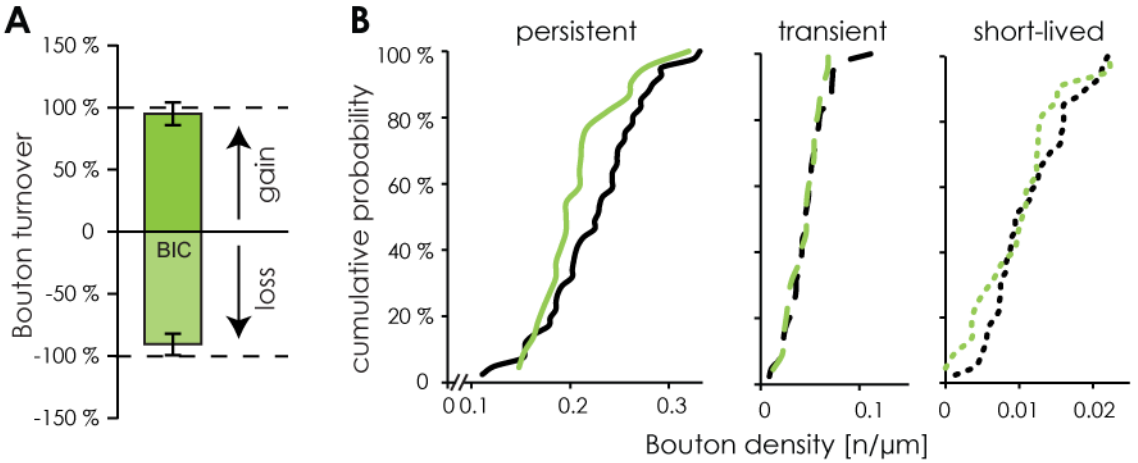

Figure 17 - GABAergic bouton turnover or density were not affected by 4 h treatment with bicuculline. A. Turnover of GABAergic boutons does not differ between 4 h treatment with bicuculline or control ACSF. **B.** Cumulative distribution of the density of persistent (solid line), transient (dashed line), and short-lived boutons (dotted line) during 4 h bicuculline treatment (green lines) if compared to treatment with control ACSF (black lines). Control: 41 axons, bicuculline: 22 axons.

In summary, the data presented here suggest that after 48 h, GABAergic axons in a slice culture cope with reduced network activity by other than structural plasticity mechanisms. These mechanisms might include changes in release probability or postsynaptic receptor density, or changes in other pre- or postsynaptic proteins (De Gois et al., 2005; Saliba et al., 2007; Saliba et al., 2009; Peng et al., 2010; Rannals and Kapur, 2011). Of course, it is possible that changes in bouton density need more time to build up and were therefore not recorded in these experiments. For enhanced network activity, the situation is less clear, due to (a) diverging effects of the two activity-enhancing drugs 4-AP and bicuculline, and (b) because of excitotoxicity induced by long-term increases in network activity.

7.4 GABAergic bouton density is not affected by 7 d manipulations of network activity.

Although *in vivo* studies suggest a regulation of GABAergic bouton density already after 24 h (Keck et al., 2011), it is possible that in organotypic slice cultures changes in GABAergic bouton density take more time to build up, for instance due to a dilution of diffusible signaling molecules. To exclude that such effects are being overlooked, bouton density of individual axons was analyzed after 7 days of TTX treatment. No difference in bouton density was found after 7 days of TTX treatment if compared to control treatment (control: 28.9 ± 1.2, TTX: 27.4 ± 0.9 boutons per 100 μm axon, $p = 0.29$), suggesting that other than structural plasticity mechanisms are the main motor of plasticity under these circumstances. Unexpectedly, GABAergic boutons were slightly larger following seven days of TTX treatment then after control treatment (control: 248.6 ± 12.7, TTX: 284.9 ± 10.8 [normalized total intensity], $p = 0.03$). This surprising finding might be explained by the differences in bouton threshold observed in this particular dataset. Unlike in other datasets, here the threshold used to distinguish a bouton from the axonal shaft was different between control and TTX treated slice cultures (control: 6650 ± 280, TTX: 5040 ± 310, $p < 0.005$). These differences in bouton threshold will affect the normalization of bouton volume which might change bouton volume measurements.

The population of axons in Gad65-GFP hippocampal slices is very heterogeneous, reflecting various interneuron types (Wierenga et al., 2010). It is therefore possible that the high variability in axon morphology masked some effects on bouton density. To exclude such effects, the same axon was imaged in the beginning and at the end of the activity manipulation (day 1 and day 7). In this experimental paradigm, the slice culture has to be transferred to the recording chamber twice. As the chamber is not a sterile environment, it was impossible to avoid contamination of the slice cultures between the first (day 1) and the second (day 7) imaging time point. If this dataset was limited to data from slices that exhibited only mild symptoms of an infection (judged by visual examination), these experiments did not reveal a difference between TTX and control treated axons with respect to bouton density (Figure 18 A; density day 1/density day 7: control: 93.1 ± 3.6 %, TTX: 88.8 ± 6.3 %, $p = 0.53$). In addition, average bouton growth or shrinkage between the two imaging time points (growth coefficient, see methods for details) was not different between the two treatments (Figure 18 B; average values: control: 0.02 ± 0.03, TTX: 0.02 ± 0.03, $p = 0.97$). Note that the mild infection of the slices might interfere with the recorded data. To draw dependable conclusions from this

dataset, the experiments should be repeated in a sterile environment where infections can be avoided.

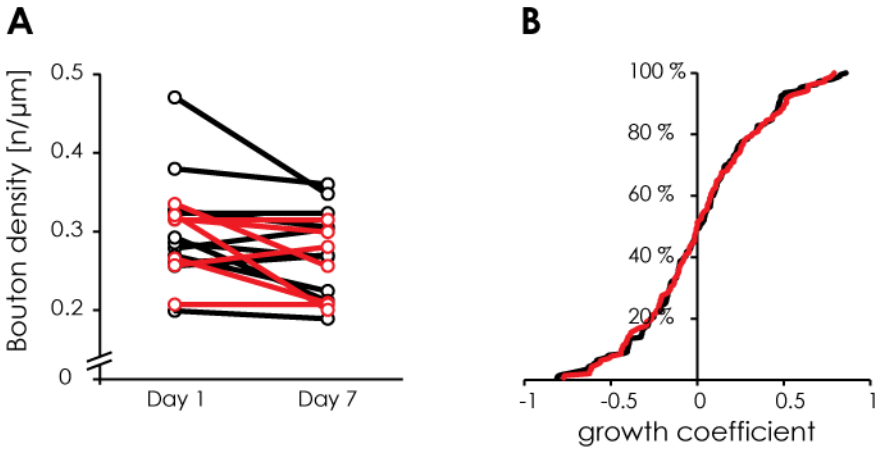

Figure 18 - 7 d activity blockade has no effect on GABAergic bouton density or volume. A. Comparison of bouton density at the beginning and the end of a 7 d treatment period with TTX. **B.** Growth coefficient of boutons found both in the beginning and at the end of a 7 d treatment period with TTX (red curve) or control ACSF (black curve). Control: 11 axons, TTX: 7 axons.

These data are consistent with data from dissociated neurons (De Gois et al., 2005; Saliba et al., 2007; Saliba et al., 2009; Peng et al., 2010; Rannals and Kapur, 2011), and suggest that other than structural plasticity mechanisms govern the response of GABAergic axons to changes in network activity in organotypic hippocampal slice cultures.

8. A role for the activation of $GABA_A$ receptors in structural plasticity of GABAergic axons

8.1 $GABA_A$ receptor activation is necessary for the 4-AP induced destabilization of GABAergic boutons.

Unlike acute application of 4-AP, acute application of 20 μM bicuculline had no effect on GABAergic bouton turnover or density in organotypic hippocampal slice cultures (Figure 17). It is possible that the lack of an effect during acute bicuculline treatment is due to an off-target effect of bicuculline (e.g. blocking calcium-dependent potassium channels in addition to $GABA_A$ receptors (Johansson et al., 2001)). To exclude such side effects, the experiment was repeated with 10 μM gabazine (a highly specific $GABA_A$ receptor blocker (Chambon et al., 1985; Heaulme et al., 1986; Hamann et al., 1988)). However, gabazine failed to change the structural dynamics of GABAergic axons, too: neither bouton turnover (Figure 19 A; bouton gain: 118.8 ± 13.0 %, bouton loss: 90.6 ± 11.0 % of control values, p = 0.33 and p = 0.60, respectively), nor density of persistent, transient, or short-lived boutons were significantly altered during a 4 h treatment with the drug (Figure 19 B; average values: persistent boutons: control: 23.7 ± 1.7, gabazine: 23.1 ± 1.3 boutons per 100 μm axon, p = 0.76; transient boutons: control: 3.8 ± 0.6, gabazine: 4.8 ± 0.7 boutons per 100 μm axon, p = 0.33; short-lived boutons: control: 0.9 ± 0.1, gabazine: 1.1 ± 0.2 boutons per 100 μm axon, p = 0.49).

These findings indicate a role for $GABA_A$ receptor activation in the induction of structural GABAergic plasticity by enhanced activity. However, it is also possible that neither the application of bicuculline nor gabazine increased neuronal activity to the same extent as 4-AP, and therefore a measurable effect on GABAergic boutons required more time to build up. This view would be supported by the lower excitotoxicity observed during 48 h bicuculline treatment if compared to 48 h 4-AP treatment and by the similar effect on GABAergic bouton dynamics that 48 h bicuculline treatment and 4 h 4-AP treatment evoked. As a consequence, 50 μM 4-AP and 20 μM bicuculline were co-applied to hippocampal slice cultures. Remarkably, 4 h of this treatment did not affect GABAergic bouton turnover (Figure 19 C; bouton gain: 89.6 ± 10.4 %, bouton loss: 81.1 ± 11.1 % of control values, p = 0.57 and p = 0.26, respectively) or density (Figure 19 D; average values: persistent boutons: control: 28.5 ± 1.8, 4-AP + bicuculline: 27.1 ± 1.2 boutons per 100 μm axon, p = 0.52; transient boutons: control: 4.6 ± 0.7, 4-AP + bicuculline: 4.6 ± 0.6 boutons per 100 μm axon, p = 0.98; short-lived boutons: control: 1.0 ± 0.2, 4-AP + bicuculline: 0.9 ±

0.1 boutons per 100 µm axon, p = 0.55), suggesting that either a $GABA_A$ receptor mediated mechanism is involved in structural GABAergic plasticity, or that bicuculline reduces the effect of 4-AP on network activity.

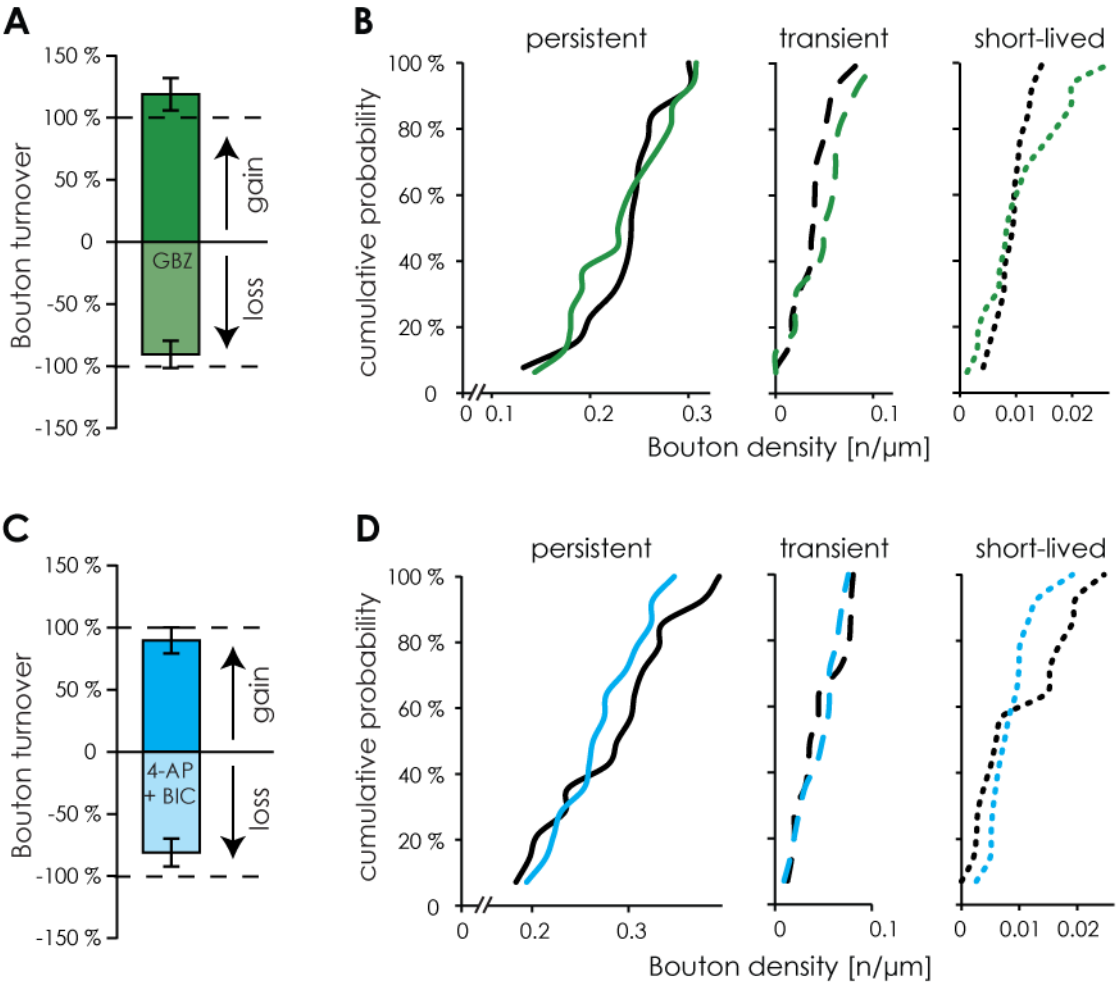

Figure 19 - Bouton turnover and density following 4 h treatment with gabazine or the combination of 4-AP and bicuculline. A. Bouton turnover during 4 h treatment with gabazine does not differ from treatment with control ACSF. **B.** Cumulative distribution of the density of persistent (solid lines), transient (dashed lines), and short-lived (dotted lines) boutons during 4 h gabazine treatment compared to treatment with control ACSF. **C.** Bouton turnover during 4 h treatment with 4-AP and bicuculline does not differ from treatment with control ACSF. **D.** Cumulative distribution of the density of persistent, transient, and short-lived boutons during 4 h 4-AP + bicuculline treatment compared to treatment with control ACSF. GABAzine series: Control: 13 axons, gabazine: 16 axons; 4-AP+bicuculline series: control: 14 axons, 4-AP+bicuculline: 14 axons.

8.2 Bicuculline does not lessen the effect of 4-AP on network activity.

Under certain circumstances, 4-AP might be able to reverse the driving force for chloride, thus making GABA an excitatory neurotransmitter (Lamsa and Taira, 2003; Zhu et al., 2008). If this were the case, co-application of 4-AP and bicuculline would reduce activity levels in hippocampal slice cultures below the activity in slices treated with 4-AP

alone. In this scenario, the blockade of $GABA_A$ receptors by bicuculline would prevent further GABA-mediated excitation of the neurons. Such a situation could also explain the divergent results on GABAergic bouton dynamics obtained from 4-AP and bicuculline treated slices. To test this hypothesis, network activity was measured with two different methods in hippocampal slice cultures that were subjected to treatment with 4-AP, bicuculline, or both substances.

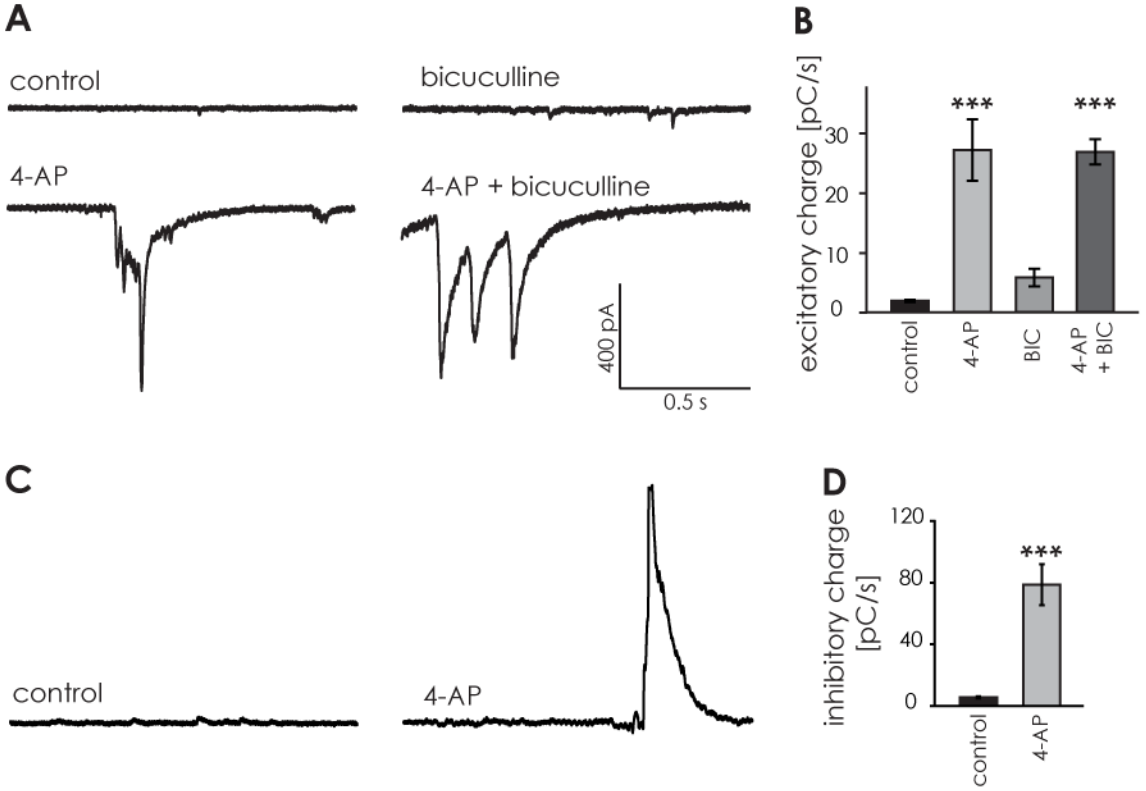

Figure 20 - Spontaneous network activity during treatment with 4-AP and/or bicuculline. A. Whole-cell recordings from visually identified CA1 pyramidal cells during different pharmacological treatments. Recordings were made at the reversal potential for inhibitory currents (-44 +/- 1.3 mV) to isolate spontaneous excitatory postsynaptic currents. **B.** Average total charge of spontaneous excitatory postsynaptic currents in CA1 pyramidal cells during treatment with different drugs. **C.** Whole-cell recordings from visually identified CA1 pyramidal cells during 4-AP and control treatment. Recordings were made at the reversal potential for excitatory currents (4.2 +/- 1.7 mV) to isolate spontaneous inhibitory postsynaptic currents. **D.** Average total charge of spontaneous inhibitory postsynaptic currents in CA1 pyramidal cells during treatment with 4-AP or control ACSF. Excitatory inputs: control: 17 cells, 4-AP: 15 cells, bicuculline: 13 cells, 4-AP + bicuculline: 13 cells; inhibitory inputs: control: 15 cells, 4-AP: 13 cells, bicuculline: 8 cells, 4-AP + bicuculline: 10 cells.

As a first test, spontaneous excitatory and inhibitory currents were recorded from visually identified CA1 pyramidal neurons in hippocampal slice cultures. The slices were treated in the same way as during the 4 h imaging experiments. Both bicuculline and 4-AP were found to enhance excitatory synaptic input to the neurons, and 4-AP did so in a much more pronounced way. Importantly, when slices were treated with bicuculline

and 4-AP simultaneously, the increase in synaptic current was comparable to that evoked by 4-AP alone (Figure 20 A, B; control: 1.8 ± 0.2, 4-AP: 27.1 ± 5.1, bicuculline: 5.7 ± 1.6, 4-AP + bicuculline: 26.8 ± 2.1 [pC/s], $p < 0.005$). Inhibitory currents could not be measured when they were inhibited by the presence of bicuculline in the bath. 4-AP treatment alone, however, strongly enhanced inhibitory currents onto CA1 pyramidal cells, as well (~14-fold increase; Figure 20 C, D; control: 5.5 ± 0.7, 4-AP: 78.7 ± 13.2 [pC/s], $p < 0.005$). In contrast to slices treated with bicuculline alone, large synchronous excitatory events were recorded almost exclusively in slices treated with 4-AP or 4-AP and bicuculline together.

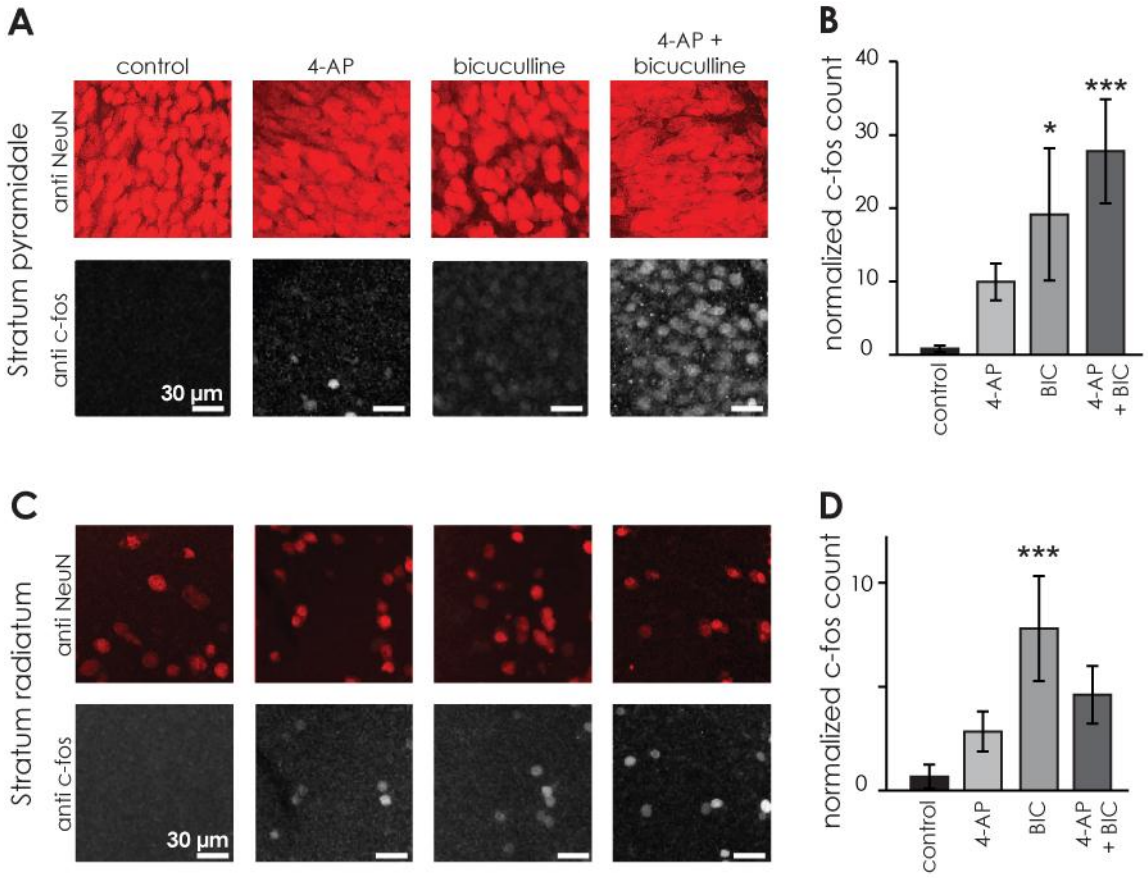

Figure 21 - C-fos activation following 4 h treatment with 4-AP and/or bicuculline. A. Immunohistochemistry for activation the immediate early gene c-fos in CA1 stratum pyramidale, co-stained with antibodies against the neuronal marker NeuN to visualize neuronal cell bodies. **B.** Cell count of c-fos positive cells in the CA1 stratum pyramidale normalized to the total intensity of the NeuN staining. **C.** Immunohistochemistry for c-fos activation and NeuN in CA1 stratum radiatum. **D.** Cell count of c-fos positive cells in the CA1 stratum pyramidale normalized to the total intensity of the NeuN staining. Control: 9 slices, 4-AP: 8 slices, bicuculline: 10 slices, 4-AP + bicuculline: 10 slices.

As a second measure for network activity, c-fos expression was assessed using post-hoc immunohistochemistry after a 4 h treatment period with either pharmacological agent or a control solution. C-fos is a transcription factor encoded by an immediate early

gene, which is activated following neuronal activity. This method has been widely used to monitor activity levels in the brain or to identify previously active neurons (Dragunow and Faull, 1989; Tischmeyer and Grimm, 1999; Schoenenberger et al., 2009; Clark et al., 2010; Rinaldi et al., 2010). C-fos levels were increased by either bicuculline or 4-AP in both *stratum pyramidale* (Figure 21 A, B; control: 0.8 ± 0.4, 4-AP: 10.0 ± 2.5, bicuculline: 19.2 ± 9.0 ($p = 0.46$ vs. control), 4-AP + bicuculline: 27.8 ± 7.1 ($p < 0.005$ vs. control) normalized cell counts per area) and *stratum radiatum* (Figure 21 C, D; control: 0.7 ± 0.6, 4-AP: 2.8 ± 1.0, bicuculline: 7.8 ± 2.5 ($p < 0.005$ vs. control), 4-AP + bicuculline: 4.6 ± 1.4 normalized cell counts per area) of the CA1 region if compared to control treatment. Combining 4-AP and bicuculline treatment lead to an even stronger increase in c-fos levels.

Both the electrophysiological and the immunohistochemical data confirm that in the experimental system used, the combination of 4-AP and bicuculline strongly enhances network activity. Furthermore, the data demonstrate that bicuculline does not reduce the effect of 4-AP on network activity. Consequently, the differential effects of 4-AP and $GABA_A$ receptor antagonists cannot be explained by differential effects on network activity. Rather, the data suggest a role for $GABA_A$ receptor activation as a sensor for increased network activity.

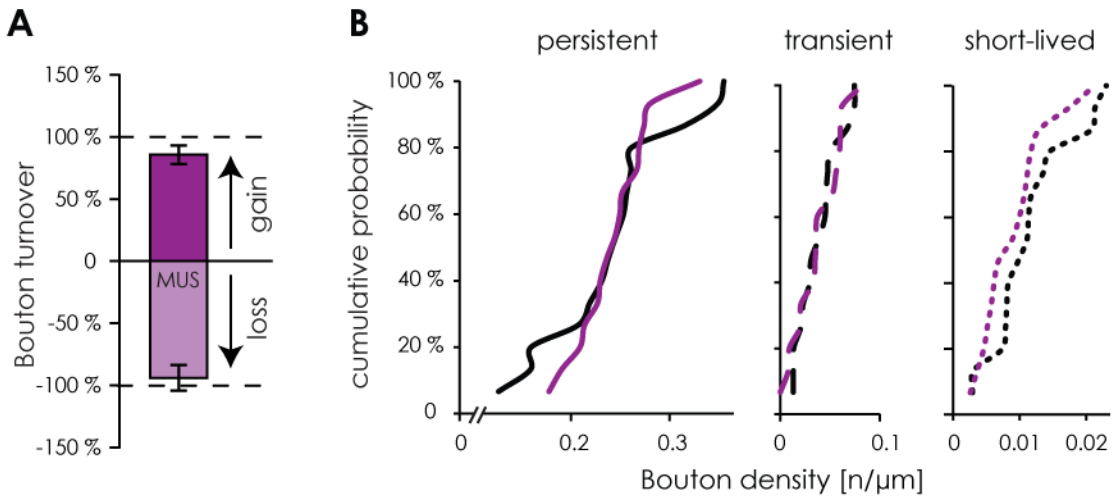

Figure 22 - 4 h treatment with muscimol has no effect on GABAergic bouton turnover or density. A. Bouton turnover during 4 h treatment with muscimol does not differ from treatment with control ACSF. **B.** Density of persistent (solid lines), transient (dashed lines), and short-lived (dotted lines) boutons is not different following 4 h muscimol treatment if compared to treatment with control ACSF. Control: 15 axons, muscimol: 15 axons.

Finally, it was investigated whether the activation of $GABA_A$ receptors alone would be sufficient to destabilize GABAergic boutons. For this purpose, the $GABA_A$ receptor agonist muscimol (10 µM) was applied to the slice cultures. Treatment with muscimol for the course of a 4 h two-photon time-lapse imaging experiment as described

above did affect neither bouton turnover (Figure 22 A; bouton gain: 85.6 ± 7.4, bouton loss: 94.1 ± 10.2 % of control values, $p = 0.26$ and $p = 0.70$, respectively) nor density (Figure 22 B; average values: persistent boutons: control: 24.3 ± 1.7, muscimol: 24.4 ± 1.0 boutons per 100 μm axon, $p = 0.96$; transient boutons: control: 3.9 ± 0.5, muscimol: 3.8 ± 0.6 boutons per 100 μm axon, $p = 0.90$; short-lived boutons: control: 1.2 ± 0.2, muscimol: 0.9 ± 0.1 boutons per 100 μm axon, $p = 0.26$).

In conclusion, only the combination of $GABA_A$ receptor activation and enhanced activity are sufficient to increase GABAergic bouton turnover and destabilize GABAergic axonal structures.

9. Analysis of bouton clustering on GABAergic axons

Recently, several studies have suggested a clustering of structural plasticity and inputs on pyramidal cell dendrites, suggesting that similar inputs (e.g. from the same neuron or the same group of neurons) culminate at the same dendritic segment (De Roo et al., 2008; Kleindienst et al., 2011; Fu et al., 2012). GABAergic axons have a tortuous morphology, probably to establish as many contacts to potential targets as possible. Therefore, it might be possible that inputs to the same postsynaptic target come from the same axonal region, which might touch the same neuron multiple times. These inputs should be regulated in parallel. In this case, boutons with similar dynamics (i.e. persistent and non-persistent boutons) would be spatially close to each other. Spatial clustering of bouton dynamics would also be predicted by spreading of locally generated plasticity signals, as has been suggested for dendritic spines (Frey and Morris, 1997; Govindarajan et al., 2011). However, a competition for limited axonal resources could also prohibit such a clustering.

To test whether persistent and non-persistent boutons were clustered along GABAergic axons, bouton arrangements were analyzed in a population of control axons. For this purpose, bouton locations and categories (persistent and non-persistent) were determined for every axon. Subsequently, the axons were simulated 1000 times with the same locations and the same number of boutons in each category. Consequently, the simulated axons had the same numbers of persistent and non-persistent boutons as experimentally observed axons, only the sequence of boutons was different. Simulated and real axons were then analyzed by different methods to asses both spatial and relative bouton clustering. All analyses were performed on datasets including and excluding short-lived boutons. These two variations of the analysis led to the same conclusions; therefore only one of them (the one including short-lived boutons) is shown here.

9.1 Analysis of relative bouton clustering

To measure the relative distance between two boutons from the same category (persistent or non-persistent), the number different boutons between them was counted (Figure 23 A, $p < 0.005$). As seen in Figure 23 B and C, the experimental data contained less directly adjacent persistent boutons then the simulated data. However, it seemed to contain more persistent bouton pairs with only one or two non-persistent boutons between them. The distribution of non-persistent boutons though, was not different from the simulated data (data not shown).

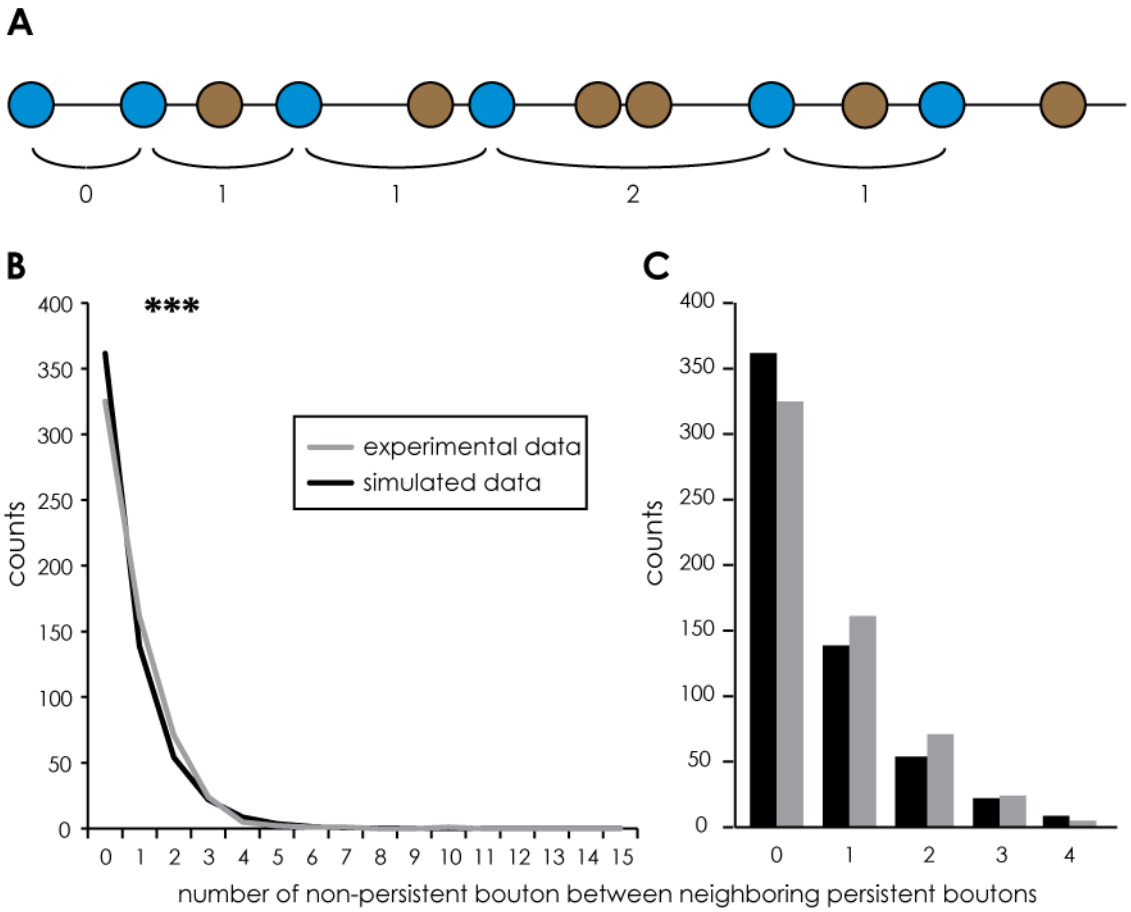

Figure 23 - Relative distances between persistent boutons in experimental and simulated data. **A.** Scheme illustrating the measurement: the number of non-persistent boutons between each pair of neighboring persistent boutons was counted for each axon and the data were pooled. **B.** Distribution of different counts (number of non-persistent boutons between neighboring persistent boutons) for experimental (grey line) and simulated (black line) data. **C.** Sama data as in B, illustrating that in the experimental data, less persistent boutons were direct neighbors (zero non-persistent boutons between them), but arrangements of one or two non-persistent boutons between two adjacent persistent boutons occurred more frequently as expected by a random distribution. 34 control-treated axons were included in this analysis.

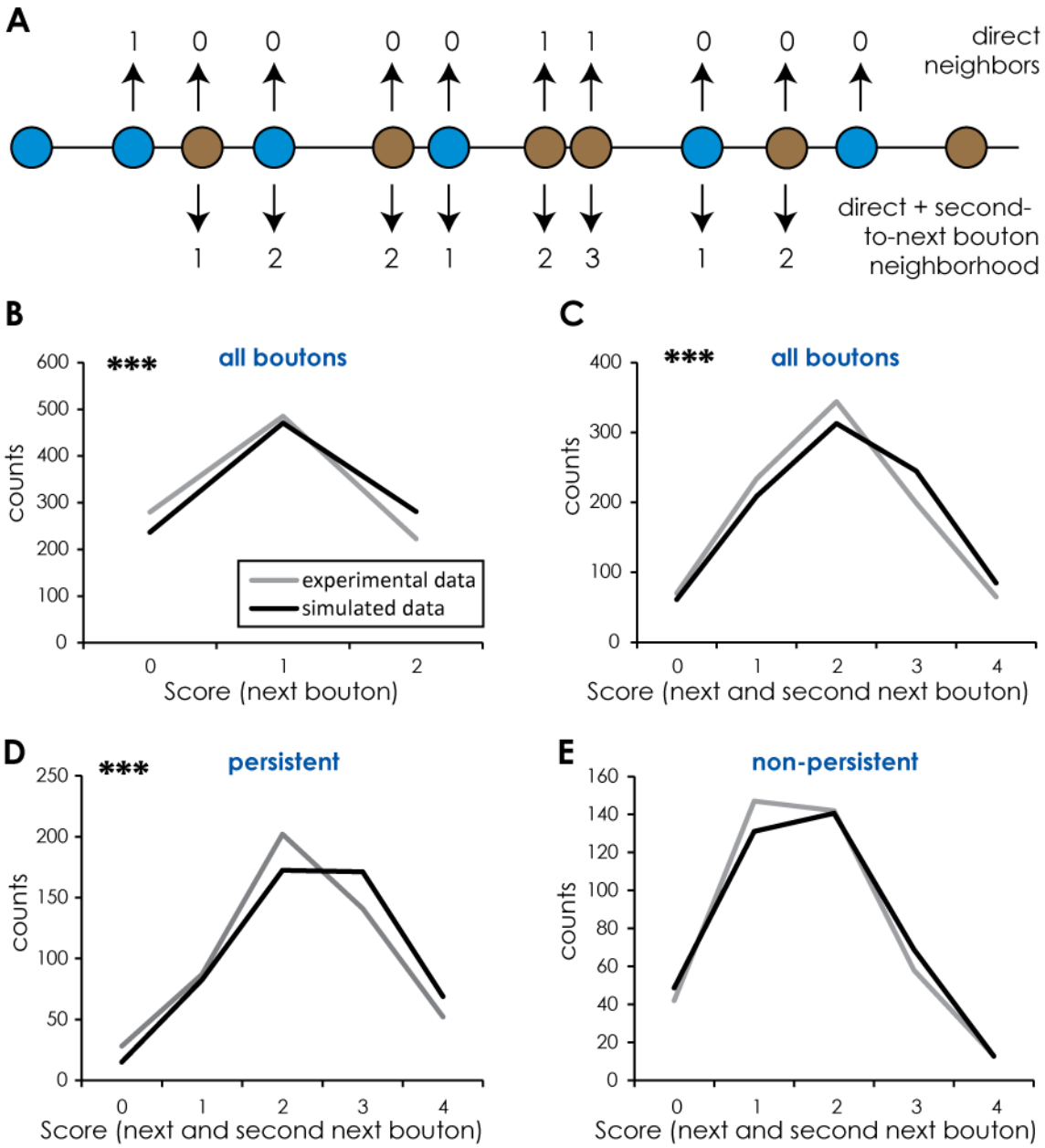

Figure 24 - Analyzing the neighborhood of persistent and non-persistent boutons. A. Schematic illustration of the method. Each bouton was assigned a score based on the number of same-category boutons in its neighborhood. Analysis of only direct neighbors: top, analysis of direct neighbors + second-to-next boutons: bottom. **B.** Distribution of experimental (grey line) and simulated (black line) data from analysis of direct neighbors. **C.** Distribution of experimental and simulated data from analysis of direct neighbors and second-to-next boutons. **D and E.** Distribution of experimental and simulated data from the analysis of direct neighbors + second-to-next boutons in the same bouton category, separated by bouton category. **D**: persistent boutons, **E**: non-persistent boutons. 34 control-treated axons were included in this analysis.

As an alternative way to assess the relative distance between boutons of the same category, a "cluster coefficient" was calculated from the neighborhood of the boutons. In brief, the next or the next and the second-to-next bouton to each side of the bouton were analyzed and the cluster coefficient was increased by one for every same-category bouton in this 2- or 4-bouton group. The cluster coefficient could consequently reach values from zero (no same-category bouton) to two or four (all boutons in the vicinity are from the same category), respectively (Figure 24 A).

In agreement with the first measurement, the distribution of the persistent bouton cluster coefficient differed between experimental and simulated data (Figure 24 B-E). The distribution of cluster coefficients from the simulated data was shifted towards higher values, indicating a greater degree of clustering. This was the case for pooled data of persistent and non-persistent boutons both if two or four neighboring boutons were analyzed (Figure 24 B, C; $p < 0.005$). Separating the data into persistent and non-persistent boutons revealed that only persistent boutons were clustered differently in experimental versus simulated data (Figure 24 D; $p < 0.005$). Non-persistent bouton clustering was indistinguishable between experimental and simulated data (Figure 24 E).

9.3 Analysis of absolute bouton clustering

As a last method, the real distance between boutons of the same category was computed. This method could unveil "interrupted" clusters, i.e. an accumulation of boutons from the same category interspersed with boutons from the other category. For this purpose, the distance between boutons of the same category was calculated (Figure 25 A). Just like the analysis of relative distances, this analysis indicated a lack of very short distances, but an excess of medium distances in the experimental data if compared to the simulated data. This conclusion was true only for persistent boutons (Figure 25 B, C; $p < 0.005$ for Figure 25 B).

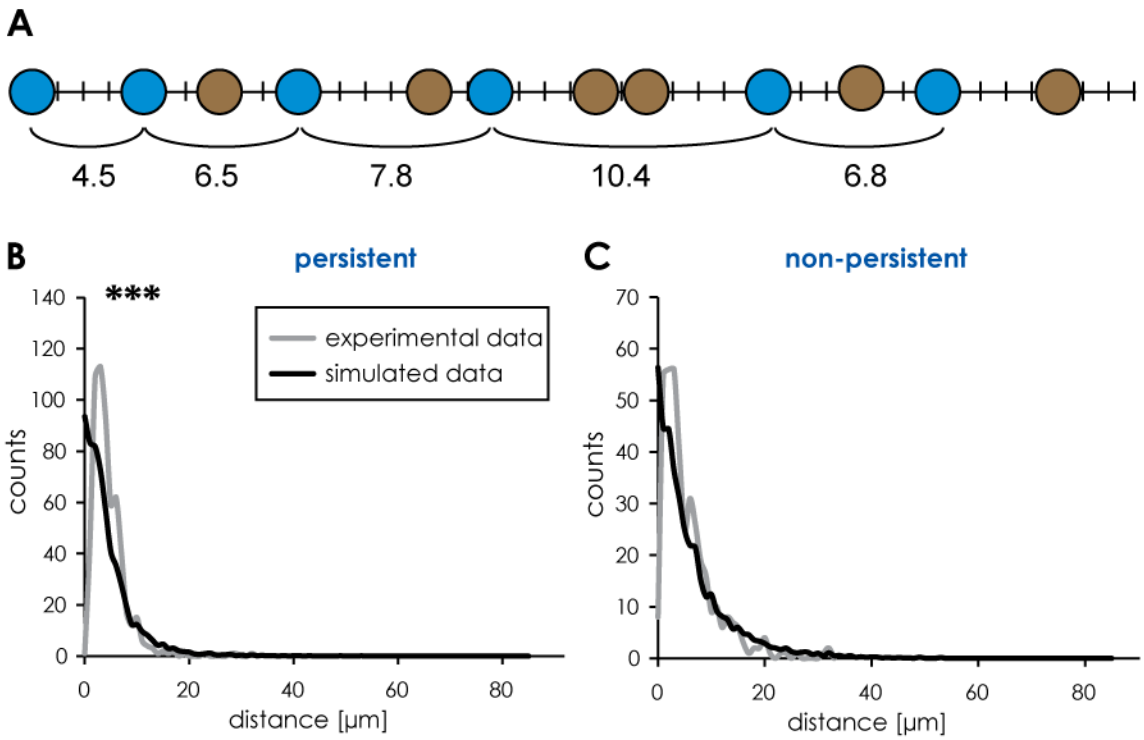

Figure 25 - Measuring the absolute distance between boutons of the same category. A. Schematic illustration of the method. The absolute distance between two boutons from the same category [µm] was determined for both non-persistent and persistent boutons (Illustration only for persistent boutons). **B.** Distribution of distances between persistent boutons for both experimental (grey line) and simulated (black line) data. **C.** Distribution of distances between non-persistent boutons for both experimental (grey line) and simulated (black line) data. 34 control-treated axons were included in the analysis.

For every bouton, this method includes the distance to the next bouton from the same category, both to the left and to the right side of the bouton. Including only distances to the nearest bouton from the same category would omit some distances and count others twice (Figure 26 A). However, the latter method has the advantage of amplifying signals from clusters (i.e. very short distances), while reducing the signal from far-off neighboring boutons. This method might be advantageous for uncovering small

clusters of just two or three boutons. Analogous to previous techniques, applying the method to experimental and simulated data revealed a lack of very short and an excess of medium distances between boutons of the same category in the experimental data (Figure 26 B, C; $p < 0.005$). Unlike previous methods, calculating the distance to the true nearest neighbor was able to uncover a difference between distances amid non-persistent boutons. Like for persistent boutons, experimental data showed a lack of very short and an excess of medium distances between non-persistent boutons. This nicely illustrates the enhanced sensitivity of the last method.

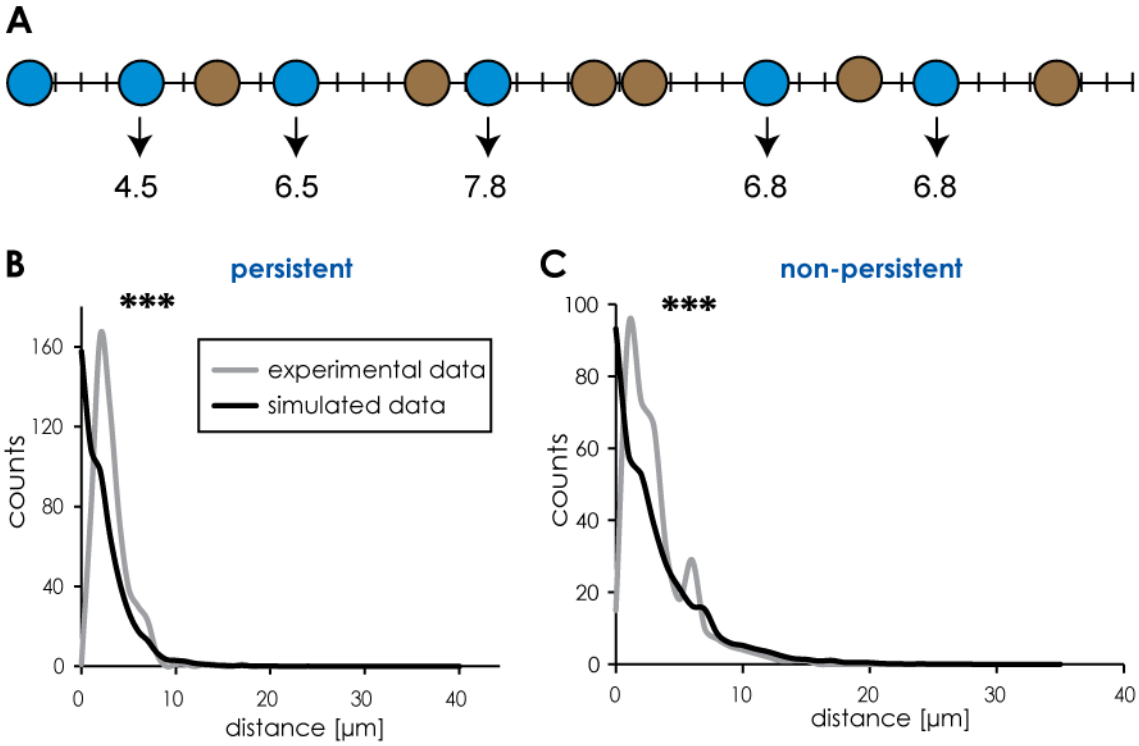

Figure 26 - Measuring the absolute distance between nearest neighbor boutons of the same category. A. Schematic illustration of the method. The absolute distance [µm] between two nearest neighbor boutons was determined for both non-persistent and persistent boutons (Illustration only for persistent boutons). **B.** Distribution of nearest neighbor distances between non-persistent boutons for both experimental (grey line) and simulated (black line) data. **C.** Distribution of nearest neighbor distances between persistent boutons for both experimental (grey line) and simulated (black line) data. 34 control-treated axons were included in the analysis.

In summary, boutons from the same category seem not to be clustered along GABAergic axons. Instead, it seems as if boutons from the same category avoid each other along GABAergic axons. However, intermediate distances are more likely to occur in the experimental data. This may argue for a propensity to evenly distribute boutons from the same category along GABAergic axons.

10. Reducing the area of network activity

Previous work on GABAergic plasticity has raised the question of whether it requires network-wide changes in activity to be induced (Hartman et al., 2006) or whether local or even cell-autonomous mechanisms suffice (Liu, 2004; Chattopadhyaya et al., 2007; Peng et al., 2010). To address these questions step-by-step, a local superfusion technique was established for organotypic hippocampal slice cultures, to manipulate network activity within a small area of the slice culture. Furthermore, initial work was done to establish the manipulation of individual cells within a hippocampal slice culture.

10.1 Reducing network activity in a restricted area of the slice culture decreases inhibitory bouton dynamics.

To reduce network activity in a small area (~300 µm x 300 µm) of the slice culture, a local superfusion technique described by Veselovsky and colleagues (Veselovsky et al., 1996) was adapted to hippocampal slice cultures. Briefly, two pipettes (between which the superfusion solution was flowing through gravity flow) were lowered to the top of the slice culture. This way, neuronal activity in a part of the CA1 area could be reduced by supplementing the superfusion solution with 0.1 µM TTX. The superfusion solution furthermore contained 10 µM Alexa 568 to highlight the manipulated region for optical control during the experiment. Images were taken both inside and outside of the manipulated region at 30 min intervals over a 4 h imaging period (Figure 27 A). Superfusion with the control solution alone already increased bouton turnover by 40-50 % (no superfusion: gain: 7.4 ± 0.9 %, loss: 6.5 ± 0.8 %; superfusion with control solution: gain: 10.6 ± 1.3 %, loss: 9.7 ± 1.1 %). However, despite this general increase, superfusion with a TTX-containing solution significantly decreased bouton turnover inside the superfusion spot (gain: 6.1 ± 1.2 % ($p = 0.003$), loss: 6.8 ± 1.2 %) compared to superfusion with the control solution (gain: 10.6 ± 1.3 %, loss: 9.7 ± 1.1 %) (Figure 27 B). In addition, the density of transient boutons was significantly decreased in regions superfused with 0.1 µM TTX, if compared to regions superfused with the control solution (Figure 27 C; control solution: 8.5 ± 1.2, TTX: 3.8 ± 0.8 transient boutons per 100 µm axon, $p = 0.002$).

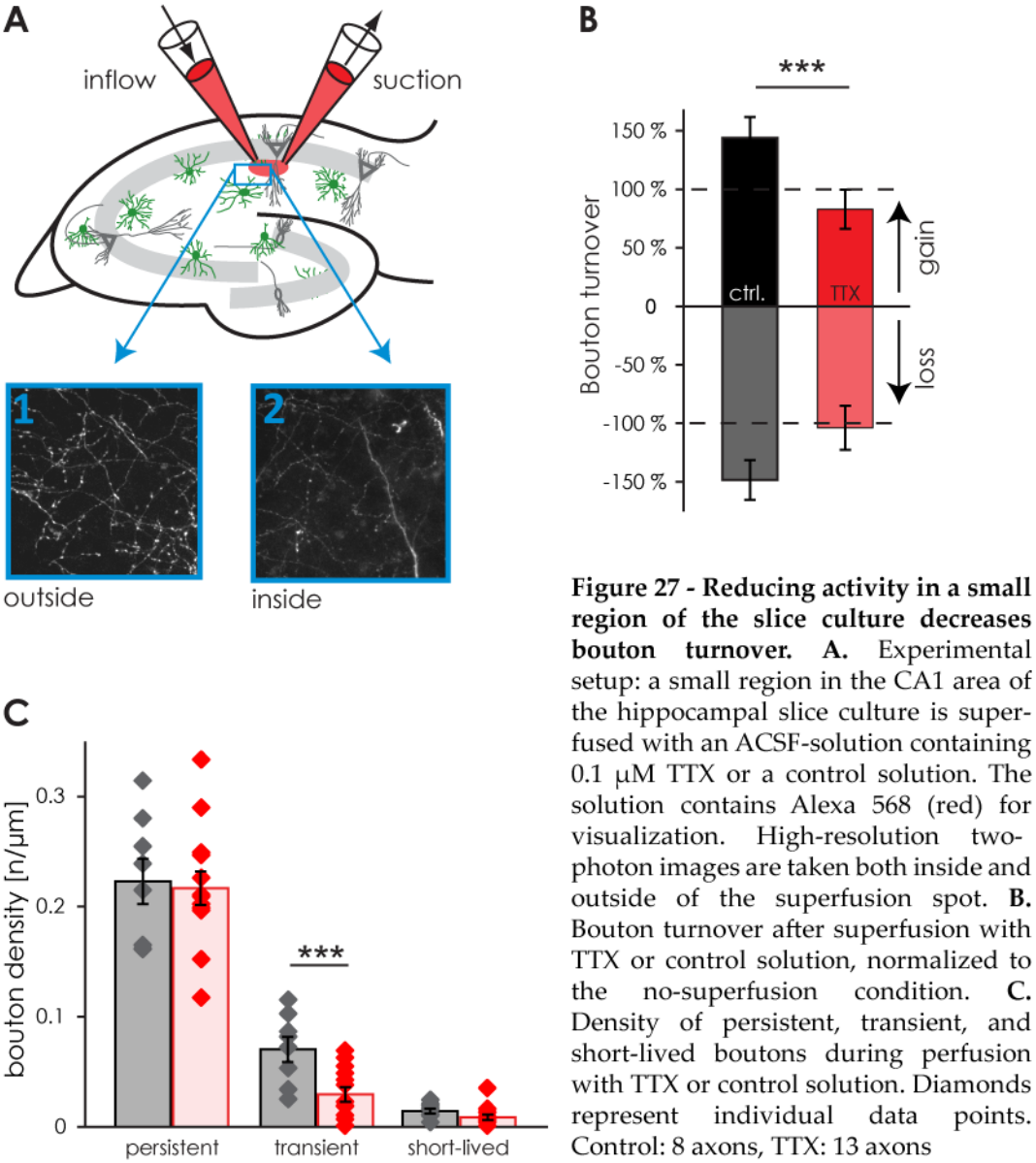

Figure 27 - Reducing activity in a small region of the slice culture decreases bouton turnover. A. Experimental setup: a small region in the CA1 area of the hippocampal slice culture is superfused with an ACSF-solution containing 0.1 µM TTX or a control solution. The solution contains Alexa 568 (red) for visualization. High-resolution two-photon images are taken both inside and outside of the superfusion spot. **B.** Bouton turnover after superfusion with TTX or control solution, normalized to the no-superfusion condition. **C.** Density of persistent, transient, and short-lived boutons during perfusion with TTX or control solution. Diamonds represent individual data points. Control: 8 axons, TTX: 13 axons

Our data indicate that superfusion with TTX decreased bouton turnover to a similar extent as bath application of TTX. This suggests that reducing activity in a restricted area of the neural network can elicit the same phenomena of structural GABAergic plasticity as manipulations of the entire slice cultures. These experiments however do not exclude the involvement of factors secreted from neighboring cells that are not contacted by the GABAergic axon. To examine if such factors are necessary for the induction of structural GABAergic plasticity, manipulating the activity of individual cells will be necessary in future experiments.

10.2 Testing promoters for expression in hippocampal slices cultures

Ultimately, the manipulation of individual pre- or postsynaptic cells will allow for the analysis of the spatial extent of structural plasticity on GABAergic axons. The development of genetic tools, such as light-driven ion channels or pumps provides intriguing opportunities for such manipulations. Light-activated ion channels derived from the green algae *Chlamydomonas reinhardtii* were optimized for mammalian expression and modified to yield variants of blue light-activated cation channels which excite neurons expressing them (Nagel et al., 2003; Lin, 2011). Analogously, an orange light-driven chloride pump which has been isolated from archaeabacteria *Natronomonas pharaonis* was modified, such that it is now available as a tool to hyperpolarize neurons expressing it (Lanyi et al., 1990; Gradinaru et al., 2008). Both molecules and their variants have become widely used tools in neuroscience (Fenno et al., 2011; Yizhar et al., 2011; Liu et al., 2012). Heterologous expression of these proteins together with a structural marker (for instance a red fluorescent protein like tdtomato (Shaner et al., 2004)) in GAD65-GFP hippocampal slice cultures would enable experiments that can clarify the spatial extent of structural plasticity in GABAergic axons.

To set the stage for such experiments, the following ubiquitous promoters were tested for expression in CA1 neurons: (1) the human cytomegalus virus immediate early promoter (CMV), which is commonly used to yield strong expression in mammalian cells but has been suggested to yield low transfection rates of neurons by a few studies (Thomsen et al., 1984; Kugler et al., 2001; Boulos et al., 2006), (2) a combination of the CMV early enhancer and the chicken beta actin promoter (CAG), (3) the human ubiquitin C promoter (UB), (4) a modified human beta actin promoter (ABES), and (5) the human elongation factor 1 alpha promoter (EF1a). Plasmid constructs containing GFP controlled by these promoters were synthesized using standard molecular biology techniques.

To test the expression driven by the different promoters in organotypic hippocampal slice cultures, the slices were transfected with these plasmids using biolistic transfection (McAllister, 2000). A few days after transfection, slices were analyzed under a stereomicroscope and green fluorescent cells were counted and sorted to three different groups (glial cells, interneurons, and pyramidal cells) according to their morphology.

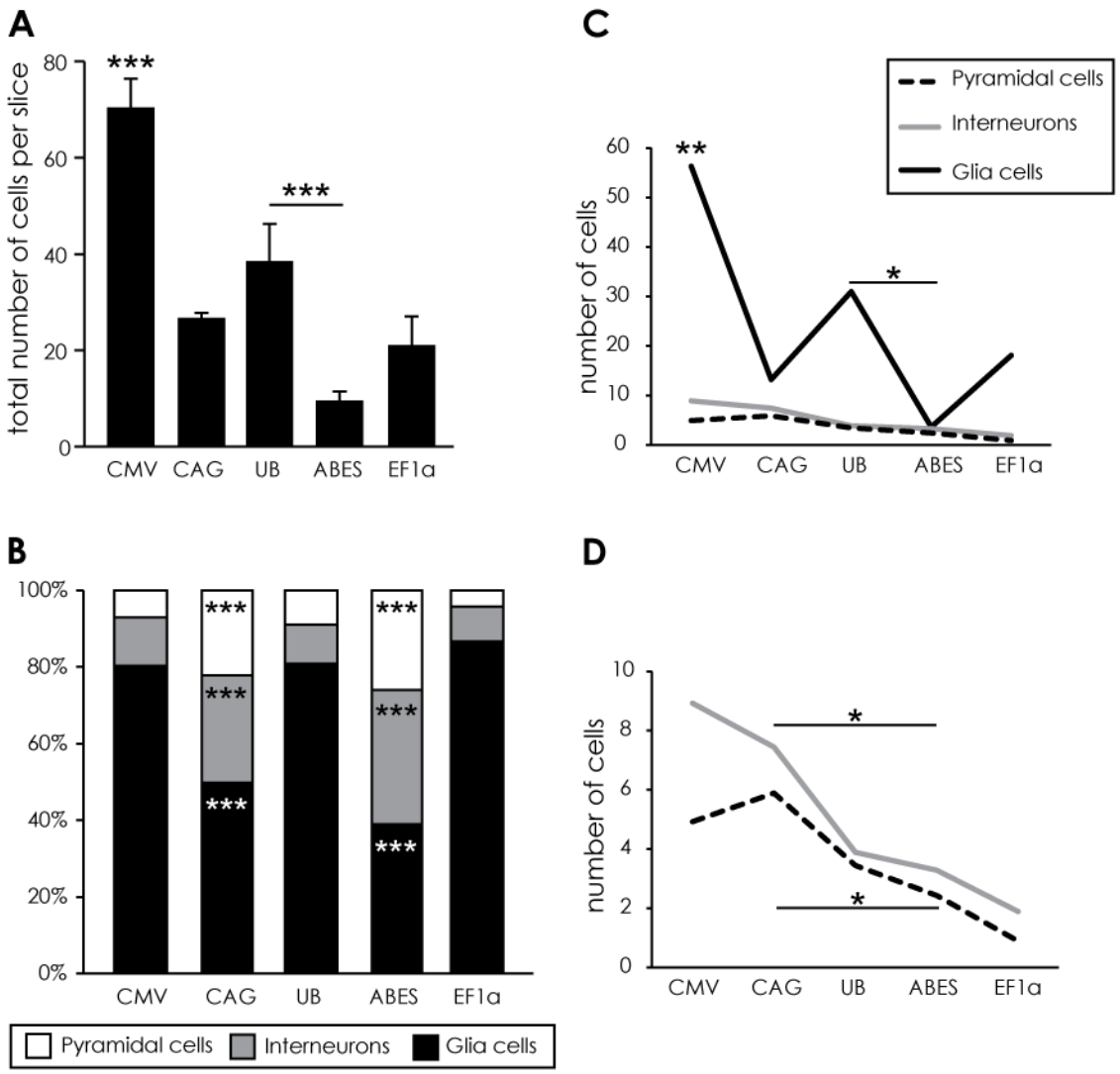

Figure 28 - Testing ubiquitous promoters for gene-expression in organotypic hippocampal slice cultures. A. Total number of GFP-positive cells per slice culture, yielded with gene-gun mediated transfection. Expressing GFP under the CMV promoter led to the highest number of cells infected per slice following gene-gun mediated transfection. **B.** Fraction of pyramidal cells, interneurons, and glia cells of all GFP-positive cells following gene-gun mediated transfection. **C and D.** Number of GFP-positive cells following gene-gun mediated transfection, separated by cell type. **Promoters:** cytomegalus early promoter (**CMV**), CMV early enhancer+chicken beta actin (**CAG**), human ubiquitin (**UB**), modified human beta actin promoter (**ABES**), and human elongation factor 1a (**EF1a**). CMV: 26 slices, CAG: 9 slices, UB: 9 slices, ABES: 14 slices, EF1a: 9 slices.

In absolute numbers, the CMV promoter caused GFP expression in the highest number of cells, while the ABES promoter yielded least GFP positive cells (CMV: 70.2 ± 6.2; CAG: 26.6 ± 6.1; UB: 38.3 ± 7.9; ABES: 9.4 ± 1.2; EF1a: 20.9 ± 2.1 cells per slice; Figure 28 A). However, for the experiments suggested above, it is desirable to achieve specific transfection of as many neurons and as few (confounding) glia as possible. Therefore, in addition to absolute numbers, it is also important to investigate the fraction of neurons transfected with each promoter. While the CMV, the UB, and the EF1a promoter

transfected mostly glia cells and only few pyramidal cells or interneurons, both the CAG and the ABES promoter transfected a significantly higher fraction of pyramidal cells and interneurons (CMV promoter: 75.9 ± 3.4 % glia cells, 15.5 ± 2.0 % interneurons, 8.6 ± 1.6 % pyramidal cells; CAG promoter: 34.5 ± 8.9 % glia cells, 33.0 ± 4.8 % interneurons, 32.5 ± 7.1 % pyramidal cells; UB promoter: 68.4 ± 8.0 % glia cells, 17.3 ± 4.8 % interneurons, 14.3 ± 4.3 % pyramidal cells; ABES promoter: 37.6 ± 3.7 % glia cells, 34.9 ± 3.8 % interneurons, 27.6 ± 2.6 % pyramidal cells; EF1a promoter: 86.2 ± 2.5 % glia cells, 8.5 ± 2.4 % interneurons, 5.3 ± 1.8 % pyramidal cells; Figure 28 B). While the ABES promoter transfected only very few cells, the number of neurons transfected with the CAG promoter were similar to those transfected with the CMV promoter (Figure 28 C, D). Therefore, the CAG promoter is most well suited for the transfection of individual neurons in organotypic hippocampal slice cultures with heterologous proteins and should be used for further experiments.

Discussion

The re-wiring of neurons is an important mechanism of synaptic plasticity. Structural dynamics on axons or dendrites might represent such re-wiring processes (Keck et al., 2008; Hofer et al., 2009; Bednarek and Caroni, 2011; Caroni et al., 2012; Lai et al., 2012). Therefore, analysis of such structural dynamics during changes in network activity can yield important information about plasticity mechanisms used by these neurons. Especially in the case of inhibitory, GABAergic synapses, such plasticity mechanisms are far from being unraveled. Therefore, the present study has employed time-lapse two-photon imaging of GAD65-GFP hippocampal slice cultures to characterize the structural dynamics of GABAergic boutons in the face of changing neuronal activity. Under baseline conditions, ~80 % of the boutons were found to be present persistently during the four hour imaging period (persistent boutons). The remaining boutons (non-persistent boutons) appeared only transiently throughout the imaging period. Interestingly, the dynamics of these populations of boutons were regulated differently following acute manipulations of network activity. Prolonged manipulations of network activity have been suggested to change either in the strength or even the density of inhibitory synapses both *in vitro* and *in vivo*. The data presented here indicate that manipulation of network activity in organotypic slice cultures immediately change GABAergic bouton dynamics. After a few days, these dynamics had returned to control levels, suggesting that long-term plasticity of GABAergic axons employs other than structural mechanisms.

11. Baseline dynamics of GABAergic boutons

Time-lapse two photon imaging of GABAergic axons in hippocampal slice cultures revealed distinct bouton categories that could be separated by their temporal appearance pattern as well as their structural properties and the likelihood to co-localize with certain synaptic markers (resulting in persistent and non-persistent boutons). Obviously, the limited imaging period of four hours and the long interval between single image stacks (30 min), make it likely that some boutons would be assigned to a different category if the imaging paradigm was changed. For instance, a transient bouton could become persistent and vice versa.

11.1 Persistent boutons

So-called **persistent boutons** were present continuously over the entire imaging period (i.e. for four hours; Figure 7 B). They were rather large and showed relatively little volume variations (CV of bouton volume; Figure 8 A, B). About 86 % of them co-localized with at least one synaptic marker (postsynaptic gephyrin and presynaptic VGAT were tested; Figure 10 A). Several arguments support the role of persistent boutons as *bona fide* synapses: First, they largely co-localized with pre- and/or postsynaptic marker proteins. A positive staining for VGAT and/or gephyrin has frequently been used as a marker for functional inhibitory synapses (Wierenga et al., 2008; Dobie and Craig, 2011; Kuriu et al., 2011). Second, their lifetime (at least 4 h) should be sufficient even for a newly formed contact to become a functional synapse (Ahmari et al., 2000; Friedman et al., 2000; Wierenga et al., 2008; Dobie and Craig, 2011). Third, the amount of structural dynamics (CV of bouton volume; Figure 8 B), possibly reflecting material exchange or growth/shrinkage of the synapse, was reduced for persistent boutons if compared to non-persistent boutons. Reduced structural dynamics have been associated with stable or mature synaptic structures before (Gray et al., 2006; Holtmaat and Svoboda, 2009), which argues in favor of a mature, synaptic nature of persistent boutons, too.

Nonetheless, persistent boutons still exhibited significant volume variations over time (Figure 8 B). These variations suggest that persistent boutons continuously exchanged synaptic material such as transmitter-filled vesicles either with neighboring boutons or with a reserve pool of presynaptic components in the axon, as has been demonstrated for excitatory axons (Darcy et al., 2006; Fernandez-Alfonso and Ryan, 2008; Tsuriel et al., 2009; Staras et al., 2010; Herzog et al., 2011). Such exchange processes have been suggested to play a crucial role in synaptic plasticity and synapse formation (Staras and Branco, 2010). Interestingly, the dynamics of large gephyrin clusters, which might represent the postsynaptic specialization in mature GABAergic synapses, are comparable

to that of persistent GABAergic boutons. In comparison to small and very mobile gephyrin clusters, large cluster were shown to have only little dynamics around their location (Hanus et al., 2006). Therefore, pre- and postsynaptic specializations of mature GABAergic synapses might have similar baseline dynamics. In fact, recent studies furthermore suggest that pre- and postsynaptic GABAergic specializations move in concert (Dobie and Craig, 2011; Kuriu et al., 2011). It can be assumed that most persistent GABAergic boutons represent *bona fide* synapses which continuously exchange small quantities of synaptic material with their neighbors or other material pools along the axonal shaft (Darcy et al., 2006).

11.2 Non-persistent boutons

Non-persistent boutons were present intermittently during the imaging period (Figure 7 B). They were only 1/3 as large as persistent boutons, but their volume was very variable (Figure 8 A, B). Furthermore, non-persistent boutons were less likely to co-localize with synaptic markers. As the likelihood of co-localizing with synaptic markers steeply increased for boutons with a minimum lifetime of more than 60 min (i.e. more than two time points; Figure 10 B), the group of non-persistent boutons was separated into **transient** and **short-lived boutons**.

Transient boutons had a lifetime of 60 to 210 min, or three to seven time points, respectively. Their average lifetime was 4.86 ± 0.09 time points or ~146 min. In about 50 % of them, at least one synaptic marker (VGAT or gephyrin) was detected by means of immunohistochemistry (Figure 10 A). The fraction of transient boutons co-localizing with one or two synaptic markers was much lower than that of persistent boutons. Therefore, the population of transient boutons is unlikely to contain only *bona fide* synapses. Nonetheless, to be classified as transient boutons, they had to occur at the same spot on the axon at least three times within four hours. It is unlikely that random transport along the axon can account for such a coincidence. Together with the average co-localization of transient boutons and synaptic marker proteins, this notion supports two different scenarios that transient boutons could represent. On the one hand, transient boutons could represent synapses in the stage of assembly or degradation. The formation of new synapses requires transport of presynaptic material (e.g. transmitter-filled vesicles) to the assembling bouton, conversely, degradation of synapses should be associated with transport of presynaptic material away from the decomposing bouton. That bouton volume CV is increased in transient boutons compared to persistent boutons (Figure 8 B) supports this hypothesis, as assembling or degrading synapses would predict a high CV

of bouton volume. On the other hand, transient boutons might represent stop sites of presynaptic material along the axon. Such sites have already been demonstrated for excitatory axons (Sabo et al., 2006; Antonova et al., 2009). They are the preferred sites for synapse formation and might be characterized by the occurrence of a specialized set of adhesion molecules (Varoqueaux et al., 2004; Chubykin et al., 2007; Huang and Scheiffele, 2008; Fu and Huang, 2011). Inhibitory axons are restricted in the sites of synapse formation per se: New inhibitory synapses preferentially form at sites where the GABAergic axon is in close proximity to the postsynaptic dendrite and the process of synapse formation does involve neither axonal nor dendritic protrusions (Wierenga et al., 2008). The formation of new GABAergic synapses is therefore restricted to these sites on the axon. Analogously to the situation in excitatory axons, it seems possible that transport entities with presynaptic proteins and synaptic vesicles (STVs, PTVs) stop at these sites. In fact, axon-dendrite crossings have been reported to frequently harbor transient GABAergic boutons and display a synapse only after a longer time period (Wierenga et al., 2008). It has even been reported that stopping transport clusters of synaptic vesicles are release competent (Kraszewski et al., 1995; Krueger et al., 2003). A stop site could occur as a transient bouton in two-photon imaging of GABAergic axons, as it would frequently be occupied by stopping synaptic material, and might even recruit postsynaptic material to the nascent site by spontaneous neurotransmitter release. Of course, a stop site would ultimately transform into an assembling bouton (see above). It is possible that non-synaptic material such as mitochondria also stops at these sites. However, that transport of mitochondria is known to be regulated by activity in ways opposing the dynamics of GABAergic boutons found here. Non-synaptic material would not be recruited to these sites but rather pass through them. Imaging non-synaptic material stopping at these sites for three or more times within four hours would be unlikely. Rather, such material would vary more with respect to its location. Therefore, synaptic material is most likely to occupy these stop sites.

In summary, the data presented here argue for transient boutons representing either synapses in the process of formation or degradation or stop-sites for synaptic material along the axon, which possibly occur in GABAergic axons, as well.

Short-lived boutons showed a trend to be slightly smaller than transient boutons, however, this difference was not significant (Figure 8 A). Furthermore, they were much less likely to co-localize with pre- or postsynaptic markers (only 12.5 % of them contained VGAT or gephyrin; Figure 10 A) than their longer-lived, “transient” counterparts.

Short-lived boutons are unlikely to represent mature GABAergic synapses for two main reasons. First, short-lived boutons hardly co-localized with pre- or postsynaptic marker proteins. The inability to detect a positive immmunohistochemical signal for pre- and postsynaptic proteins in short-lived boutons was most likely not due to their small overall size and therefore the likelihood of a positive fluorescence signal below the detection limit. It was confirmed that persistent or transient boutons with a size comparable to that of short-lived boutons could be co-localized with a fluorescence signal for VGAT or gephyrin. Second, the lifetime of a short-lived bouton would not be sufficient for synapse formation. Several studies suggest that synapse formation takes at least a few hours (Friedman et al., 2000; McAllister, 2007; Wierenga et al., 2008; Owald and Sigrist, 2009).

Short-lived boutons probably represent other axonal processes, such as (1) the initial phase of synapse formation with a transient bouton appearing at a future synaptic location, (2) nascent synaptic contacts with a non-target cell, which for this reason are not maintained, or (3) the transport of large amounts of material along the axon. Such material could include presynaptic transport clusters of presynaptic material (STVs and PTVs), mitochondria, or other cellular material (Goldstein et al., 2008). Given the low probability of synaptic marker association with short-lived boutons, the first two alternatives seem unlikely, as even nascent contacts which only probe a potential location would already co-localize with synaptic markers to a certain degree. Consequently, short-lived boutons probably reflect the transport of material along the axon. As the dynamics of mitochondria are at odds with the dynamics of short-term boutons following manipulations of network activity (Cai and Sheng, 2009; Ohno et al., 2011), short-lived boutons probably reflect transport of synaptic or other cellular material.

11.3 Synapse formation on GABAergic axons

The formation of GABAergic synapses is an important process both in developing and mature neural tissues. However, the precise sequence of events leading to the formation of a GABAergic synapse is still unclear. Data collected here from VGAT and gephyrin staining of hippocampal slice cultures present the opportunity to investigate some aspects of GABAergic synapse formation. Owing to the accumulation of synaptic material, newly forming synapses are expected to grow. Degrading synapses on the other hand would be expected to shrink due to the loss of synaptic material. Interestingly, the growing and shrinking behavior of persistent boutons varied dependent on their synaptic marker content: boutons co-localizing with VGAT alone contained the largest fraction of growing boutons, and they also showed the strongest growth (Figure 12 B, C). Boutons

co-localizing with gephyrin alone however, contained the largest fraction of shrinking boutons and furthermore showed the strongest shrinking overall (Figure 12 B, C). In boutons co-localizing with both VGAT and gephyrin together, volume changes were smaller and balanced over the population, suggesting that these boutons are mature synapses in a state of equilibrium. Boutons co-localizing with only one synaptic marker are less likely to represent mature boutons (Gray et al., 2006; Holtmaat and Svoboda, 2009). It is more likely that these boutons are in the state of assembly or degradation, where they do not contain all the material that usually defines *bona fide* synapses.

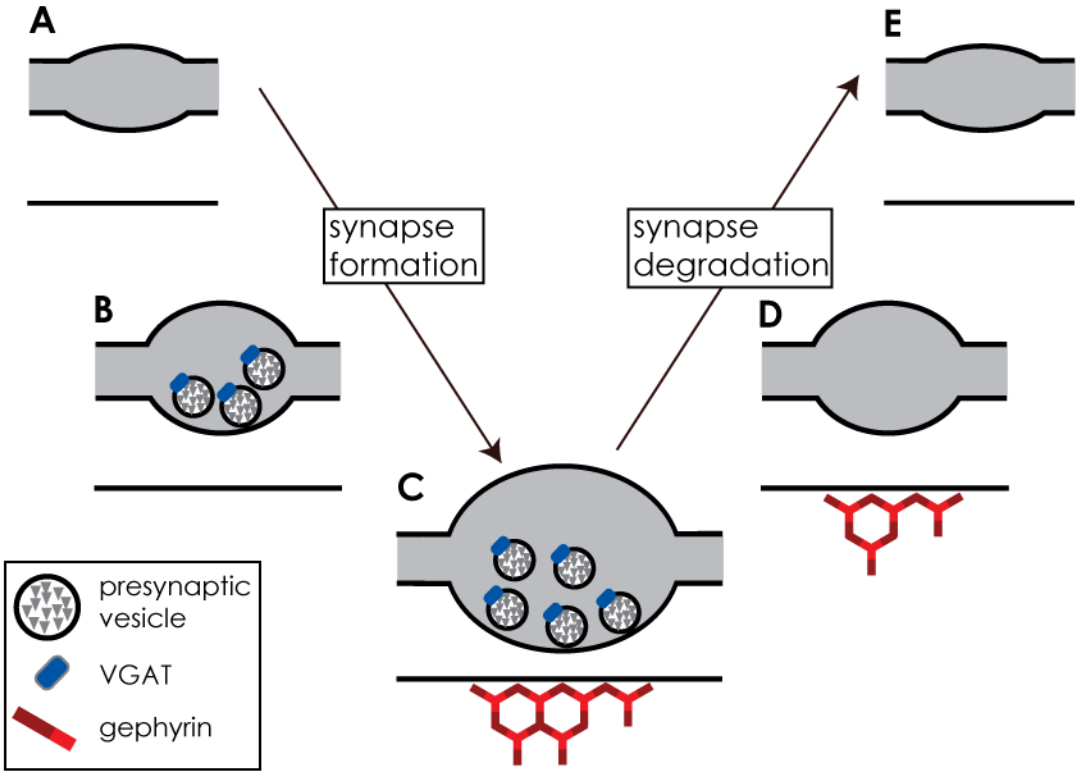

Figure 29 - Model of GABAergic synapse formation and degradation. The data presented here argue that during the process of synapse formation (**A-C**), presynaptic material is acquired before postsynaptic material. Conversely, during the process of synapse degradation (**C-E**), presynaptic material is lost prior to postsynaptic material.

The data presented here suggest that boutons co-localizing with VGAT alone rather grow, while those that co-localize with gephyrin alone rather shrink. This is consistent with the idea that newly forming and therefore growing boutons acquire VGAT first, while those that begin to degrade and therefore shrink have lost VGAT before they will lose gephyrin, consequently they co-localize with gephyrin alone (Figure 29). The hypothesis that assembling synapses acquire presynaptic markers before postsynaptic ones is in line with other reports on inhibitory and excitatory synapse formation (Friedman et al., 2000; Wierenga et al., 2008; Dobie and Craig, 2011).

11.4 Clustering of structural dynamics along GABAergic axons

Several recent studies suggest that synaptic plasticity does not occur in a spatially random fashion, but that it is clustered, probably due to the clustering of similar inputs (Kleindienst et al., 2011; Fu et al., 2012). Therefore, a computer simulation was conducted to reveal similar phenomena in GABAergic axons. Interestingly, persistent and non-persistent boutons that are described here seemed not to be clustered along the axons. Rather, they seemed to avoid too close proximity to boutons from the same category (Figures 23-26).

One possible explanation for this phenomenon is that new presynaptic boutons can be generated by splitting off pre-existing, larger boutons or that they can get lost by merging with neighboring boutons. These pre-existing boutons have been described to be rather large, therefore it is reasonable to assume that they would appear as persistent boutons in this study (Krueger et al., 2003; McAllister, 2007; Dobie and Craig, 2011). If these processes would dominate over other processes of synapse formation and degradation, persistent boutons would be expected to be interspersed with non-persistent boutons. However, analyzing splitting and merging events in the dataset used here suggested that bouton assembly and degradation mostly occur without the involvement of splitting and merging processes (Figure 8 C).

Another possibility is that axonal resources for bouton dynamics (such as motor proteins, plasticity signals or tags that attract transport packets, etc.) are scarce along the axon. Local competition for such resources would then prohibit the spatial clustering of non-persistent boutons. The analyses performed here suggest that competition would restrict non-persistent bouton clustering within a range of up to two μm (Figure 26 C). Clustering within intermediate distances of ~ 2-8 μm was actually more likely to occur in the experimental data. These data would suggest an extremely local competition whose spatial scale does not exceed 1-2 μm. Competition hindering the clustering of plasticity at this scale has not been reported in recent literature, dynamics structures rather seem to be clustered at this spatial scale (Fu et al., 2012). Furthermore, known plasticity signals seem to be able to spread over tens of micrometers or more, also arguing against the restriction of plasticity clustering at very small spatial scales (Frey and Morris, 1997; Govindarajan et al., 2011). Nonetheless, a recent study has demonstrated that dynamic dendritic spines do not cluster with each other, but rather with dynamic inhibitory synapses (Chen et al., 2012). Such an avoidance of structures from the same category would be in line with the data presented in this study. Of course, all the data referred to above were recorded in different systems than GABAergic axons in hippocampal slice cultures. It should

therefore not be excluded that a clustering of axonal dynamics occurs at exactly the limited spatial scale that is described here.

Finally, it is also possible that the non-clustering of bouton types along the axon is caused by an artifact of the simulation. While the simulation includes bouton numbers and positions, it does not take into account the spatial extent of boutons. As data from this thesis demonstrates, persistent boutons are about three times as large as non-persistent boutons, so if boutons were assumed to be perfect spheres, the diameter of persistent boutons would be about 1.44 times as wide as that of non-persistent boutons. This difference in the spatial extent of boutons is not accounted for in the simulated data. Therefore, it is possible that in the simulated data spatially close positions along the axon are assigned to two boutons that would overlap if their spatial extent was taken into account. Such a scenario could not exist in the experimental data. It would appear as one bouton due to the resolution limit of light microscopy (Figure 30). Consequently, the simulation does so far not perfectly mirror the real data.

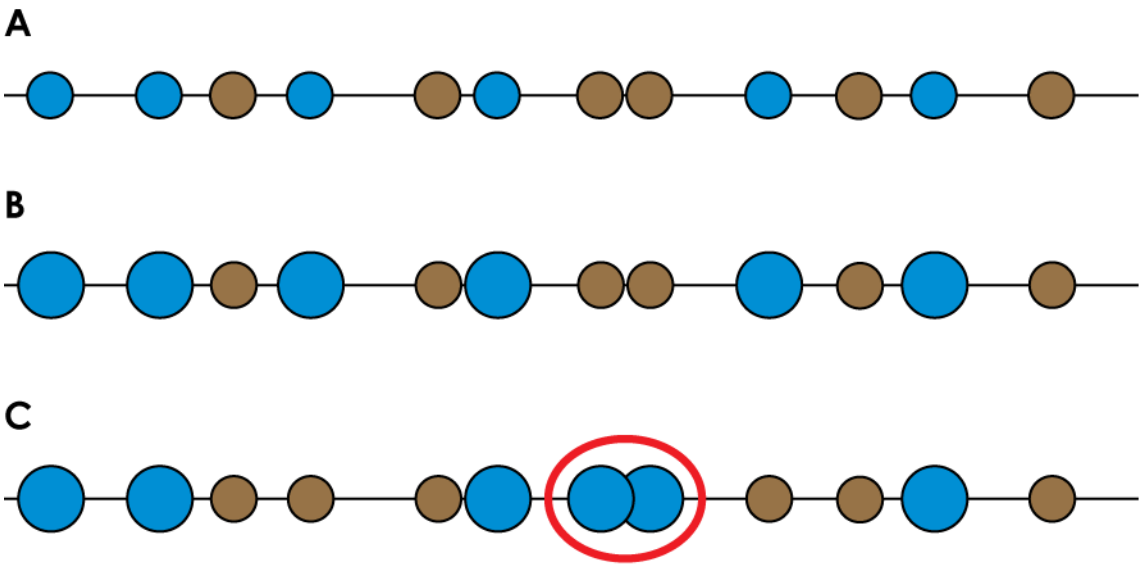

Figure 30 - Illustration of a potential caveat of the simulation of bouton positions. A. In the simulation used here, persistent (blue) and non-persistent (brown) boutons do not differ with respect to their spatial extent, therefore, the spatial extent is not included in the simulation. **B.** Experimental measurements have demonstrated that the volume of persistent boutons is ~3-times as large as that of non-persistent boutons. **C.** Including volume differences in the simulation used here would render some arrangements impossible. One such example is depicted here: the two persistent boutons in the red circle overlap. This would be detected as only one bouton with two-photon microscopy. Therefore, the simulation does not perfectly mirror the real data.

In summary, analysis of clustering revealed that very close proximity or direct neighborhood between boutons with similar dynamics occurred with a lower probability in experimental data. This interpretation is partially supported by previous data. Nonetheless, the data presented here could be refined by including the spatial extent of GABAergic boutons in the simulation.

12. Structural plasticity of GABAergic boutons

Few studies have analyzed the structural dynamics of GABAergic axons or synapses. While Dobie and Craig have described the dynamics of pre- and postsynaptic proteins under control conditions (Dobie and Craig, 2011), Kuriu and colleagues have investigated the effect of 48 h TTX treatment on the dynamics of GABAergic synapses (Kuriu et al., 2011). The study presented here extends previous data by establishing between three different axonal structures and by analyzing the likelihood of these structures to represent synapses. Furthermore, this study provides data on the regulation of these structures by both enhanced and reduced network activity. Most importantly, data presented in this thesis attempts to unveil mechanisms of structural GABAergic plasticity immediately after the onset of activity manipulations. Axonal dynamics have so far not been investigated at this timescale. Nonetheless, the data might provide important insights about the mechanisms through which interneurons re-wire their synaptic connections in the face of changing network activity.

Only axons which are labeled with GFP in GAD65-GFP mice were analyzed. These axons represent a diverse population (Wierenga et al., 2010) of axons contacting different target cells and having different molecular and functional characteristics (Klausberger and Somogyi, 2008). It is possible that some axons express different plasticity mechanisms than others. Due to this fact, some plasticity mechanisms might be occluded in this dataset. In the future, labeling of single interneuron populations could be used to uncover plasticity mechanisms of more confined populations of interneurons (Taniguchi et al., 2011).

12.1 Structural dynamics of GABAergic axons are affected by acute (4 h) manipulations of network activity

This study demonstrates that the structural dynamics of GABAergic axons are rapidly affected by changes in overall network activity. Interestingly, different manipulations of network activity affected very specific aspects of these dynamics.

Reducing network activity with TTX distinctively reduced transient and short-lived boutons while leaving persistent boutons unaffected (Figure 13 B). In accordance with the interpretation of transient bouton function, this suggests that reducing network activity decreases the occupation or density of potential synaptic sites (i.e. stop sites for synaptic material), as well as the formation and degradation of GABAergic synapses. The invariability of persistent bouton density suggests that established synaptic sites are maintained following the reduction of network activity. Furthermore, the CV of persistent

bouton volume was decreased during this treatment (Figure 14 D, Figure 15). Therefore, also material transport into and out of GABAergic boutons was reduced by acute TTX treatment. This idea is also supported by the reduction of short-lived boutons. Interestingly, a similar phenomenon has already been described for excitatory synapses: analyses of PSD-95 puncta revealed that individual puncta change their size over time. Following the addition of TTX, however, this relative remodeling slowed down (Minerbi et al., 2009), suggesting a reduced amount of material transport into and out of these synaptic structures. The decrease in material transport goes hand in hand with the decreased occupation or density of synaptic sites. An overall decrease in the transport of synaptic material would entail both phenomena.

Conversely, **enhancing network activity** with 4-AP mainly reduced the density of persistent boutons. The density of short-lived boutons tended to be increased following 4-AP treatment (Figure 13 C). Interestingly, 4-AP treatment specifically increased the volume of large persistent boutons (Figure 14 C). This finding suggests that despite the general loss of persistent boutons, an already strong – and consequently large – subset of persistent boutons is strengthened even further (i. e. grows). Intriguingly, the extent of bouton growth seemed to be correlated with bouton size, such that the largest boutons grew most strongly. Such a behavior would be consistent with the idea of homeostatic scaling (Turrigiano et al., 1998), where the strength of an entire population of synapses is changed as a function of their initial strength. This way, individual synaptic weights and the information stored through them are preserved. The mechanism of scaling found here was slightly different from that found by Turrigiano and colleagues: While Turrigiano and colleagues reported a multiplicative scaling by the same factor (Turrigiano et al., 1998), this study reports a scaling of large volumes by multiplication with a continuously increasing factor (Figure 15). This discrepancy could be explained by different measures analyzed (mEPSC amplitudes versus bouton volumes) or different experimental systems used. Although homeostatic scaling was typically reported to occur at timescales of many hours to days, shorter timescales like those investigated here were reported as well (Hartmann et al., 2008). Other persistent boutons were destabilized and probably fell prey to enhanced competition for limited (presynaptic) resources (Govindarajan et al., 2011; Ratnayaka et al., 2012). The data presented here is in line with previous data from excitatory neurons, reporting an enhanced mobility of presynaptic components following increased neuronal activity (Tsuriel et al., 2006; Frischknecht et al., 2008). The idea of enhanced trafficking of GABAergic presynaptic material is furthermore supported by the slight increase of short-lived boutons and the increase in persistent bouton volume CV (Figure 14 D). As opposed to the data on presynaptic components presented here, some

studies demonstrate that the mobility of postsynaptic components is rather decreased by enhanced neuronal activity (Okabe et al., 2001; Hanus et al., 2006; Ehlers et al., 2007). Therefore, enhanced activity might regulate the dynamics of pre- and postsynaptic components differently.

Overall, acute treatment with 4-AP seemed to induce two phenomena of structural plasticity on GABAergic axons. First of all, a population of large presynaptic boutons was subjected to homeostatic scaling, increasing their size in a size-dependent manner. Second, material transport along the GABAergic axon was increased while persistent boutons were de-stabilized, this probably reflects enhanced competition for presynaptic resources by the GABAergic boutons.

It should be emphasized that TTX and 4-AP did not have directly opposing effects on the structural dynamics of GABAergic boutons. While TTX treatment mostly affected the exploration of new synaptic sites, 4-AP rather changed material transport along the axon. Of course, TTX and 4-AP also do not modify the same facet of neuronal activity: while TTX treatment prevents action potential generation, 4-AP broadens the repolarizing phase of the action potential, thereby keeping the action potential threshold low and allowing for burst firing. Therefore, it might not be surprising that the two treatments also affect different aspects of GABAergic bouton dynamics.

12.2 $GABA_A$ receptor activation is required for high-activity induced changes in GABAergic bouton dynamics

A surprising finding of this study was the interconnection of enhanced structural dynamics of GABAergic axons and the activation of $GABA_A$ receptors (Figure 19). This suggests that a rapid increase in neuronal activity and consequently GABA release could be sensed by the activation of $GABA_A$ receptors, which would then increase structural dynamics of the axon via as yet unknown downstream mechanisms. $GABA_A$ receptors are known as ionotropic receptors. No downstream signaling has been reported for them. Also chloride – the ion chiefly passed by $GABA_A$ receptors – is not known to be a second messenger like for instance calcium ions can be. Despite this lack of data supporting any other role for $GABA_A$ receptors than passing chloride ions, $GABA_A$ receptor activation has been suggested to be involved in the formation and/or maturation of GABAergic synapses "through as yet unknown structural or signaling mechanisms" (Huang and Scheiffele, 2008). In development, addition of the $GABA_A$ receptor antagonist bicuculline has been shown to halt normal maturation of GABAergic development (i.e. the developmental switch from excitatory to inhibitory function (Ganguly et al., 2001; Leitch et al., 2005). However, downstream signaling might be different in such

experimental conditions due to the depolarizing action of GABA in development (Chen et al., 1996; Owens et al., 1996; Rivera et al., 1999).

In addition to their typical postsynaptic location, $GABA_A$ receptors can also occur at presynaptic sites in various brain regions, e.g. the hippocampus and the cerebellum (Vautrin et al., 1994; Pouzat and Marty, 1999; Kullmann et al., 2005; Draguhn et al., 2008). Activation of presynaptic $GABA_A$ receptors in the hippocampus has been reported to reduce transmitter release and thus act as a negative feedback mechanism upon GABA release (Axmacher et al., 2004). One could speculate that activation of these presynaptic $GABA_A$ receptors does not only regulate GABA release during fast repetitive spiking patterns (Draguhn et al., 2008), but also serves as a detector for the level of GABA release from a given interneuron or even synapse. Such a detector could then induce downstream signaling cascades that ultimately would increase dynamics of presynaptic material. This mechanism would explain why the application of bicuculline disrupted the structural plasticity phenomena induced by acute 4-AP treatment.

Another possible scenario explaining the role of $GABA_A$ receptors in structural plasticity of GABAergic axons can be derived from the interactions of $GABA_A$ receptors with other neurotransmitter systems. It has been shown that $GABA_A$ receptor activation interferes with dopamine signaling through D2 and D5 receptors (Perez de la Mora et al., 1997; Liu et al., 2000). In both cases, the activation of $GABA_A$ receptors hampered the effect induced by dopamine (e. g. cAMP generation (Liu et al., 2000)). In theory, similar interactions of $GABA_A$ receptors and other neuronal signaling systems could underlie the observed increase in presynaptic transport processes. The blockade of $GABA_A$ receptors would hamper normal signaling of these hypothetical pathways.

Although $GABA_A$ receptor activation seems to be required for the 4-AP induced effect described here, $GABA_A$ receptor activation alone was not sufficient for an increase the structural dynamics of GABAergic axons (Figure 22). In fact, muscimol application rather showed a trend towards decreasing structural dynamics on GABAergic axons. Of course, muscimol, being an agonist of $GABA_A$ receptors (Johnston et al., 1968; Brehm et al., 1972; Giotti et al., 1983), will reduce neuronal activity by enhancing inhibition. Therefore, it seems likely that the combination of enhanced neuronal activity and $GABA_A$ receptor activation go hand in hand to increase structural dynamics of GABAergic axons. The precise role of $GABA_A$ receptor activation in this process remains elusive and will require further investigations.

12.3 Long-term manipulations of network activity

Many studies both *in vivo* and *in vitro* suggest that long-term manipulations of network activity can change the density of inhibitory synapses (Marty et al., 2004; Chen et al., 2011; Keck et al., 2011; van Versendaal et al., 2012). It is possible, that acute changes in GABAergic bouton dynamics, as observed in this study, will ultimately result in changes in inhibitory bouton density. Indeed, changes in the transport of synaptic material and/or the exploration of potential synaptic sites might be able to lay the groundwork for the formation of new or the degradation of old synapses.

Nonetheless, the data presented here do not reveal differences in bouton density following a longer manipulation of neuronal activity (Figures 16, 18). Remarkably, also bouton dynamics, which were affected within the first hours after the start of the activity manipulations, were not altered after the slice had been kept in the activity altering solution for several days. Two scenarios could explain these data.

Especially specific learning paradigms, such as motor learning tasks, seem to induce a remodeling of existing synapses rather than an overall increase in synapse density (Xu et al., 2009; Yang et al., 2009; Caroni et al., 2012). Such re-wiring of synaptic connections might be employed by the experimental system used here. It is possible, that these re-arrangements – represented as changes in GABAergic bouton turnover – might be completed before the long-term imaging starts (at least 48 h after the start of the activity manipulation). Therefore, no changes in bouton density or structural bouton dynamics were detected with two-photon imaging of GABAergic axons.

Of course, it is also possible that the combinations of activity manipulations and experimental system used here do not change GABAergic synapses over a timescale of 48 h to seven days. However, it seems more plausible, that although the activity manipulations do not change the density of GABAergic boutons, they affected synaptic strength by other means. In fact, several other *in vitro* studies did not report changes in GABAergic bouton density following prolonged manipulations of network activity (Rutherford et al., 1997; Kilman et al., 2002; Hartman et al., 2006; Swanwick et al., 2006; Kuriu et al., 2011; Rannals and Kapur, 2011). The alterations that were detected in these studies encompassed changes in both pre- and postsynaptic markers of inhibitory synapses, including $GABA_A$ receptors, GABA, GAD65 and the size of presynaptic varicosities, and suggested alterations of presynaptic vesicle filling (Kilman et al., 2002; Hartman et al., 2006; Swanwick et al., 2006), and postsynaptic receptor density (Kilman et al., 2002; Swanwick et al., 2006; Rannals and Kapur, 2011). These effects could occur without changes in the size of presynaptic varicosities, and therefore would have gone unnoticed in the current study.

In contrast to the present study, Kuriu and colleagues detected a decrease in the volume of presynaptic varicosities along inhibitory axons following 48 h treatment with 1 μM TTX (Kuriu et al., 2011). Following 48 h manipulations of activity, the present study failed to detect a difference in GABAergic bouton volumes between treated slice cultures and untreated controls. This apparent discrepancy could be explained by the different experimental systems used (dissociated cell cultures vs. organotypic hippocampal slice cultures). A slice culture maintains many features of neuronal development and tissue architecture that are found *in vivo*. Furthermore, the tissue might represent a diffusion barrier for soluble factors such as BDNF or TNFα, and enable their proper signaling in slice cultures compared to dissociated cells.

In summary, the data presented here support the view that short-term changes in structural dynamics of GABAergic axons precede long-term alterations of synapse function. These alterations seem not to be expressed by structural means, but might encompass variations in synaptic function that do not lead to changes in the structure of GABAergic axons.

12.4 Spatial scale of structural plasticity of GABAergic axons

Although plasticity of GABAergic synapses in various paradigms is now a well-accepted fact, the spatial scale at which these mechanisms work is still a matter of debate. GABAergic plasticity has been reported to critically rely on network activity levels in the entire neuronal network (Burrone et al., 2002; Hartman et al., 2006), as well as to be regulated on a cellular level (Chattopadhyaya et al., 2007; Peng et al., 2010) or even on individual dendritic branches (Liu, 2004). While a network-wide plasticity mechanism is believed to employ diffusible factors or intracellular molecules as plasticity-inducing signals (Rutherford et al., 1997; Brunig et al., 2001; Beattie et al., 2002; Stellwagen and Malenka, 2006; Swanwick et al., 2006), more localized plasticity mechanisms could be induced by additional signals, including trans-synaptic signaling and adhesion molecules or local intracellular signals (Sutton et al., 2006; Hou et al., 2008; Ibata et al., 2008; Turrigiano, 2008).

To investigate the spatial scale of the specific plasticity mechanisms discovered in this study, a fraction of the slice culture was manipulated using an adapted local superfusion technique (Veselovsky et al., 1996). If activity reduction was confined to the superfused fraction of the slice culture, axons within the superfusion spot still exhibited less structural dynamics than their non-manipulated neighbors in the slice culture (Figure 27 B, C). This observation is consistent with the effect of activity reduction in the entire slice culture. Furthermore, it suggests that also more localized alterations of network

activity have the ability to evoke structural plasticity of GABAergic synapses. Notwithstanding, the paradigm used here affects a continuous block of neuronal tissue, where even the signaling via diffusible factors might still be intact. Therefore, future studies will need to include the manipulation of individual cells and even subcellular compartments to truly assess the spatial scale of this form of GABAergic plasticity. The present study has established a method for biolistic transfection of individual cells in hippocampal slice cultures, and set the groundwork for further experiments on a single-cell level (Figure 28).

13. Conclusion

In summary, the experimental work performed for this thesis yields three main findings on the subject of structural dynamics and plasticity of GABAergic axons:

(1) The data presented here demonstrate different populations of presynaptic boutons on GABAergic axons. Most persistent boutons are suggested to represent *bona fide* GABAergic synapses. Transient boutons could constitute both prospective sites for synapse formation as well as assembling or degrading synapses. Short-lived boutons probably reflect transport events along the GABAergic axon. Boutons with the same dynamics were found not to cluster on the axon.

(2) Reduction of neuronal activity in the network reduces the structural dynamics of GABAergic axons, mostly by reducing the exploration of prospective synaptic sites and synapse assembly/degradation. However, this reaction is not translated into changes in bouton density over the course of several days, suggesting that rather the connectivity and/or strength of inhibitory synapses are changed in response to large-scale, long-term manipulation of neuronal activity.

(3) Enhancing neuronal activity in the network increased structural dynamics of GABAergic axons, mostly facilitating material exchange and competition for axonal resources. Interestingly, this effect required the activation of $GABA_A$ receptors, suggesting a novel role in signaling for these receptors.

Outlook

Plasticity of both excitatory and inhibitory synapses is crucial for balancing the activity level in a neuronal network. The importance of this balance of excitation and inhibition is highlighted by the severe neurological phenotypes that can arise from disturbing it (Yizhar et al., 2011; Chattopadhyaya and Cristo, 2012). Understanding both excitatory and inhibitory plasticity mechanisms that contribute to the balance of excitation and inhibition will ultimately allow for better therapies of neurological disorders like autism and schizophrenia.

The aim of this thesis was to shed light on the structural characteristics and plasticity mechanisms of inhibitory, GABAergic synapses to contribute to filling the gap of knowledge between excitatory and inhibitory synaptic plasticity. Different types of GABAergic boutons were described on the axon, the majority of which likely represented mature synapses. Baseline structural dynamics were expressed as bouton turnover, the density of different bouton categories, or variations in bouton volumes. These dynamics were found to be affected by network-wide activity manipulations within a few hours. Interestingly, high-activity induced structural plasticity was found to critically depend on

the activation of $GABA_A$ receptors. Long-term (48 h to 7 d) activity manipulations did affect neither the density nor the dynamics of GABAergic boutons, suggesting that other than structural mechanisms are employed to deal with GABAergic plasticity after such periods. Data presented in this thesis set the groundwork for further experiments in at least two different directions.

First, the established experimental setup will allow for the investigation of the molecular mechanisms underlying the observed mechanisms of structural GABAergic plasticity. Diffusible factors such as BDNF or TNFα have been implemented in various plasticity paradigms, also at inhibitory synapses. Subjecting hippocampal slice cultures to the activity manipulations described here, while blocking different signaling cascades activated by BDNF or TNFα would be an obvious first step to determining the molecular mechanisms underlying structural GABAergic plasticity. Furthermore, the intriguing role of $GABA_A$ receptors in these paradigms should be investigated. As discussed above, possible explanations for the involvement of $GABA_A$ receptors in structural dynamics of GABAergic axons could be signaling induced by the presynaptic population of $GABA_A$ receptors or the interaction of $GABA_A$ receptors with other signaling systems. By knocking out the expression of $GABA_A$ receptors in either individual GABAergic interneurons or candidate signaling systems while enhancing neuronal activity with 4-AP could shed light on these questions, respectively.

Second, the work presented in this thesis has already set the groundwork for investigating the spatial scale of the structural plasticity of GABAergic synapses. Using single-cell transfection with light-gated ion channels and fluorescent marker proteins will enable the analysis of structural GABAergic plasticity following manipulations at the single cell level. Also, the manipulation of individual interneurons is plausible. It will be important to determine the spatial scale on which the observed structural plasticity of GABAergic synapses operates. This knowledge could furthermore help to determine the molecular and cellular mechanisms that evoke this form of plasticity.

Acknowledgements

First of all, I would like **Corette Wierenga, PhD**, for supervising my thesis work and introducing me to the field of synaptic plasticity. I am very grateful for the time she took to introduce me to two-photon microscopy and in-depth data analysis. Both professionally and personally, it was a great pleasure to work with her. I am very grateful to **Prof. Dr. Tobias Bonhoeffer**, for giving me the opportunity to carry out my thesis work in his department. I would like to thank him for his continuous support of my scientific career. I appreciate that he always took the time for guidance and advice, despite his busy schedule. I would furthermore like to thank **Prof. Dr. Andreas Herz** for being a very supportive and helpful member of my thesis advisor committee. I am thankful to **Prof. Dr. Stefan Kröger** for reviewing this thesis, and for his scientific enthusiasm when discussing my work.

A big thank you goes to **Volker Staiger, Frank Voss, and Claudia Huber**. Volker was a great help with the local superfusion and other technical problems. Frank prepared wonderful slice cultures and did not lose his mind when the mice went on their annual strike. Claudia helped with all kinds of molecular biology. Thanks also to the MPIN workshop, IT, and administration staff. Overall, it was a wonderful experience to work in the **Bonhoeffer lab**. I would like to thank all present and past members of the **Bonhoeffer and the Stein lab** with whom I overlapped during my stay. Thanks for coffee breaks, running and badminton sessions and all the good conversations. I would like to thank **Dr. Matthias Traut** for comments on this thesis.

Thanks also to the **Boehringer Ingelheim Fonds** for almost three years of monetary and continued personal support. Being part of the BIF family continues to be a wonderful experience! Furthermore, the **IMPRS** and the **GSN** enabled me to do a fast-track PhD and supported me throughout my entire PhD. Thanks!

I would like to thank **Prof. Dr. Eleni Roussa** for introducing me to the field of neurosciences and scientific work in general. **Prof. Dr. Lei Wang** truly sparked my passion for science. It was his visionary thinking, his great ideas and the opportunity to design my own research with him that made time at the Salk Institute a wonderful experience. I am grateful for his continued support.

I would like to thank all **my friends**, who made these past years in Munich so enjoyable, be it in Munich, on the Volleyball court, or travelling.
All my love goes to **Matthias**, for his constant support and his cheerfulness.
Most importantly, I would like to thank my family. **Mama, Papa, Lisa, Lorenz**, without you I would neither be who I am nor where I am.

Bibliography

Ahmari SE, Buchanan J, Smith SJ (2000) Assembly of presynaptic active zones from cytoplasmic transport packets. Nat Neurosci 3:445-451.

Ang ES, Jr., Haydar TF, Gluncic V, Rakic P (2003) Four-dimensional migratory coordinates of GABAergic interneurons in the developing mouse cortex. J Neurosci 23:5805-5815.

Antonova I, Lu FM, Zablow L, Udo H, Hawkins RD (2009) Rapid and long-lasting increase in sites for synapse assembly during late-phase potentiation in rat hippocampal neurons. PLoS One 4:e7690.

Axmacher N, Winterer J, Stanton PK, Draguhn A, Muller W (2004) Two-photon imaging of spontaneous vesicular release in acute brain slices and its modulation by presynaptic GABAA receptors. Neuroimage 22:1014-1021.

Bannai H, Levi S, Schweizer C, Inoue T, Launey T, Racine V, Sibarita JB, Mikoshiba K, Triller A (2009) Activity-dependent tuning of inhibitory neurotransmission based on GABAAR diffusion dynamics. Neuron 62:670-682.

Baulac S, Huberfeld G, Gourfinkel-An I, Mitropoulou G, Beranger A, Prud'homme JF, Baulac M, Brice A, Bruzzone R, LeGuern E (2001) First genetic evidence of GABA(A) receptor dysfunction in epilepsy: a mutation in the gamma2-subunit gene. Nat Genet 28:46-48.

Beattie EC, Stellwagen D, Morishita W, Bresnahan JC, Ha BK, Von Zastrow M, Beattie MS, Malenka RC (2002) Control of synaptic strength by glial TNFalpha. Science 295:2282-2285.

Bednarek E, Caroni P (2011) beta-Adducin is required for stable assembly of new synapses and improved memory upon environmental enrichment. Neuron 69:1132-1146.

Bellocchio EE, Reimer RJ, Fremeau RT, Jr., Edwards RH (2000) Uptake of glutamate into synaptic vesicles by an inorganic phosphate transporter. Science 289:957-960.

Berninger B, Marty S, Zafra F, da Penha Berzaghi M, Thoenen H, Lindholm D (1995) GABAergic stimulation switches from enhancing to repressing BDNF expression in rat hippocampal neurons during maturation in vitro. Development 121:2327-2335.

Bliss TV, Lomo T (1973) Long-lasting potentiation of synaptic transmission in the dentate area of the anaesthetized rabbit following stimulation of the perforant path. J Physiol 232:331-356.

Bortone D, Polleux F (2009) KCC2 expression promotes the termination of cortical interneuron migration in a voltage-sensitive calcium-dependent manner. Neuron 62:53-71.

Bosch M, Hayashi Y (2011) Structural plasticity of dendritic spines. Curr Opin Neurobiol 22:383-388.

Boulos S, Meloni BP, Arthur PG, Bojarski C, Knuckey NW (2006) Assessment of CMV, RSV and SYN1 promoters and the woodchuck post-transcriptional regulatory element in adenovirus vectors for transgene expression in cortical neuronal cultures. Brain Res 1102:27-38.

Bourne JN, Harris KM (2011) Coordination of size and number of excitatory and inhibitory synapses results in a balanced structural plasticity along mature hippocampal CA1 dendrites during LTP. Hippocampus 21:354-373.

Brehm L, Hjeds H, Krogsgaard-Larsen P (1972) The structure of muscimol, a GABA analogue of restricted conformation. Acta Chem Scand 26:1298-1299.

Bresler T, Shapira M, Boeckers T, Dresbach T, Futter M, Garner CC, Rosenblum K, Gundelfinger ED, Ziv NE (2004) Postsynaptic density assembly is fundamentally different from presynaptic active zone assembly. J Neurosci 24:1507-1520.

Brunig I, Penschuck S, Berninger B, Benson J, Fritschy JM (2001) BDNF reduces miniature inhibitory postsynaptic currents by rapid downregulation of GABA(A) receptor surface expression. Eur J Neurosci 13:1320-1328.

Burrone J, O'Byrne M, Murthy VN (2002) Multiple forms of synaptic plasticity triggered by selective suppression of activity in individual neurons. Nature 420:414-418.

Bury LA, Sabo SL (2010) How it's made: the synapse. Mol Interv 10:282-292.

Bury LA, Sabo SL (2011) Coordinated trafficking of synaptic vesicle and active zone proteins prior to synapse formation. Neural Dev 6:24.

Butt SJ, Fuccillo M, Nery S, Noctor S, Kriegstein A, Corbin JG, Fishell G (2005) The temporal and spatial origins of cortical interneurons predict their physiological subtype. Neuron 48:591-604.

Buzsaki G, Horvath Z, Urioste R, Hetke J, Wise K (1992) High-frequency network oscillation in the hippocampus. Science 256:1025-1027.

Cai Q, Sheng ZH (2009) Mitochondrial transport and docking in axons. Exp Neurol 218:257-267.

Carmona MA, Pozas E, Martinez A, Espinosa-Parrilla JF, Soriano E, Aguado F (2006) Age-dependent spontaneous hyperexcitability and impairment of GABAergic function in the hippocampus of mice lacking trkB. Cereb Cortex 16:47-63.

Caroni P, Donato F, Muller D (2012) Structural plasticity upon learning: regulation and functions. Nat Rev Neurosci 13:478-490.

Castillo PE, Chiu CQ, Carroll RC (2011) Long-term plasticity at inhibitory synapses. Curr Opin Neurobiol 21:328-338.

Chambon JP, Feltz P, Heaulme M, Restle S, Schlichter R, Biziere K, Wermuth CG (1985) An arylaminopyridazine derivative of gamma-aminobutyric acid (GABA) is a selective and competitive antagonist at the GABAA receptor site. Proc Natl Acad Sci U S A 82:1832-1836.

Chattopadhyaya B, Cristo GD (2012) GABAergic circuit dysfunctions in neurodevelopmental disorders. Front Psychiatry 3:51.

Chattopadhyaya B, Di Cristo G, Higashiyama H, Knott GW, Kuhlman SJ, Welker E, Huang ZJ (2004) Experience and activity-dependent maturation of perisomatic GABAergic innervation in primary visual cortex during a postnatal critical period. J Neurosci 24:9598-9611.

Chattopadhyaya B, Di Cristo G, Wu CZ, Knott G, Kuhlman S, Fu Y, Palmiter RD, Huang ZJ (2007) GAD67-mediated GABA synthesis and signaling regulate inhibitory synaptic innervation in the visual cortex. Neuron 54:889-903.

Chen G, Trombley PQ, van den Pol AN (1996) Excitatory actions of GABA in developing rat hypothalamic neurones. J Physiol 494 (Pt 2):451-464.
Chen JL, Lin WC, Cha JW, So PT, Kubota Y, Nedivi E (2011) Structural basis for the role of inhibition in facilitating adult brain plasticity. Nat Neurosci 14:587-594.
Chen JL, Villa KL, Cha JW, So PT, Kubota Y, Nedivi E (2012) Clustered dynamics of inhibitory synapses and dendritic spines in the adult neocortex. Neuron 74:361-373.
Chevaleyre V, Heifets BD, Kaeser PS, Sudhof TC, Castillo PE (2007) Endocannabinoid-mediated long-term plasticity requires cAMP/PKA signaling and RIM1alpha. Neuron 54:801-812.
Cho KO, Hunt CA, Kennedy MB (1992) The rat brain postsynaptic density fraction contains a homolog of the Drosophila discs-large tumor suppressor protein. Neuron 9:929-942.
Chubykin AA, Atasoy D, Etherton MR, Brose N, Kavalali ET, Gibson JR, Sudhof TC (2007) Activity-dependent validation of excitatory versus inhibitory synapses by neuroligin-1 versus neuroligin-2. Neuron 54:919-931.
Cingolani LA, Goda Y (2008) Differential involvement of beta3 integrin in pre- and postsynaptic forms of adaptation to chronic activity deprivation. Neuron Glia Biol 4:179-187.
Citri A, Malenka RC (2008) Synaptic plasticity: multiple forms, functions, and mechanisms. Neuropsychopharmacology 33:18-41.
Clark PJ, Kohman RA, Miller DS, Bhattacharya TK, Haferkamp EH, Rhodes JS (2010) Adult hippocampal neurogenesis and c-Fos induction during escalation of voluntary wheel running in C57BL/6J mice. Behav Brain Res 213:246-252.
Craddock N, Jones L, Jones IR, Kirov G, Green EK, Grozeva D, Moskvina V, Nikolov I, Hamshere ML, Vukcevic D, Caesar S, Gordon-Smith K, Fraser C, Russell E, Norton N, Breen G, St Clair D, Collier DA, Young AH, Ferrier IN, Farmer A, McGuffin P, Holmans PA, Donnelly P, Owen MJ, O'Donovan MC (2010) Strong genetic evidence for a selective influence of GABAA receptors on a component of the bipolar disorder phenotype. Mol Psychiatry 15:146-153.
Curtis DR, Hosli L, Johnston GA (1968a) A pharmacological study of the depression of spinal neurones by glycine and related amino acids. Exp Brain Res 6:1-18.
Curtis DR, Hosli L, Johnston GA, Johnston IH (1968b) The hyperpolarization of spinal motoneurones by glycine and related amino acids. Exp Brain Res 5:235-258.
Curtis DR, Duggan AW, Felix D, Johnston GA (1970) GABA, bicuculline and central inhibition. Nature 226:1222-1224.
Cuzon VC, Yeh PW, Cheng Q, Yeh HH (2006) Ambient GABA promotes cortical entry of tangentially migrating cells derived from the medial ganglionic eminence. Cereb Cortex 16:1377-1388.
Dalva MB, McClelland AC, Kayser MS (2007) Cell adhesion molecules: signalling functions at the synapse. Nat Rev Neurosci 8:206-220.
Darcy KJ, Staras K, Collinson LM, Goda Y (2006) Constitutive sharing of recycling synaptic vesicles between presynaptic boutons. Nat Neurosci 9:315-321.
De Gois S, Schafer MK, Defamie N, Chen C, Ricci A, Weihe E, Varoqui H, Erickson JD (2005) Homeostatic scaling of vesicular glutamate and GABA transporter expression in rat neocortical circuits. J Neurosci 25:7121-7133.

De Paola V, Arber S, Caroni P (2003) AMPA receptors regulate dynamic equilibrium of presynaptic terminals in mature hippocampal networks. Nat Neurosci 6:491-500.
De Roo M, Klauser P, Muller D (2008) LTP promotes a selective long-term stabilization and clustering of dendritic spines. PLoS Biol 6:e219.
De Simoni A, Griesinger CB, Edwards FA (2003) Development of rat CA1 neurones in acute versus organotypic slices: role of experience in synaptic morphology and activity. J Physiol 550:135-147.
Di Cristo G, Chattopadhyaya B, Kuhlman SJ, Fu Y, Belanger MC, Wu CZ, Rutishauser U, Maffei L, Huang ZJ (2007) Activity-dependent PSA expression regulates inhibitory maturation and onset of critical period plasticity. Nat Neurosci 10:1569-1577.
Dobie FA, Craig AM (2011) Inhibitory synapse dynamics: coordinated presynaptic and postsynaptic mobility and the major contribution of recycled vesicles to new synapse formation. J Neurosci 31:10481-10493.
Dong N, Qi J, Chen G (2007) Molecular reconstitution of functional GABAergic synapses with expression of neuroligin-2 and GABAA receptors. Mol Cell Neurosci 35:14-23.
Draguhn A, Axmacher N, Kolbaev S (2008) Presynaptic ionotropic GABA receptors. Results Probl Cell Differ 44:69-85.
Dragunow M, Faull R (1989) The use of c-fos as a metabolic marker in neuronal pathway tracing. J Neurosci Methods 29:261-265.
Eccles J, McIntyre A (1951) Plasticity of mammalian monosynaptic reflexes. Nature 167:466-468.
Ehlers MD, Heine M, Groc L, Lee MC, Choquet D (2007) Diffusional trapping of GluR1 AMPA receptors by input-specific synaptic activity. Neuron 54:447-460.
Engert F, Bonhoeffer T (1999) Dendritic spine changes associated with hippocampal long-term synaptic plasticity. Nature 399:66-70.
Essrich C, Lorez M, Benson JA, Fritschy JM, Luscher B (1998) Postsynaptic clustering of major GABAA receptor subtypes requires the gamma 2 subunit and gephyrin. Nat Neurosci 1:563-571.
Fazzari P, Paternain AV, Valiente M, Pla R, Lujan R, Lloyd K, Lerma J, Marin O, Rico B (2010) Control of cortical GABA circuitry development by Nrg1 and ErbB4 signalling. Nature 464:1376-1380.
Fenno L, Yizhar O, Deisseroth K (2011) The development and application of optogenetics. Annu Rev Neurosci 34:389-412.
Fernandez-Alfonso T, Ryan TA (2008) A heterogeneous "resting" pool of synaptic vesicles that is dynamically interchanged across boutons in mammalian CNS synapses. Brain Cell Biol 36:87-100.
Fiumelli H, Woodin MA (2007) Role of activity-dependent regulation of neuronal chloride homeostasis in development. Curr Opin Neurobiol 17:81-86.
Fogarty M, Grist M, Gelman D, Marin O, Pachnis V, Kessaris N (2007) Spatial genetic patterning of the embryonic neuroepithelium generates GABAergic interneuron diversity in the adult cortex. J Neurosci 27:10935-10946.
Frey U, Morris RG (1997) Synaptic tagging and long-term potentiation. Nature 385:533-536.
Friedman HV, Bresler T, Garner CC, Ziv NE (2000) Assembly of new individual excitatory synapses: time course and temporal order of synaptic molecule recruitment. Neuron 27:57-69.

Frischknecht R, Fejtova A, Viesti M, Stephan A, Sonderegger P (2008) Activity-induced synaptic capture and exocytosis of the neuronal serine protease neurotrypsin. J Neurosci 28:1568-1579.
Fritschy JM, Harvey RJ, Schwarz G (2008) Gephyrin: where do we stand, where do we go? Trends Neurosci 31:257-264.
Fritschy JM, Panzanelli P, Kralic JE, Vogt KE, Sassoe-Pognetto M (2006) Differential dependence of axo-dendritic and axo-somatic GABAergic synapses on GABAA receptors containing the alpha1 subunit in Purkinje cells. J Neurosci 26:3245-3255.
Fu M, Yu X, Lu J, Zuo Y (2012) Repetitive motor learning induces coordinated formation of clustered dendritic spines in vivo. Nature 483:92-95.
Fu Y, Huang ZJ (2011) Differential dynamics and activity-dependent regulation of alpha- and beta-neurexins at developing GABAergic synapses. Proc Natl Acad Sci U S A 107:22699-22704.
Gähwiler BH (1981) Organotypic monolayer cultures of nervous tissue. J Neurosci Methods 4:329-342.
Ganguly K, Schinder AF, Wong ST, Poo M (2001) GABA itself promotes the developmental switch of neuronal GABAergic responses from excitation to inhibition. Cell 105:521-532.
Garner CC, Kindler S, Gundelfinger ED (2000) Molecular determinants of presynaptic active zones. Curr Opin Neurobiol 10:321-327.
Garner CC, Waites CL, Ziv NE (2006) Synapse development: still looking for the forest, still lost in the trees. Cell Tissue Res 326:249-262.
Gibson HE, Edwards JG, Page RS, Van Hook MJ, Kauer JA (2008) TRPV1 channels mediate long-term depression at synapses on hippocampal interneurons. Neuron 57:746-759.
Giotti A, Luzzi S, Spagnesi S, Zilletti L (1983) GABAA and GABAB receptor-mediated effects in guinea-pig ileum. Br J Pharmacol 78:469-478.
Goddard CA, Butts DA, Shatz CJ (2007) Regulation of CNS synapses by neuronal MHC class I. Proc Natl Acad Sci U S A 104:6828-6833.
Goldstein AY, Wang X, Schwarz TL (2008) Axonal transport and the delivery of pre-synaptic components. Curr Opin Neurobiol 18:495-503.
Govindarajan A, Israely I, Huang SY, Tonegawa S (2011) The dendritic branch is the preferred integrative unit for protein synthesis-dependent LTP. Neuron 69:132-146.
Gradinaru V, Thompson KR, Deisseroth K (2008) eNpHR: a Natronomonas halorhodopsin enhanced for optogenetic applications. Brain Cell Biol 36:129-139.
Graf ER, Zhang X, Jin SX, Linhoff MW, Craig AM (2004) Neurexins induce differentiation of GABA and glutamate postsynaptic specializations via neuroligins. Cell 119:1013-1026.
Gray EG (1963) Electron microscopy of presynaptic organelles of the spinal cord. J Anat 97:101-106.
Gray NW, Weimer RM, Bureau I, Svoboda K (2006) Rapid redistribution of synaptic PSD-95 in the neocortex in vivo. PLoS Biol 4:e370.
Hamann M, Desarmenien M, Desaulles E, Bader MF, Feltz P (1988) Quantitative evaluation of the properties of a pyridazinyl GABA derivative (SR 95531) as a GABAA competitive antagonist. An electrophysiological approach. Brain Res 442:287-296.

Hanus C, Ehrensperger MV, Triller A (2006) Activity-dependent movements of postsynaptic scaffolds at inhibitory synapses. J Neurosci 26:4586-4595.
Harms KJ, Craig AM (2005) Synapse composition and organization following chronic activity blockade in cultured hippocampal neurons. J Comp Neurol 490:72-84.
Harris KM, Kater SB (1994) Dendritic spines: cellular specializations imparting both stability and flexibility to synaptic function. Annu Rev Neurosci 17:341-371.
Hartman KN, Pal SK, Burrone J, Murthy VN (2006) Activity-dependent regulation of inhibitory synaptic transmission in hippocampal neurons. Nat Neurosci 9:642-649.
Hartmann K, Bruehl C, Golovko T, Draguhn A (2008) Fast homeostatic plasticity of inhibition via activity-dependent vesicular filling. PLoS One 3:e2979.
Heaulme M, Chambon JP, Leyris R, Molimard JC, Wermuth CG, Biziere K (1986) Biochemical characterization of the interaction of three pyridazinyl-GABA derivatives with the GABAA receptor site. Brain Res 384:224-231.
Hebb D (1949) The organization of behavior. New York: John Wiley Sons.
Heifets BD, Chevaleyre V, Castillo PE (2008) Interneuron activity controls endocannabinoid-mediated presynaptic plasticity through calcineurin. Proc Natl Acad Sci U S A 105:10250-10255.
Hendry SH, Schwark HD, Jones EG, Yan J (1987) Numbers and proportions of GABA-immunoreactive neurons in different areas of monkey cerebral cortex. J Neurosci 7:1503-1519.
Hensch TK, Fagiolini M, Mataga N, Stryker MP, Baekkeskov S, Kash SF (1998) Local GABA circuit control of experience-dependent plasticity in developing visual cortex. Science 282:1504-1508.
Herzog E, Nadrigny F, Silm K, Biesemann C, Helling I, Bersot T, Steffens H, Schwartzmann R, Nagerl UV, El Mestikawy S, Rhee J, Kirchhoff F, Brose N (2011) In vivo imaging of intersynaptic vesicle exchange using VGLUT1 Venus knock-in mice. J Neurosci 31:15544-15559.
Hofer SB, Mrsic-Flogel TD, Bonhoeffer T, Hubener M (2009) Experience leaves a lasting structural trace in cortical circuits. Nature 457:313-317.
Holtmaat A, Svoboda K (2009) Experience-dependent structural synaptic plasticity in the mammalian brain. Nat Rev Neurosci 10:647-658.
Holtmaat AJ, Trachtenberg JT, Wilbrecht L, Shepherd GM, Zhang X, Knott GW, Svoboda K (2005) Transient and persistent dendritic spines in the neocortex in vivo. Neuron 45:279-291.
Hong EJ, McCord AE, Greenberg ME (2008) A biological function for the neuronal activity-dependent component of Bdnf transcription in the development of cortical inhibition. Neuron 60:610-624.
Hou Q, Zhang D, Jarzylo L, Huganir RL, Man HY (2008) Homeostatic regulation of AMPA receptor expression at single hippocampal synapses. Proc Natl Acad Sci U S A 105:775-780.
Huang ZJ, Scheiffele P (2008) GABA and neuroligin signaling: linking synaptic activity and adhesion in inhibitory synapse development. Curr Opin Neurobiol 18:77-83.
Ibata K, Sun Q, Turrigiano GG (2008) Rapid synaptic scaling induced by changes in postsynaptic firing. Neuron 57:819-826.
Iversen LL, Mitchell JF, Srinivasan V (1971) The release of gamma-aminobutyric acid during inhibition in the cat visual cortex. J Physiol 212:519-534.

Jacob TC, Bogdanov YD, Magnus C, Saliba RS, Kittler JT, Haydon PG, Moss SJ (2005) Gephyrin regulates the cell surface dynamics of synaptic GABAA receptors. J Neurosci 25:10469-10478.

Jiao Y, Zhang Z, Zhang C, Wang X, Sakata K, Lu B, Sun QQ (2011) A key mechanism underlying sensory experience-dependent maturation of neocortical GABAergic circuits in vivo. Proc Natl Acad Sci U S A 108:12131-12136.

Johansson S, Druzin M, Haage D, Wang MD (2001) The functional role of a bicuculline-sensitive Ca2+-activated K+ current in rat medial preoptic neurons. J Physiol 532:625-635.

Johnston GA, Curtis DR, De Groat WC, Duggan AW (1968) Central actions of ibotenic acid and muscimol. Biochem Pharmacol 17:2488-2489.

Kaneko M, Stellwagen D, Malenka RC, Stryker MP (2008) Tumor necrosis factor-alpha mediates one component of competitive, experience-dependent plasticity in developing visual cortex. Neuron 58:673-680.

Keck T, Mrsic-Flogel TD, Vaz Afonso M, Eysel UT, Bonhoeffer T, Hubener M (2008) Massive restructuring of neuronal circuits during functional reorganization of adult visual cortex. Nat Neurosci 11:1162-1167.

Keck T, Scheuss V, Jacobsen RI, Wierenga CJ, Eysel UT, Bonhoeffer T, Hubener M (2011) Loss of sensory input causes rapid structural changes of inhibitory neurons in adult mouse visual cortex. Neuron 71:869-882.

Kerschensteiner D, Morgan JL, Parker ED, Lewis RM, Wong RO (2009) Neurotransmission selectively regulates synapse formation in parallel circuits in vivo. Nature 460:1016-1020.

Kilman V, van Rossum MC, Turrigiano GG (2002) Activity deprivation reduces miniature IPSC amplitude by decreasing the number of postsynaptic GABA(A) receptors clustered at neocortical synapses. J Neurosci 22:1328-1337.

Kittler JT, Thomas P, Tretter V, Bogdanov YD, Haucke V, Smart TG, Moss SJ (2004) Huntingtin-associated protein 1 regulates inhibitory synaptic transmission by modulating gamma-aminobutyric acid type A receptor membrane trafficking. Proc Natl Acad Sci U S A 101:12736-12741.

Klassen MP, Wu YE, Maeder CI, Nakae I, Cueva JG, Lehrman EK, Tada M, Gengyo-Ando K, Wang GJ, Goodman M, Mitani S, Kontani K, Katada T, Shen K (2010) An Arf-like small G protein, ARL-8, promotes the axonal transport of presynaptic cargoes by suppressing vesicle aggregation. Neuron 66:710-723.

Klausberger T, Somogyi P (2008) Neuronal diversity and temporal dynamics: the unity of hippocampal circuit operations. Science 321:53-57.

Kleindienst T, Winnubst J, Roth-Alpermann C, Bonhoeffer T, Lohmann C (2011) Activity-dependent clustering of functional synaptic inputs on developing hippocampal dendrites. Neuron 72:1012-1024.

Kneussel M, Brandstatter JH, Laube B, Stahl S, Muller U, Betz H (1999) Loss of postsynaptic GABA(A) receptor clustering in gephyrin-deficient mice. J Neurosci 19:9289-9297.

Kraszewski K, Mundigl O, Daniell L, Verderio C, Matteoli M, De Camilli P (1995) Synaptic vesicle dynamics in living cultured hippocampal neurons visualized with CY3-conjugated antibodies directed against the lumenal domain of synaptotagmin. J Neurosci 15:4328-4342.

Krueger SR, Kolar A, Fitzsimonds RM (2003) The presynaptic release apparatus is functional in the absence of dendritic contact and highly mobile within isolated axons. Neuron 40:945-957.
Kugler S, Meyn L, Holzmuller H, Gerhardt E, Isenmann S, Schulz JB, Bahr M (2001) Neuron-specific expression of therapeutic proteins: evaluation of different cellular promoters in recombinant adenoviral vectors. Mol Cell Neurosci 17:78-96.
Kullmann DM, Ruiz A, Rusakov DM, Scott R, Semyanov A, Walker MC (2005) Presynaptic, extrasynaptic and axonal GABAA receptors in the CNS: where and why? Prog Biophys Mol Biol 87:33-46.
Kuriu T, Yanagawa Y, Konishi S (2011) Activity-dependent coordinated mobility of hippocampal inhibitory synapses visualized with presynaptic and postsynaptic tagged-molecular markers. Mol Cell Neurosci 49:184-195.
Kwon HB, Sabatini BL (2011) Glutamate induces de novo growth of functional spines in developing cortex. Nature 474:100-104.
Lai CS, Franke TF, Gan WB (2012) Opposite effects of fear conditioning and extinction on dendritic spine remodelling. Nature 483:87-91.
Lamsa K, Taira T (2003) Use-dependent shift from inhibitory to excitatory GABAA receptor action in SP-O interneurons in the rat hippocampal CA3 area. J Neurophysiol 90:1983-1995.
Lanyi JK, Duschl A, Varo G, Zimanyi L (1990) Anion binding to the chloride pump, halorhodopsin, and its implications for the transport mechanism. FEBS Lett 265:1-6.
Lau CG, Murthy VN (2012) Activity-dependent regulation of inhibition via GAD67. J Neurosci 32:8521-8531.
Lee HH, Deeb TZ, Walker JA, Davies PA, Moss SJ (2011) NMDA receptor activity downregulates KCC2 resulting in depolarizing GABAA receptor-mediated currents. Nat Neurosci 14:736-743.
Leitch E, Coaker J, Young C, Mehta V, Sernagor E (2005) GABA type-A activity controls its own developmental polarity switch in the maturing retina. J Neurosci 25:4801-4805.
Li RW, Yu W, Christie S, Miralles CP, Bai J, Loturco JJ, De Blas AL (2005) Disruption of postsynaptic GABA receptor clusters leads to decreased GABAergic innervation of pyramidal neurons. J Neurochem 95:756-770.
Lin JY (2011) A user's guide to channelrhodopsin variants: features, limitations and future developments. Exp Physiol 96:19-25.
Liodis P, Denaxa M, Grigoriou M, Akufo-Addo C, Yanagawa Y, Pachnis V (2007) Lhx6 activity is required for the normal migration and specification of cortical interneuron subtypes. J Neurosci 27:3078-3089.
Liu F, Wan Q, Pristupa ZB, Yu XM, Wang YT, Niznik HB (2000) Direct protein-protein coupling enables cross-talk between dopamine D5 and gamma-aminobutyric acid A receptors. Nature 403:274-280.
Liu G (2004) Local structural balance and functional interaction of excitatory and inhibitory synapses in hippocampal dendrites. Nat Neurosci 7:373-379.
Liu X, Ramirez S, Pang PT, Puryear CB, Govindarajan A, Deisseroth K, Tonegawa S (2012) Optogenetic stimulation of a hippocampal engram activates fear memory recall. Nature 484:381-385.

Lopez-Bendito G, Sturgess K, Erdelyi F, Szabo G, Molnar Z, Paulsen O (2004) Preferential origin and layer destination of GAD65-GFP cortical interneurons. Cereb Cortex 14:1122-1133.

LoTurco JJ, Owens DF, Heath MJ, Davis MB, Kriegstein AR (1995) GABA and glutamate depolarize cortical progenitor cells and inhibit DNA synthesis. Neuron 15:1287-1298.

Ludwig A, Li H, Saarma M, Kaila K, Rivera C (2003) Developmental up-regulation of KCC2 in the absence of GABAergic and glutamatergic transmission. Eur J Neurosci 18:3199-3206.

Luscher B, Fuchs T, Kilpatrick CL (2011) GABAA receptor trafficking-mediated plasticity of inhibitory synapses. Neuron 70:385-409.

Lushnikova I, Skibo G, Muller D, Nikonenko I (2009) Synaptic potentiation induces increased glial coverage of excitatory synapses in CA1 hippocampus. Hippocampus 19:753-762.

Lushnikova I, Skibo G, Muller D, Nikonenko I (2011) Excitatory synaptic activity is associated with a rapid structural plasticity of inhibitory synapses on hippocampal CA1 pyramidal cells. Neuropharmacology 60:757-764.

Ma DQ, Whitehead PL, Menold MM, Martin ER, Ashley-Koch AE, Mei H, Ritchie MD, Delong GR, Abramson RK, Wright HH, Cuccaro ML, Hussman JP, Gilbert JR, Pericak-Vance MA (2005) Identification of significant association and gene-gene interaction of GABA receptor subunit genes in autism. Am J Hum Genet 77:377-388.

Maric D, Liu QY, Maric I, Chaudry S, Chang YH, Smith SV, Sieghart W, Fritschy JM, Barker JL (2001) GABA expression dominates neuronal lineage progression in the embryonic rat neocortex and facilitates neurite outgrowth via GABA(A) autoreceptor/Cl- channels. J Neurosci 21:2343-2360.

Marik SA, Yamahachi H, McManus JN, Szabo G, Gilbert CD (2010) Axonal dynamics of excitatory and inhibitory neurons in somatosensory cortex. PLoS Biol 8:e1000395.

Marsden KC, Beattie JB, Friedenthal J, Carroll RC (2007) NMDA receptor activation potentiates inhibitory transmission through GABA receptor-associated protein-dependent exocytosis of GABA(A) receptors. J Neurosci 27:14326-14337.

Marty S, Wehrle R, Fritschy JM, Sotelo C (2004) Quantitative effects produced by modifications of neuronal activity on the size of GABAA receptor clusters in hippocampal slice cultures. Eur J Neurosci 20:427-440.

Matsuzaki M, Honkura N, Ellis-Davies GC, Kasai H (2004) Structural basis of long-term potentiation in single dendritic spines. Nature 429:761-766.

Matsuzaki M, Ellis-Davies GC, Nemoto T, Miyashita Y, Iino M, Kasai H (2001) Dendritic spine geometry is critical for AMPA receptor expression in hippocampal CA1 pyramidal neurons. Nat Neurosci 4:1086-1092.

McAllister AK (2000) Biolistic transfection of neurons. Sci STKE 2000:pl1.

McAllister AK (2007) Dynamic aspects of CNS synapse formation. Annu Rev Neurosci 30:425-450.

McBain CJ, Kauer JA (2009) Presynaptic plasticity: targeted control of inhibitory networks. Curr Opin Neurobiol 19:254-262.

McIntire SL, Reimer RJ, Schuske K, Edwards RH, Jorgensen EM (1997) Identification and characterization of the vesicular GABA transporter. Nature 389:870-876.

McKernan RM, Whiting PJ (1996) Which GABAA-receptor subtypes really occur in the brain? Trends Neurosci 19:139-143.
Megias M, Emri Z, Freund TF, Gulyas AI (2001) Total number and distribution of inhibitory and excitatory synapses on hippocampal CA1 pyramidal cells. Neuroscience 102:527-540.
Miller KD (1996) Synaptic economics: competition and cooperation in synaptic plasticity. Neuron 17:371-374.
Minerbi A, Kahana R, Goldfeld L, Kaufman M, Marom S, Ziv NE (2009) Long-term relationships between synaptic tenacity, synaptic remodeling, and network activity. PLoS Biol 7:e1000136.
Morales B, Choi SY, Kirkwood A (2002) Dark rearing alters the development of GABAergic transmission in visual cortex. J Neurosci 22:8084-8090.
Murthy VN, Schikorski T, Stevens CF, Zhu Y (2001) Inactivity produces increases in neurotransmitter release and synapse size. Neuron 32:673-682.
Nagel G, Szellas T, Huhn W, Kateriya S, Adeishvili N, Berthold P, Ollig D, Hegemann P, Bamberg E (2003) Channelrhodopsin-2, a directly light-gated cation-selective membrane channel. Proc Natl Acad Sci U S A 100:13940-13945.
Narahashi T, Deguchi T, Urakawa N, Ohkubo Y (1960) Stabilization and rectification of muscle fiber membrane by tetrodotoxin. Am J Physiol 198:934-938.
Ohno N, Kidd GJ, Mahad D, Kiryu-Seo S, Avishai A, Komuro H, Trapp BD (2011) Myelination and axonal electrical activity modulate the distribution and motility of mitochondria at CNS nodes of Ranvier. J Neurosci 31:7249-7258.
Okabe S, Miwa A, Okado H (2001) Spine formation and correlated assembly of presynaptic and postsynaptic molecules. J Neurosci 21:6105-6114.
Owald D, Sigrist SJ (2009) Assembling the presynaptic active zone. Curr Opin Neurobiol 19:311-318.
Owens DF, Kriegstein AR (2002) Is there more to GABA than synaptic inhibition? Nat Rev Neurosci 3:715-727.
Owens DF, Boyce LH, Davis MB, Kriegstein AR (1996) Excitatory GABA responses in embryonic and neonatal cortical slices demonstrated by gramicidin perforated-patch recordings and calcium imaging. J Neurosci 16:6414-6423.
Papadopoulos T, Korte M, Eulenburg V, Kubota H, Retiounskaia M, Harvey RJ, Harvey K, O'Sullivan GA, Laube B, Hulsmann S, Geiger JR, Betz H (2007) Impaired GABAergic transmission and altered hippocampal synaptic plasticity in collybistin-deficient mice. Embo J 26:3888-3899.
Paradis S, Harrar DB, Lin Y, Koon AC, Hauser JL, Griffith EC, Zhu L, Brass LF, Chen C, Greenberg ME (2007) An RNAi-based approach identifies molecules required for glutamatergic and GABAergic synapse development. Neuron 53:217-232.
Patrizi A, Scelfo B, Viltono L, Briatore F, Fukaya M, Watanabe M, Strata P, Varoqueaux F, Brose N, Fritschy JM, Sassoe-Pognetto M (2008) Synapse formation and clustering of neuroligin-2 in the absence of GABAA receptors. Proc Natl Acad Sci U S A 105:13151-13156.
Pelhate M, Pichon Y (1974) Proceedings: Selective inhibition of potassium current in the giant axon of the cockroach. J Physiol 242:90P-91P.
Pelkey KA, McBain CJ (2008) Target-cell-dependent plasticity within the mossy fibre-CA3 circuit reveals compartmentalized regulation of presynaptic function at divergent release sites. J Physiol 586:1495-1502.

Peng YR, Zeng SY, Song HL, Li MY, Yamada MK, Yu X (2010) Postsynaptic spiking homeostatically induces cell-autonomous regulation of inhibitory inputs via retrograde signaling. J Neurosci 30:16220-16231.
Perez de la Mora M, Ferre S, Fuxe K (1997) GABA-dopamine receptor-receptor interactions in neostriatal membranes of the rat. Neurochem Res 22:1051-1054.
Pfeiffer F, Graham D, Betz H (1982) Purification by affinity chromatography of the glycine receptor of rat spinal cord. J Biol Chem 257:9389-9393.
Pouille F, Scanziani M (2001) Enforcement of temporal fidelity in pyramidal cells by somatic feed-forward inhibition. Science 293:1159-1163.
Pouzat C, Marty A (1999) Somatic recording of GABAergic autoreceptor current in cerebellar stellate and basket cells. J Neurosci 19:1675-1690.
Rannals MD, Kapur J (2011) Homeostatic strengthening of inhibitory synapses is mediated by the accumulation of GABA(A) receptors. J Neurosci 31:17701-17712.
Ratnayaka A, Marra V, Bush D, Burden JJ, Branco T, Staras K (2012) Recruitment of resting vesicles into recycling pools supports NMDA receptor-dependent synaptic potentiation in cultured hippocampal neurons. J Physiol 590:1585-1597.
Rial Verde EM, Lee-Osbourne J, Worley PF, Malinow R, Cline HT (2006) Increased expression of the immediate-early gene arc/arg3.1 reduces AMPA receptor-mediated synaptic transmission. Neuron 52:461-474.
Richter K, Langnaese K, Kreutz MR, Olias G, Zhai R, Scheich H, Garner CC, Gundelfinger ED (1999) Presynaptic cytomatrix protein bassoon is localized at both excitatory and inhibitory synapses of rat brain. J Comp Neurol 408:437-448.
Rinaldi A, Romeo S, Agustin-Pavon C, Oliverio A, Mele A (2010) Distinct patterns of Fos immunoreactivity in striatum and hippocampus induced by different kinds of novelty in mice. Neurobiol Learn Mem 94:373-381.
Rivera C, Voipio J, Payne JA, Ruusuvuori E, Lahtinen H, Lamsa K, Pirvola U, Saarma M, Kaila K (1999) The K+/Cl- co-transporter KCC2 renders GABA hyperpolarizing during neuronal maturation. Nature 397:251-255.
Rivera C, Voipio J, Thomas-Crusells J, Li H, Emri Z, Sipila S, Payne JA, Minichiello L, Saarma M, Kaila K (2004) Mechanism of activity-dependent downregulation of the neuron-specific K-Cl cotransporter KCC2. J Neurosci 24:4683-4691.
Rivera C, Li H, Thomas-Crusells J, Lahtinen H, Viitanen T, Nanobashvili A, Kokaia Z, Airaksinen MS, Voipio J, Kaila K, Saarma M (2002) BDNF-induced TrkB activation down-regulates the K+-Cl- cotransporter KCC2 and impairs neuronal Cl- extrusion. J Cell Biol 159:747-752.
Roberts E, Frankel S (1950) gamma-Aminobutyric acid in brain: its formation from glutamic acid. J Biol Chem 187:55-63.
Roberts E, Frankel S (1951) Glutamic acid decarboxylase in brain. J Biol Chem 188:789-795.
Rosier AM, Arckens L, Demeulemeester H, Orban GA, Eysel UT, Wu YJ, Vandesande F (1995) Effect of sensory deafferentation on immunoreactivity of GABAergic cells and on GABA receptors in the adult cat visual cortex. J Comp Neurol 359:476-489.
Rossignol E (2011) Genetics and function of neocortical GABAergic interneurons in neurodevelopmental disorders. Neural Plast 2011:649325.
Royle SJ, Lagnado L (2010) Clathrin-mediated endocytosis at the synaptic terminal: bridging the gap between physiology and molecules. Traffic 11:1489-1497.

Rudolph U, Mohler H (2004) Analysis of GABAA receptor function and dissection of the pharmacology of benzodiazepines and general anesthetics through mouse genetics. Annu Rev Pharmacol Toxicol 44:475-498.
Ruthazer ES, Li J, Cline HT (2006) Stabilization of axon branch dynamics by synaptic maturation. J Neurosci 26:3594-3603.
Rutherford LC, Nelson SB, Turrigiano GG (1998) BDNF has opposite effects on the quantal amplitude of pyramidal neuron and interneuron excitatory synapses. Neuron 21:521-530.
Rutherford LC, DeWan A, Lauer HM, Turrigiano GG (1997) Brain-derived neurotrophic factor mediates the activity-dependent regulation of inhibition in neocortical cultures. J Neurosci 17:4527-4535.
Sabo SL, Gomes RA, McAllister AK (2006) Formation of presynaptic terminals at predefined sites along axons. J Neurosci 26:10813-10825.
Saiyed T, Paarmann I, Schmitt B, Haeger S, Sola M, Schmalzing G, Weissenhorn W, Betz H (2007) Molecular basis of gephyrin clustering at inhibitory synapses: role of G- and E-domain interactions. J Biol Chem 282:5625-5632.
Saliba RS, Gu Z, Yan Z, Moss SJ (2009) Blocking L-type voltage-gated Ca2+ channels with dihydropyridines reduces gamma-aminobutyric acid type A receptor expression and synaptic inhibition. J Biol Chem 284:32544-32550.
Saliba RS, Michels G, Jacob TC, Pangalos MN, Moss SJ (2007) Activity-dependent ubiquitination of GABA(A) receptors regulates their accumulation at synaptic sites. J Neurosci 27:13341-13351.
Sassoe-Pognetto M, Frola E, Pregno G, Briatore F, Patrizi A (2011) Understanding the molecular diversity of GABAergic synapses. Front Cell Neurosci 5:4.
Sassoe-Pognetto M, Kirsch J, Grunert U, Greferath U, Fritschy JM, Mohler H, Betz H, Wassle H (1995) Colocalization of gephyrin and GABAA-receptor subunits in the rat retina. J Comp Neurol 357:1-14.
Schikorski T, Stevens CF (1997) Quantitative ultrastructural analysis of hippocampal excitatory synapses. J Neurosci 17:5858-5867.
Schoenenberger P, Gerosa D, Oertner TG (2009) Temporal control of immediate early gene induction by light. PLoS One 4:e8185.
Seeburg DP, Feliu-Mojer M, Gaiottino J, Pak DT, Sheng M (2008) Critical role of CDK5 and Polo-like kinase 2 in homeostatic synaptic plasticity during elevated activity. Neuron 58:571-583.
Shaner NC, Campbell RE, Steinbach PA, Giepmans BN, Palmer AE, Tsien RY (2004) Improved monomeric red, orange and yellow fluorescent proteins derived from Discosoma sp. red fluorescent protein. Nat Biotechnol 22:1567-1572.
Shapira M, Zhai RG, Dresbach T, Bresler T, Torres VI, Gundelfinger ED, Ziv NE, Garner CC (2003) Unitary assembly of presynaptic active zones from Piccolo-Bassoon transport vesicles. Neuron 38:237-252.
Shepherd JD, Rumbaugh G, Wu J, Chowdhury S, Plath N, Kuhl D, Huganir RL, Worley PF (2006) Arc/Arg3.1 mediates homeostatic synaptic scaling of AMPA receptors. Neuron 52:475-484.
Soghomonian JJ, Martin DL (1998) Two isoforms of glutamate decarboxylase: why? Trends Pharmacol Sci 19:500-505.
Somogyi P, Klausberger T (2005) Defined types of cortical interneurone structure space and spike timing in the hippocampus. J Physiol 562:9-26.

Song JY, Ichtchenko K, Sudhof TC, Brose N (1999) Neuroligin 1 is a postsynaptic cell-adhesion molecule of excitatory synapses. Proc Natl Acad Sci U S A 96:1100-1105.
Staras K, Branco T (2010) Sharing vesicles between central presynaptic terminals: implications for synaptic function. Front Synaptic Neurosci 2:20.
Staras K, Branco T, Burden JJ, Pozo K, Darcy K, Marra V, Ratnayaka A, Goda Y (2010) A vesicle superpool spans multiple presynaptic terminals in hippocampal neurons. Neuron 66:37-44.
Stellwagen D, Malenka RC (2006) Synaptic scaling mediated by glial TNF-alpha. Nature 440:1054-1059.
Stepanyants A, Tamas G, Chklovskii DB (2004) Class-specific features of neuronal wiring. Neuron 43:251-259.
Sudhof TC, Rizo J (2011) Synaptic vesicle exocytosis. Cold Spring Harb Perspect Biol 3.
Sutton MA, Ito HT, Cressy P, Kempf C, Woo JC, Schuman EM (2006) Miniature neurotransmission stabilizes synaptic function via tonic suppression of local dendritic protein synthesis. Cell 125:785-799.
Swanwick CC, Murthy NR, Kapur J (2006) Activity-dependent scaling of GABAergic synapse strength is regulated by brain-derived neurotrophic factor. Mol Cell Neurosci 31:481-492.
Takahashi H, Katayama K, Sohya K, Miyamoto H, Prasad T, Matsumoto Y, Ota M, Yasuda H, Tsumoto T, Aruga J, Craig AM (2012) Selective control of inhibitory synapse development by Slitrk3-PTPdelta trans-synaptic interaction. Nat Neurosci 15:389-398, S381-382.
Takamori S, Rhee JS, Rosenmund C, Jahn R (2000) Identification of a vesicular glutamate transporter that defines a glutamatergic phenotype in neurons. Nature 407:189-194.
Takata M, Sabe H, Hata A, Inazu T, Homma Y, Nukada T, Yamamura H, Kurosaki T (1994) Tyrosine kinases Lyn and Syk regulate B cell receptor-coupled Ca2+ mobilization through distinct pathways. Embo J 13:1341-1349.
Taniguchi H, He M, Wu P, Kim S, Paik R, Sugino K, Kvitsiani D, Fu Y, Lu J, Lin Y, Miyoshi G, Shima Y, Fishell G, Nelson SB, Huang ZJ (2011) A resource of Cre driver lines for genetic targeting of GABAergic neurons in cerebral cortex. Neuron 71:995-1013.
Tao HW, Poo MM (2005) Activity-dependent matching of excitatory and inhibitory inputs during refinement of visual receptive fields. Neuron 45:829-836.
Terauchi A, Johnson-Venkatesh EM, Toth AB, Javed D, Sutton MA, Umemori H (2010) Distinct FGFs promote differentiation of excitatory and inhibitory synapses. Nature 465:783-787.
Thiagarajan TC, Piedras-Renteria ES, Tsien RW (2002) alpha- and betaCaMKII. Inverse regulation by neuronal activity and opposing effects on synaptic strength. Neuron 36:1103-1114.
Thomas P, Mortensen M, Hosie AM, Smart TG (2005) Dynamic mobility of functional GABAA receptors at inhibitory synapses. Nat Neurosci 8:889-897.
Thomsen DR, Stenberg RM, Goins WF, Stinski MF (1984) Promoter-regulatory region of the major immediate early gene of human cytomegalovirus. Proc Natl Acad Sci U S A 81:659-663.
Tischmeyer W, Grimm R (1999) Activation of immediate early genes and memory formation. Cell Mol Life Sci 55:564-574.

Tokuoka H, Goda Y (2008) Activity-dependent coordination of presynaptic release probability and postsynaptic GluR2 abundance at single synapses. Proc Natl Acad Sci U S A 105:14656-14661.
Tretter V, Moss SJ (2008) GABA(A) Receptor Dynamics and Constructing GABAergic Synapses. Front Mol Neurosci 1:7.
Tsuriel S, Fisher A, Wittenmayer N, Dresbach T, Garner CC, Ziv NE (2009) Exchange and redistribution dynamics of the cytoskeleton of the active zone molecule bassoon. J Neurosci 29:351-358.
Tsuriel S, Geva R, Zamorano P, Dresbach T, Boeckers T, Gundelfinger ED, Garner CC, Ziv NE (2006) Local sharing as a predominant determinant of synaptic matrix molecular dynamics. PLoS Biol 4:e271.
Turrigiano G (2007) Homeostatic signaling: the positive side of negative feedback. Curr Opin Neurobiol 17:318-324.
Turrigiano GG (1999) Homeostatic plasticity in neuronal networks: the more things change, the more they stay the same. Trends Neurosci 22:221-227.
Turrigiano GG (2008) The self-tuning neuron: synaptic scaling of excitatory synapses. Cell 135:422-435.
Turrigiano GG, Nelson SB (2004) Homeostatic plasticity in the developing nervous system. Nat Rev Neurosci 5:97-107.
Turrigiano GG, Leslie KR, Desai NS, Rutherford LC, Nelson SB (1998) Activity-dependent scaling of quantal amplitude in neocortical neurons. Nature 391:892-896.
Ullrich B, Ushkaryov YA, Sudhof TC (1995) Cartography of neurexins: more than 1000 isoforms generated by alternative splicing and expressed in distinct subsets of neurons. Neuron 14:497-507.
Umemori H, Linhoff MW, Ornitz DM, Sanes JR (2004) FGF22 and its close relatives are presynaptic organizing molecules in the mammalian brain. Cell 118:257-270.
van Versendaal D, Rajendran R, Saiepour MH, Klooster J, Smit-Rigter L, Sommeijer JP, De Zeeuw CI, Hofer SB, Heimel JA, Levelt CN (2012) Elimination of inhibitory synapses is a major component of adult ocular dominance plasticity. Neuron 74:374-383.
Varoqueaux F, Jamain S, Brose N (2004) Neuroligin 2 is exclusively localized to inhibitory synapses. Eur J Cell Biol 83:449-456.
Varoqueaux F, Sigler A, Rhee JS, Brose N, Enk C, Reim K, Rosenmund C (2002) Total arrest of spontaneous and evoked synaptic transmission but normal synaptogenesis in the absence of Munc13-mediated vesicle priming. Proc Natl Acad Sci U S A 99:9037-9042.
Vautrin J, Schaffner AE, Barker JL (1994) Fast presynaptic GABAA receptor-mediated Cl- conductance in cultured rat hippocampal neurones. J Physiol 479 (Pt 1):53-63.
Verhage M, Maia AS, Plomp JJ, Brussaard AB, Heeroma JH, Vermeer H, Toonen RF, Hammer RE, van den Berg TK, Missler M, Geuze HJ, Sudhof TC (2000) Synaptic assembly of the brain in the absence of neurotransmitter secretion. Science 287:864-869.
Veselovsky NS, Engert F, Lux HD (1996) Fast local superfusion technique. Pflugers Arch 432:351-354.
Weyhersmuller A, Hallermann S, Wagner N, Eilers J (2011) Rapid active zone remodeling during synaptic plasticity. J Neurosci 31:6041-6052.

Wierenga CJ, Walsh MF, Turrigiano GG (2006) Temporal regulation of the expression locus of homeostatic plasticity. J Neurophysiol 96:2127-2133.
Wierenga CJ, Becker N, Bonhoeffer T (2008) GABAergic synapses are formed without the involvement of dendritic protrusions. Nat Neurosci 11:1044-1052.
Wierenga CJ, Mullner FE, Rinke I, Keck T, Stein V, Bonhoeffer T (2010) Molecular and electrophysiological characterization of GFP-expressing CA1 interneurons in GAD65-GFP mice. PLoS One 5:e15915.
Wonders CP, Anderson SA (2006) The origin and specification of cortical interneurons. Nat Rev Neurosci 7:687-696.
Woodin MA, Ganguly K, Poo MM (2003) Coincident pre- and postsynaptic activity modifies GABAergic synapses by postsynaptic changes in Cl- transporter activity. Neuron 39:807-820.
Wu X, Fu Y, Knott G, Lu J, Di Cristo G, Huang ZJ (2012) GABA signaling promotes synapse elimination and axon pruning in developing cortical inhibitory interneurons. J Neurosci 32:331-343.
Xu T, Yu X, Perlik AJ, Tobin WF, Zweig JA, Tennant K, Jones T, Zuo Y (2009) Rapid formation and selective stabilization of synapses for enduring motor memories. Nature 462:915-919.
Xu W (2011) PSD-95-like membrane associated guanylate kinases (PSD-MAGUKs) and synaptic plasticity. Curr Opin Neurobiol 21:306-312.
Yang G, Pan F, Gan WB (2009) Stably maintained dendritic spines are associated with lifelong memories. Nature 462:920-924.
Yizhar O, Fenno LE, Prigge M, Schneider F, Davidson TJ, O'Shea DJ, Sohal VS, Goshen I, Finkelstein J, Paz JT, Stehfest K, Fudim R, Ramakrishnan C, Huguenard JR, Hegemann P, Deisseroth K (2011) Neocortical excitation/inhibition balance in information processing and social dysfunction. Nature 477:171-178.
Yuste R, Bonhoeffer T (2004) Genesis of dendritic spines: insights from ultrastructural and imaging studies. Nat Rev Neurosci 5:24-34.
Zhai R, Olias G, Chung WJ, Lester RA, tom Dieck S, Langnaese K, Kreutz MR, Kindler S, Gundelfinger ED, Garner CC (2000) Temporal appearance of the presynaptic cytomatrix protein bassoon during synaptogenesis. Mol Cell Neurosci 15:417-428.
Zhai RG, Vardinon-Friedman H, Cases-Langhoff C, Becker B, Gundelfinger ED, Ziv NE, Garner CC (2001) Assembling the presynaptic active zone: a characterization of an active one precursor vesicle. Neuron 29:131-143.
Zhu L, Polley N, Mathews GC, Delpire E (2008) NKCC1 and KCC2 prevent hyperexcitability in the mouse hippocampus. Epilepsy Res 79:201-212.
Ziv NE, Smith SJ (1996) Evidence for a role of dendritic filopodia in synaptogenesis and spine formation. Neuron 17:91-102.